UNIVERSITÀ DEGLI STUDI DI UDINE
hic sunt futura

www.uniud.it

PhD Course in:

"Agricultural Sciences and Biotechnology"

Cycle 33°

Thesis title

"Development of synthetic methods, namely oligonucleotide aptamers, in order to stimulate the plant defence response in *Arabidopsis thaliana*"

PhD Candidate

Federico Bosetto

Supervisor

Prof. Giuseppe Firrao

Coordinator

Prof. Francesco Nazzi

Year 2021

INDEX

1. ABSTRACT

Aptamers are small single stranded synthetic nucleic acids that fold into a well-defined three-dimensional structure to bind to a variety of diverse molecular targets specifically and tightly. Aptamers are evolved from random oligonucleotide pools by an *in vitro* selection process called Systemic Evolution of Ligands by EXponential enrichment (SELEX).

A new methodology based on oligonucleotide aptamers was experimented in *Arabidopsis thaliana* to protect plants facing disease as an alternative to the use of pesticides. An attempt was made to select two aptamers specifically targeting both the plant cell and the flagellin from *Pseudomonas syringae* pv. *tomato* DC3000.

These two aptamers were to be combined in a chimeric synthetic biosensor, which is expected, when properly stimulated by the pathogen, to activate the defence response thanks to the cell-internalization of AtlsiRNA-1, a dsRNA known to be involved in the plant defence mechanism.

For the first time a Cell-SELEX strategy was introduced on plant cells and, although further optimization of the washing and elution steps is still required, a suitable protocol was designed and applied. Cell-SELEX was used to select specific DNA aptamers which targeted the cell surface receptors and/or internalize into the cell cytoplasm. The selection progress was monitored by a combined approach based on Real Time PCR and High Resolution Melting (HRM) analysis, which showed for cell-extracted oligonucleotides a shift of the melting peak from 74 °C to 81 °C. Some potential-internalizing aptamers have been tested for their capability of internalize into plant cells. Real Time PCR of the cell lysate allowed the identification of three potential aptamers which were successfully internalized in a higher amount. The amount of potential aptamer 132 that was internalized was found to be 89 folds larger than aptamer 106 and 136 folds larger than aptamer 120. While for potential aptamers 118 and 35-259 was found to be 63 folds larger than aptamer 106 and 96 folds larger than aptamer 120.

The second part of the work was dedicated to the selection of DNA aptamers against the flagellin of *Pseudomonas syringae* pv. *tomato* DC3000 (*Pto*).

Pto is a well-known pathogen used in experimental infections of *Arabidopsis thaliana* plants. The selection of aptamers against the flagellin provides a highly specific molecular tool which could be integrated in the synthetic previously described biosensor. To this end, the *Pto*-flagellin gene was cloned, expressed and purified under denaturing conditions, then refolded to be used as target for SELEX. The monitoring of the selection progress by Real-Time PCR and HRM analysis and the

sequence analysis of the products of round 8 confirmed the selection of potential specific aptamers, whose affinity to the target is yet to be determined.

A third SELEX was performed against the lactate dehydrogenase from *Plasmodium falciparum* to select for cubane-modified aptamers or cubamers, in order to practice on SELEX with chemically-modification on aptamers to develop the technological basis for the selection of specific cubamers against the *Pto*-flagellin.

In the end, a model of a structure switching aptamer-based biosensor to simulate *in vivo* the plant defence response stimulation in a pathogen-specific manner is proposed starting from the sequences of the potential aptamers selected with this work.

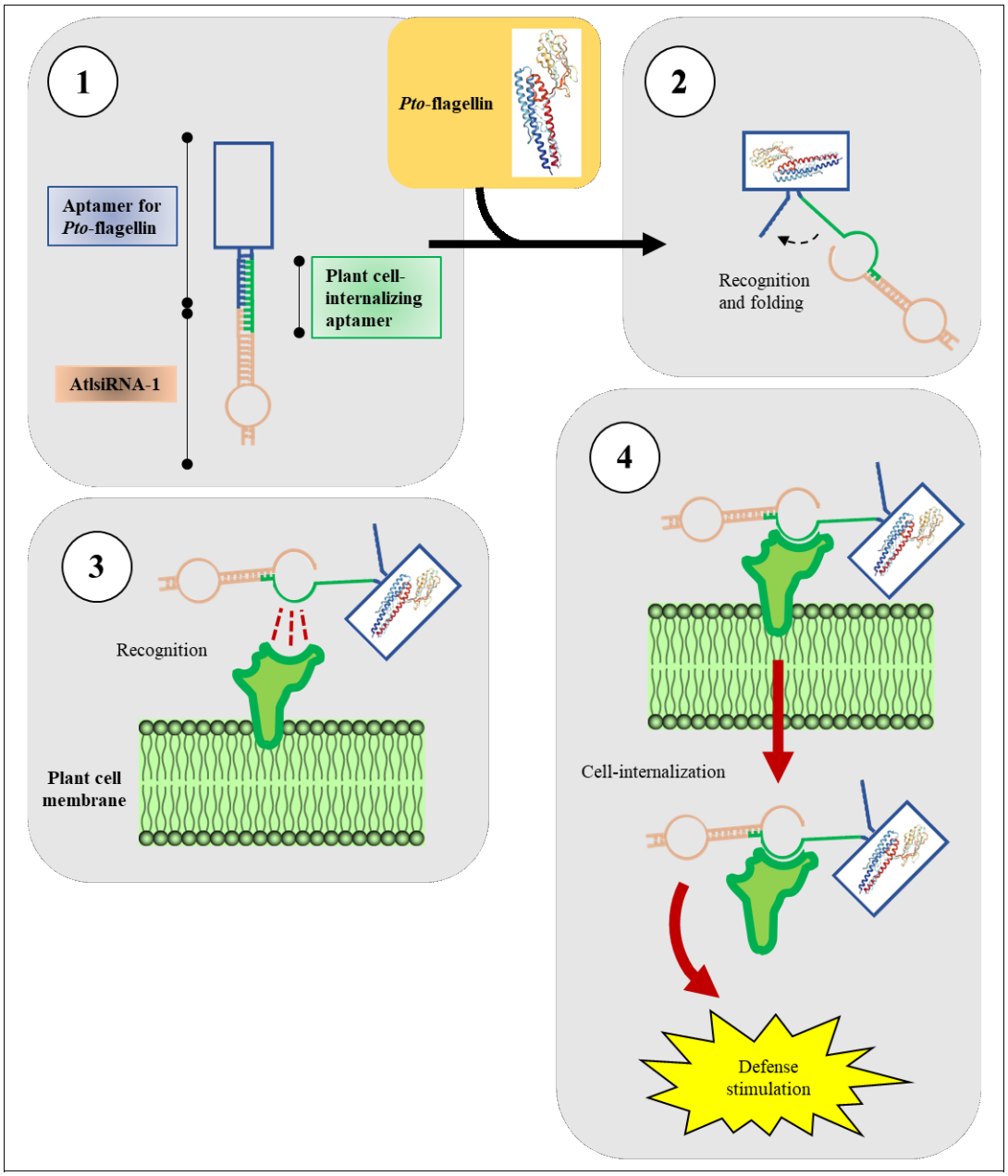

2. INTRODUCTION

2.1 Aptamer properties

Aptamers are small single stranded synthetic nucleic acids or small peptide molecules that fold into a well-defined three-dimensional structure to bind to a variety of diverse molecular targets specifically and tightly (Figure 1) [Gopinath, 2016; Song et al., 2012; Yüce et al., 2015]. Metal ions, small molecules, proteins and whole cells are commonly bound by aptamers [Cai et al., 2018].

Aptamers are evolved from random oligonucleotide pools by an *in vitro* selection process called Systemic Evolution of Ligands by EXponential enrichment (SELEX) [Ellington and Szostak, 1990; Tuerk and Gold, 1990]. One SELEX round is structured in four major steps: incubation of random oligonucleotide pools with the molecular target, separation of bound from unbound sequences, elution and amplification of bound nucleic acids. At the end of the selection, aptamers are characterized and checked for their affinity and specificity to the target.

Aptamers possess secondary structures constituted by stems, loops, bulges, hairpins, pseudoknots, triplexes and G-quadruplexes which form unique three-dimensional structures necessary for the molecular recognition of the cognate targets [Gopinath, 2016; Stoltenburg et al., 2007; Strehlitz et al., 2012; Zhou and Rossi, 2017].

The aptamer-target binding occurs by structure compatibility, hydrogen bonding, electrostatic interactions, hydrophobic effect, π-π stacking and van der Walls forces [Hermann and Patel, 2000; Tan et al., 2016]. Hence, the chemical composition of the selection environment, in terms of metal ions and pH, and the temperature, impact the binding affinity of aptamers [Tan et al., 2016]. Oligonucleotide aptamers are negatively charged molecules due by the phosphate groups, the presence of monovalent and divalent cations help to screen this charge and enhance the stabilization of aptamer secondary structures [Cai et al., 2018; Carothers et al., 2010; Tan et al., 2016; Walter et al., 2012]. In fact, Carothers and colleagues reported that aptamer binding of amino acids, proteins and nucleotides were performed in presence of 5 - 10 mM Mg^{2+} [Carothers et al., 2010]. However, also target-inherent properties such as pI [Mayer, 2009; Zhou and Rossi, 2017], charge and hydrophilicity [Zhou and Rossi, 2017] modulate the binding affinity with aptamers.

Together, all mentioned variables contribute specifically to the binding stringency, which in turn affect the affinity and the function of selected aptamers [Zhou and Rossi, 2017].

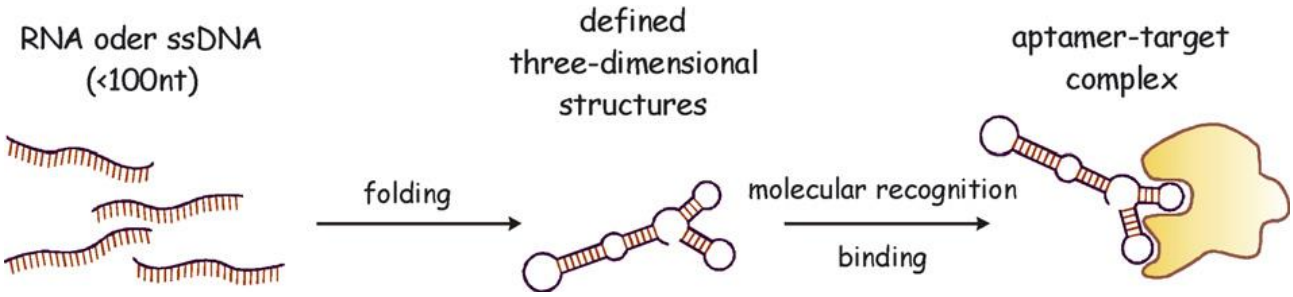

Figure 1. Representation of how an aptamer recognizes its specific target. Aptamers are small single stranded oligonucleotides of DNA or RNA that fold in a well-defined three-dimensional structure to bind their targets specifically and tightly [modified from Stoltenburg et al., 2007].

2.1.1 Aptamers versus Antibodies

Based on their high affinity and specificity, aptamers are considered as valid alternatives to antibodies in several biological and biotechnological applications. Although, nowadays antibodies are used routinely in most of diagnostic tests as biorecognition tools and are still dominating the global medicine marketplace, they possess several drawbacks compared to aptamers.

The selection of aptamers is a complete *in vitro* process, meaning that it does not rely on living animals and *in vivo* conditions, which are strictly required for antibodies. The chemical synthesis of aptamers is inexpensive and yields a uniformity of aptamer population with minimal batch to batch variability [Jayasena, 1999; Kim and Gu, 2014; Luzi et al., 2003; Song et al., 2012; Yüce et al., 2015; Zhou and Rossi, 2017].

Besides, aptamers are easily chemically modified to increase their stability and binding affinity [Luzi et al., 2003; Song et al., 2012; Yüce et al., 2015; Zhou and Rossi, 2017] or with reporter molecules to localize them [Jayasena, 1999; Kim and Gu, 2014; Song et al., 2012; Yüce et al., 2015].

Toxins and non-immunogenic molecules can be used as target to select high affinity aptamers, whereas the antibody production to recognize same molecules is scarcely realizable [Jayasena, 1999; Song et al., 2012; Zhou and Rossi, 2017].

Moreover, if denatured, aptamers can regain their conformation whereas a denatured antibody is hardly recoverable [Jayasena, 1999; Kim and Gu, 2014; Luzi et al., 2003; Song et al., 2012; Zhou and Rossi, 2017].

Thanks to their small size, aptamers display a superior cell-penetration capability compared to antibodies, raising different therapeutic opportunities [Kim and Gu, 2014; Xiang et al., 2015; Yüce et al., 2015]. Hence, their small size allows them to bind to small molecules or some hidden binding domains that are inaccessible for antibodies [Song et al., 2012; Yüce et al., 2015; Zhou and Rossi, 2017].

2.1.2 Chemical modifications on Aptamers

Oligonucleotide aptamers, like any oligonucleotide, suffer of rapid degradation by endo- and exo- nucleases *in vivo*. Moreover, the chemical diversity of oligonucleotide aptamers is only based on the five structural elements and in this view, they compare poorly with antibodies. However, chemical modifications have been designed and successfully applied in order to increase their stability and their binding affinity, particularly valuable for their efficient application in therapeutics and in the diagnostic field (Figure 2). Chemically modified aptamers can be generated by post-SELEX modifications or by using modified nucleoside triphosphates during the selection process [Diafa and Hollenstein, 2015; Ni et al., 2017; Röthlisberger and Hollenstein, 2018; Tolle and Mayer, 2013].

Improvements of nuclease resistance of aptamers include modifications of the sugar ring and of the phosphate groups [Diafa and Hollenstein, 2015; Gao et al., 2016; Lapa et al., 2016; Ni et al., 2017; Tolle and Mayer, 2013]. Modifications of the 2′ position of ribose and deoxyribose with 2′-NH_2, 2′-F and 2′-O-CH_3 nucleotides are particularly important for RNA aptamers but as a rule they are not well-tolerated by canonical polymerases [Röthlisberger and Hollenstein, 2018]. Modification of the α-phosphate group at one non-bridging oxygen atom with sulfur generates α-phosphorothioates where only the S diastereomer can be processed by canonical polymerases [Lapa et al., 2016]. Both kind of modifications have been extensively used to enhance the biological stability of oligonucleotides [Diafa and Hollenstein, 2015; Gao et al., 2016; Lapa et al., 2016; Ni et al., 2017; Röthlisberger and Hollenstein, 2018; Tolle and Mayer, 2013]. An exhaustive description of other kind of chemical modifications of aptamers to avoid nuclease cleavage is reviewed by Röthlisberger and Hollenstein [Röthlisberger and Hollenstein, 2018].

As pointed out above, aptamers can be also chemically modified to enhance their binding affinity with targets. These modifications mostly involve hydrophobic groups that might introduce additional possibilities of secondary structures and different types of molecular interactions with cognate targets that unmodified aptamers cannot exploit. Modifications with hydrophobic moieties are typically localized on the nucleobases at the C8- and N7- positions for purines and at the C5 position for pyrimidines, generally these modified sites are well tolerated by canonical polymerases [Diafa and Hollenstein, 2015; Lapa et al., 2016; Röthlisberger and Hollenstein, 2018; Tolle and Mayer, 2013]. Additionally, there is evidence that in certain cases the incorporation of hydrophobic modifications on the nucleobase also positively impacts the oligonucleotide resistance to nuclease degradation [Rohloff et al., 2014; Röthlisberger and Hollenstein, 2018].

Examples of chemically modified aptamers with very low dissociation rate constants for the target are the Slow Off-rate Modified Aptamers or SOMAmers. SOMAmers are modified aptamers with moieties of amino acid side chains that create hydrophobic surfaces on the oligonucleotide and

permit it to strictly interact with the hydrophobic counterparts of the target [Diafa and Hollenstein, 2015; Rohloff et al., 2014; Röthlisberger and Hollenstein, 2018; Tolle and Mayer, 2013].

Cubane is another useful hydrophobic modification that can be applied to the nucleobases of oligonucleotides to increase their binding affinity. Cubanes are bioisosteres derived from benzene, which show unique characteristics and some advantages. Cubanes compared benzene are biologically stable, non-toxic and more water soluble due to the disruption of π-stacking. Moreover, cubanes form unusual C-H···O hydrogen bonds caused by the strong s-character in the C-H bonds itself induced by the p-character of the C-C bonds [Kuduva et al., 1999].

So far, cubanes have been successfully exploited as important functional groups of pharmaceuticals and agrochemicals [Houston et al., 2019]. Recently, Cheung and colleagues, have been the first to apply chemical modifications based on cubane to DNA aptamers to design an efficient molecular tool for malaria diagnosis. They showed that cubane-modified aptamers (cubamers) specifically recognise the lactate dehydrogenase from *Plasmodium vivax* (*Pv*LDH), the most widespread agent of malaria, thanks to the hydrophobic interactions which take place between the cubane and the enzyme. Moreover, the selected cubamers bind to the variable region of *Pv*LDH, enabling to discriminate this enzyme from the homologous isoform of *Plasmodium falciparum*, the most virulent agent of malaria [Cheung et al., 2020].

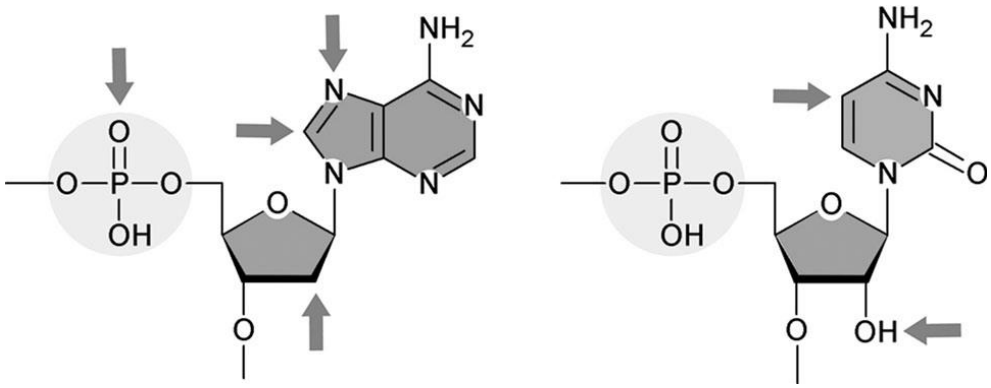

Figure 2. Modification sites in natural NTPs: 2′ position of the sugar, α-phosphate group, C8 and N7 in purine nucleobases and C5 in pyrimidine nucleobases [modified from Lapa et al., 2016].

2.1.3 Aptamer applications

As pointed out before, aptamers are employed in a myriad of applications thanks to the high affinity and specificity of their binding capacity and their well-known peculiarity to recognize almost every kind of target (Figure 3).

Aptasensors are biosensors that use an aptamer to detect a specific ligand coupled to a physical transducer which converts the target recognition event in a detectable response [Mairal et al., 2008; Luzi et al., 2003; O'Sullivan, 2002], such as an optical [Kim and Gu, 2014; Luzi et al., 2003; Mairal et al., 2008; O'Sullivan, 2002; Song et al., 2012; Strehlitz et al., 2012; Zhang et al., 2019], electrochemical [Kim and Gu, 2014; Luzi et al., 2003; Mairal et al., 2008; Song et al., 2012; Strehlitz et al., 2012; Zhang et al., 2019] or mass-sensitive [Luzi et al., 2003; Song et al., 2012] signal.

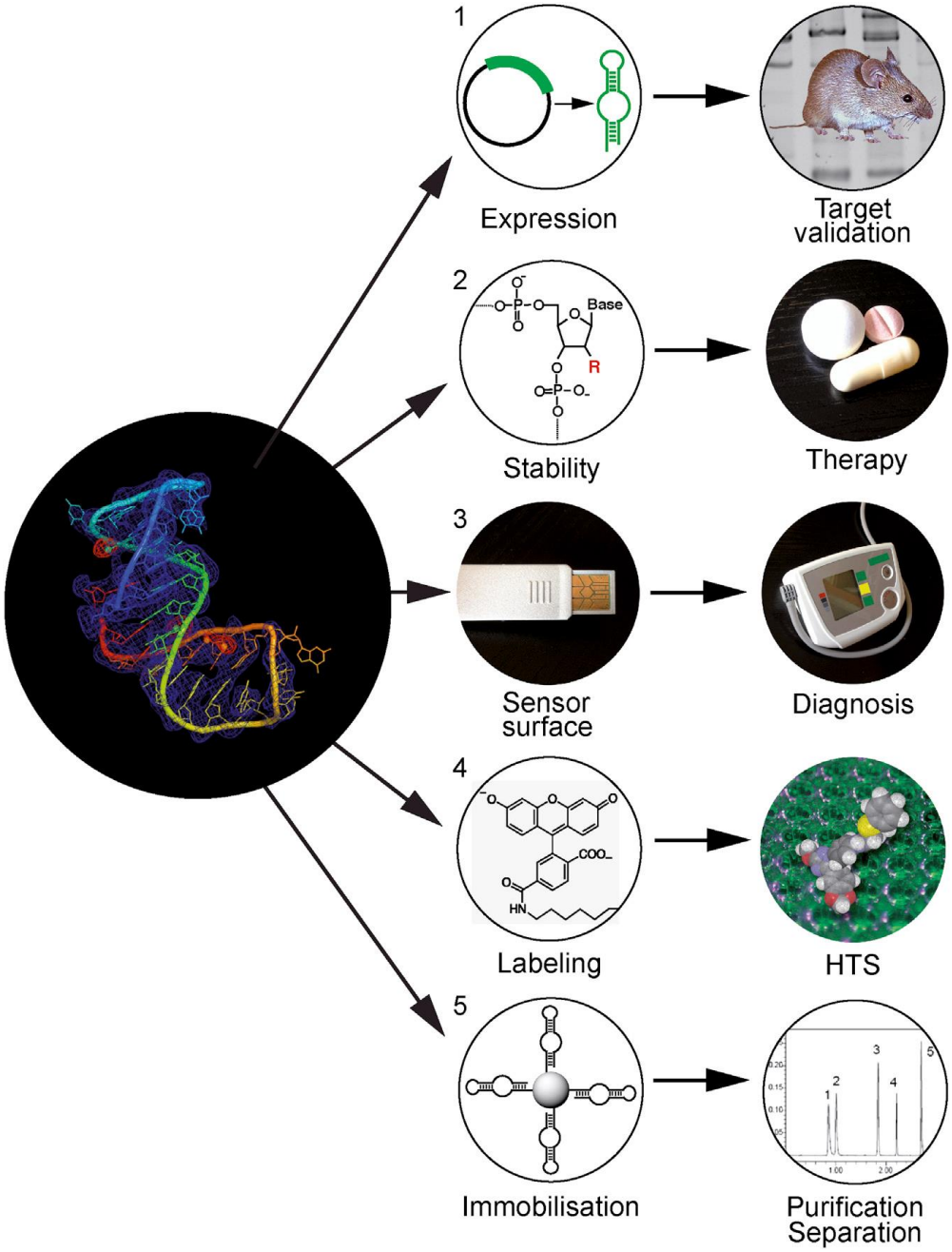

Figure 3. Aptamer applications. 1) Aptamer *in vivo* and in cell expressions permit to validate targets. 2) Aptamer chemical modifications increase their stability for therapeutic purposes. 3) Aptamers included in sensors are important

for diagnosis. 4) Aptamers labelled with probes allow to conduct high-throughput screening (HTS). 5) Immobilised aptamers are applied in purification and separation techniques [modified from Famulok and Mayer, 2014].

Aptasensors and aptamers have been successfully developed against harmful targets for the human health, such as cancer cells [Ciancio et al., 2018; Mayer, 2009; Mercier et al., 2017; Ohuchi, 2012; Xiang et al., 2015; Zhang et al., 2019; Zhou and Rossi, 2017; Zhuo et al., 2017], pathogenic microorganisms [Davydova et al., 2016; Zhang et al., 2019] including microbes [Özalp et al., 2013], viruses [Yüce et al., 2015] and unicellular parasites [Ohuchi, 2012], and biocontaminants like antibiotics [Strehlitz et al., 2012; Zhang et al., 2019] and toxins [Mairal et al., 2008; Song et al., 2012; Yüce et al., 2015; Zhang et al., 2019].

Besides, aptamers have been utilised as therapeutic tools to either directly work as drugs [Mayer, 2009; Mercier et al., 2017; Song et al., 2012; Xiang et al., 2015; Zhang et al., 2019; Zhou and Rossi, 2017; Zhuo et al., 2017] or as carriers to deliver other kind of drugs [Mayer, 2009; Mercier et al., 2017; Song et al., 2012; Yüce et al., 2015; Zhang et al., 2019; Zhou and Rossi, 2017; Zhuo et al., 2017].

Moreover, aptamers have been exploited as tools for imaging [Song et al., 2012; Xiang et al., 2015] and diagnostic [Zhang et al., 2019; Zhuo et al., 2017] applications which help target validation [Ciancio et al., 2018; Mayer, 2009; Mercier et al., 2017; Famulok and Mayer, 2014; Yüce et al., 2015].

Despite the great success of aptamer applications in biological and biotechnological fields mainly relative to the human health, there are very few examples of important applications in the plant field.

The ever-increasing human population increases the demands for food at global level both in terms of quality and quantity. Plants play a central role to guarantee the human sustenance and therefore need to be preserved by every negative aspect which impacts their growth, especially from biotic stresses coming from pathogens which account for important crop losses.

To date, examples of the aptamer approach applied in the plant field include the efficient suppression of viral infections in transgenic plants expressing small peptide aptamers and the *in vivo* and *ex vivo* applications of a synthetic peptide which impairs oomycete spreading. An in-depth study of the application of peptide aptamers in plant viral- and oomycete- infections it is reviewed at the next paragraph.

2.1.4 Aptamers as plant protection tools

Advancement in biotechnology has led to the development of novel approaches based on aptamers to counteract pathogen spreading in plants. Specifically, peptide aptamers have been successfully selected for controlling plant viruses and recently also oomycetes. Peptide aptamers are selected starting from random peptide libraries that are screened on protein targets. In fact, the goal of peptide aptamers is to interact tight with a protein target and inhibit its molecular function. In plant viral infections, peptide aptamers have been selected to primary functions of the virus, such as DNA replication, assembly of replication complexes and protein complex binding nucleic acids [Colombo et al., 2010; Mendoza-Figueroa et al., 2014], while to impair oomycete spreading on plants, peptide aptamers have been selected against a fundamental enzyme as the cellulase synthase 2 [Colombo et al., 2020].

The first report of the peptide aptamer approach concerned *Nicotiana benthamiana* plants which have been made resistant to five different tospoviruses. Rudolph and colleagues [2003] selected a 29 aa long peptide which strongly interacted with one of the nucleocapside protein homodimerization domains that are involved in many essential functions, such as homopolymerization, packaging of the viral genomic RNA and interaction with the movement protein. Transgenic plant lines expressing the peptide aptamer showed reduced symptoms of viral infection [Rudolph et al., 2003].

Later, Lopez-Ochoa and colleagues [2006] successfully exploited the peptide aptamer strategy to block geminivirus replication in tobacco protoplasts. Geminivirus are responsible of major economic losses in a broad range of vegetables and field crops, with multiple viruses often contributing to disease in a given crop. Starting from a random peptide library, based on *E. coli* thioredoxin, with 2.9×10^9 random 20-mer peptides in its active site, they selected a set of peptide aptamers that bound to the N terminus of highly conserved replication initiator protein (Rep/AL1) of *Tobacco golden mosaic virus* [Lopez-Ochoa et al., 2006]. Besides, the same research group showed that two peptide aptamers, among the previously selected, named A22 and A64 were able to strongly bind the Rep/AL1 proteins from nine different viruses belonging to the three major *Geminiviridae* genera. Transgenic tomato plants expressing A22 and A64 and infected with unrelated geminiviruses, *Tomato yellow leaf curl virus* and *Tomato mottle virus*, displayed reduced symptoms and decreased viral DNA loads [Reyes et al., 2013].

Recently, an 8 amino acid long peptide was developed to efficiently stop *Plasmopara viticola* infection of *Vitis vinifera* green tissues. Colombo and colleagues demonstrated that NoPv1 peptide aptamer prevents the germ tube formation by impairing the activity of the cellulase synthase 2, namely *Pv*Cesa2. Moreover, they showed that the selected peptide aptamer was not affecting the

growth of non-target organisms, including human cells. Due to the high homology among the cellulose synthase enzyme sequences, they also found that NoPv1 was able to contrast the growth of another oomycete, *Phytophthora infestans*, the causal agent of late blight in tomato and potato [Colombo et al., 2020].

Although the three described examples clearly showed that the peptide aptamer approach can strongly reduce viral- and oomycete- infections at broad-spectrum, more applications, also looking at the oligonucleotide aptamers, should be taken in account to extent the plant immunity to several diseases originating from other organisms, such as bacteria and fungi. Hence, the usage of transgenic plants, not only to express aptamers *in planta*, is highly complexed and strictly ruled in the marketplace. Therefore, alternatives to directly apply aptamers on plants are needed. In this view, cell-penetrating peptides have been successfully applied to transfer peptide aptamers into plant cells [Colombo et al., 2010].

2.2 Systemic Evolution of Ligands by EXponential enrichment (SELEX)

Combinatorial chemistry is an important technology to discover and synthesize new drugs and molecules of interest to provide innovative solutions in the biological and biotechnological research [Stoltenburg et al., 2007]. In the view of oligonucleotide aptamers, large libraries, representing a huge pool of unique molecules, are screened against the target of interest. Only the sequences which adopt peculiar secondary and tertiary structures to tightly bind the target are selected and successively amplified by PCR to start a new selection cycle [Stoltenburg et al., 2007]. At the end of the selection, only few highly specific aptamers are selected and characterized for their specificity for the target.

Systematic Evolution of Ligands by EXponential Enrichment or SELEX is the *in vitro* procedure adopted to generate aptamers [Ellington and Szostak, 1990; Tuerk and Gold, 1990].

SELEX relies on iterative cycles of *in vitro* selection and amplification that mimic a darwinian selection process where the evolutionary pressure is exerted by the target binding affinity [Stoltenburg et al., 2007]. Figure 4 illustrates the common SELEX steps [Jayasena, 1999; Luzi et al., 2003; Mairal et al., 2008; Mercier et al., 2017; Ozer et al., 2014; Stoltenburg et al., 2007; Tan et al., 2016; Yüce et al., 2015; Zhang et al., 2019; Zhuo et al., 2017].

Starting from the design of a random oligonucleotide library, a common SELEX experiment comprises a binding step between library and target, a partition step with the removal of unbound

sequences, an elution step of the specifically bound oligonucleotides, the amplification and monitoring of the selected oligonucleotides and a final condition step to prepare the selected oligonucleotides for the next SELEX round. When the SELEX procedure is finished, a sidestep is the cloning part which is necessary for the sequencing and the aptamer characterization.

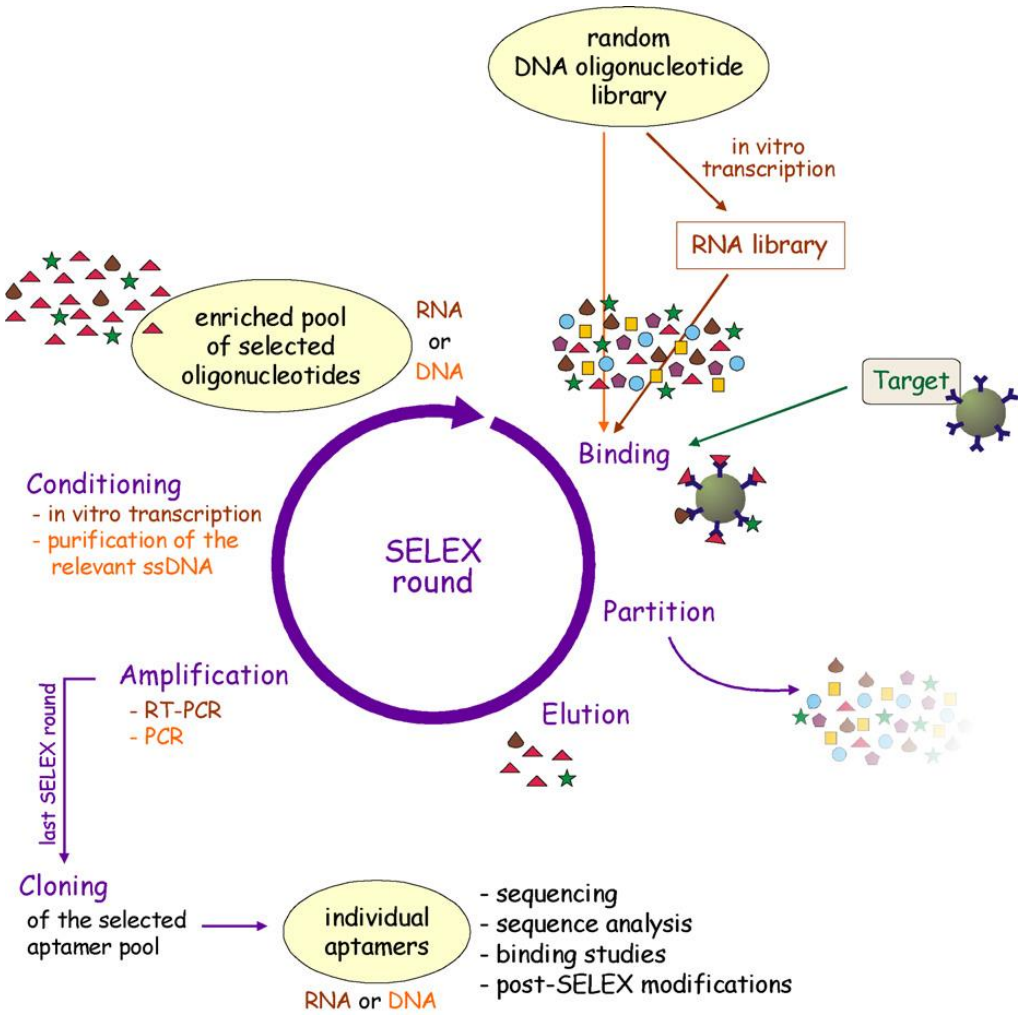

Figure 4. General SELEX procedure. Random DNA oligonucleotide library can be directly incubated with the target or can be first *in vitro* transcribed in an RNA library. With the partition step all the sequences that are not specifically bound to the target are discarded, while those ones that remain attached to the target are eluted and recovered. The eluted sequences are amplified and treated to regenerate the single stranded structure of random oligonucleotide library to start a new SELEX round. When the selection is finished, the selected pool is cloned and sequenced to characterize the individual candidates [modified from Stoltenburg et al., 2007].

2.2.1 The SELEX cycle

A SELEX experiment requires a random DNA or RNA oligonucleotide library which is usually structured with two constant regions where annealing of primers take place and a central

random region (Figure 5) [Gopinath, 2016; Jayasena, 1999; Kim and Gu, 2014; Luzi et al., 2003; Mairal et al., 2008; Stoltenburg et al., 2007]. The library complexity or diversity is dependent on the length of the random region because each position (N) can be taken by one of the four nucleotides, generating in this way 4^N unique and different sequences. For example, an oligonucleotide library with a random region of 40 nucleotides has a maximum theoretical diversity of $4^{40} = 1.2 \times 10^{24}$. Notwithstanding, from a practical point of view, an oligonucleotide library is representative of no more of $10^{14} – 10^{15}$ individual sequences, which still permits the selection of specific aptamer families for the target of interest [Gopinath, 2016; Jayasena, 1999; Kim and Gu, 2014; Luzi et al., 2003; Mairal et al., 2008].

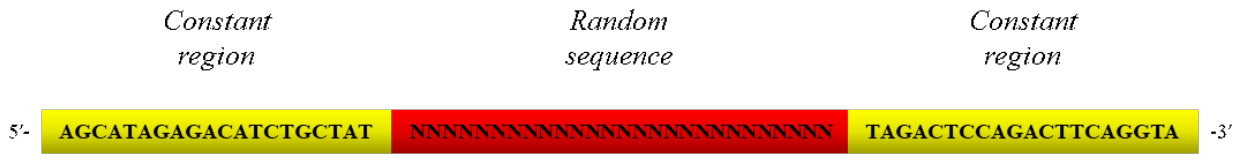

Figure 5. Schematic representation of a random oligonucleotide library. The yellow portions are the constant regions, the red portion is the random sequence where N can be dA/dG/dC/dT.

The SELEX cycle starts when the random oligonucleotide library is incubated with the target of interest. During the binding step, every sequence interacts with the target assuming specific conformational changes which are strictly dependent by the random region and the target properties. Besides, the aptamer-target binding is highly influenced by the chemical composition of the reaction buffer, the pH and the temperature which determine the binding stringency, as above mentioned.

Since not all the sequences are able to bind the desired target with high affinity it is important to devise a partition strategy. The partition step allows the removal of unbound and low binding affinity sequences. Thanks to a specifically formulated washing buffer based on the target characteristics, unwanted sequences are discarded from the selection process.

After partitioning, the aptamer-target complex is recovered. As for the partition, the elution step can be carried out according to the target properties. The most used methods include affinity [Famulok, 1994], heat separation [Sefah et al., 2010; Stoltenburg et al., 2005; Walter et al., 2012], denaturing agents [Bianchini et al., 2001; Walter et al., 2012], increasing of ionic strength and alteration of pH [Hernandez et al., 2013; Walter et al., 2012].

After the target-binding aptamers have been eluted, the subsequent steps are the aptamer pool amplification and the monitoring of the selection process.

The amplification step is performed using standard PCR, qPCR and RT-PCR procedures. However, carefulness is required because random libraries do not behave as common genomic DNA templates due to the nature of the random sequences [Musheev and Krylov, 2006; Wang et al., 2019]. When comparing the amplification of a genomic DNA to the random aptamer library, Musheev and co-workers discovered that the random library design is responsible for the amplification issues. They distinguished a PCR by-product and a genomic PCR non-specific product. The difference lies in the fact that while non-specific products are due to primer-primer hybridization accumulating over the cycles, a by-product is the result of a type of ss/dsDNA formed by product-product hybridization [Musheev and Krylov, 2006]. Tolle and his group identified two mechanisms by which these by-products are produced: a ladder and non-ladder type by-product formation [Tolle et al., 2014].

The monitoring of the selection progress is adopted to verify the successful selection of high affinity and specificity aptamers. Multiple assays have been developed with this purpose, such as restriction fragment length polymorphism analysis [Mencin et al., 2014], quantification of selected ssDNA by fluorescence or by Real-Time PCR measurements [Mencin et al., 2014], determination of pool dissociation constants (K_{Ds}) [Mencin et al., 2014] and melting curve analysis [Luo et al., 2017; Mencin et al., 2014; Vanbrabant et al., 2014].

As Luo and co-workers reported, an important aspect of the SELEX process is to determine when to stop the selection. The gold standard for monitoring the enrichment during SELEX is the affinity assay. Though, this method suffers from limitations especially when non-specific oligonucleotides are still present, putting aside the fact that probing the aptamer pool after each round can be time consuming [Luo et al., 2017].

The strategy that Luo and colleagues adopts to monitor the selection progress is the evaluation of the decreasing of the aptamer diversity by the progression of the selection. An actual aptamer class selection from the library is expected to be associated with a peak fluorescence shift from lower to higher melting temperatures, implying that convergence of aptamer species is occurring [Luo et al., 2017]. Mencin and Vanbrabant described the diversity as the number of different full-length sequences in a PCR product: the starting diversity of the random oligonucleotide library decreases as the selection progresses and more similar sequences start to appear [Mencin et al., 2014; Vanbrabant et al., 2014].

Before to proceed to the next SELEX round, ssDNA is generated from dsDNA. Some common methods exploited to create ssDNA are asymmetric PCR amplification [Marimuthu et al., 2012; Svobodová et al., 2012], λ-exonuclease digestion [Civit et al., 2012; Svobodová et al., 2012] and bead-based separation [Civit et al., 2012; Sefah et al., 2010].

Asymmetric-PCR requires the optimization of the number of amplification cycles and the primer ratio to increase the ssDNA synthesis, avoiding unspecific and smeared DNA bands [Marimuthu et al., 2012]. However, asymmetric PCR amplification produces both ssDNA and dsDNA, therefore λ-exonuclease digestion has to be performed on the PCR product to completely digest the unwanted strand [Svobodová et al., 2012]. When using λ-exonuclease, a primer phosphorylated, at 5′ the position is required for the digestion of the undesired DNA strand [Civit et al., 2012; Svobodová et al., 2012].

Bead-based separation consists of using a biotin-labelled primer to immobilise the PCR product onto streptavidin-coated beads. The desired DNA strand is washed away by alkaline treatment and eluted while the undesired DNA strand remains attached on the beads [Civit et al., 2012; Sefah et al., 2010]. Once that ssDNA synthesis has been accomplished, the next SELEX round can be started.

After every SELEX round, the aptamer diversity should decrease, and larger fraction of target-binding aptamers is selected. When SELEX ends, the recovered selected library is sequenced, most often after previous cloning. Aptamer candidates are analysed to assess their complexity and to find shared domains, the latter being usually responsible for the target binding capacity. Aptamer binding activity of individual clones can be confirmed by different methods to validate their affinity and specificity for the target [Jayasena 1999; Luzi et al., 2003; Mairal et al., 2008; Ozer et al., 2014; Stoltenburg et al., 2007].

2.2.2 Cell-SELEX and Cell-internalization SELEX

Cell-SELEX is a rather novel type of SELEX which uses whole living cells as target of interest (Figure 6). Cell-SELEX strategy is particularly interesting because aptamers can be selected against surface molecules in their native states and, furthermore, a prior knowledge of targets is not required [Bayat et al., 2018; Chen et al., 2016; Gopinath et al., 2016; Guo et al., 2008; Ozer et al., 2014; Ye et al., 2012; Yüce et al., 2015; Zhang et al., 2019].

Due by the myriad of potential targets present on the cell surface, the principle of Cell-SELEX is that aptamers are selected on positive cells which expose the target on interest. Therefore, an efficient aptamer selection is only possible if negative cells, which do not present the target, are used to remove all off-target oligonucleotides [Bayat et al., 2018; Chen et al., 2016; Gopinath et al., 2016; Guo et al., 2008; Ohuchi, 2012; Ozer et al., 2014; Sefah et al., 2010; Song et al., 2012; Ye et al., 2012]. Cell-SELEX is commonly used to target cancer cells [Chen et al., 2016; Mercier et al., 2017;

Ohuchi, 2012; Ye et al., 2012; Zhang et al., 2019] which, in the selection process, represent the positive cells, instead the corresponding healthy cells represent the negative cells.

Cell condition is also important in Cell-SELEX because dead cells will lead to the selection of non-specific oligonucleotides which contaminate the specific aptamer pool [Bayat et al., 2018; Chen et al., 2016; Gopinath et al., 2016; Ohuchi, 2012; Ozer et al., 2014; Sefah et al., 2010].

Cell-internalization SELEX is a variant of Cell-SELEX and is performed to select aptamers which internalize into the cell cytoplasm upon binding of their cognate target (Figure 6). Cell-internalizing aptamers were successfully selected against cancer cells to specifically deliver therapeutic agents such as drugs or other nucleic acids [Gopinath et al., 2016; Ohuchi, 2012; Thiel et al., 2012; Xiao et al., 2012].

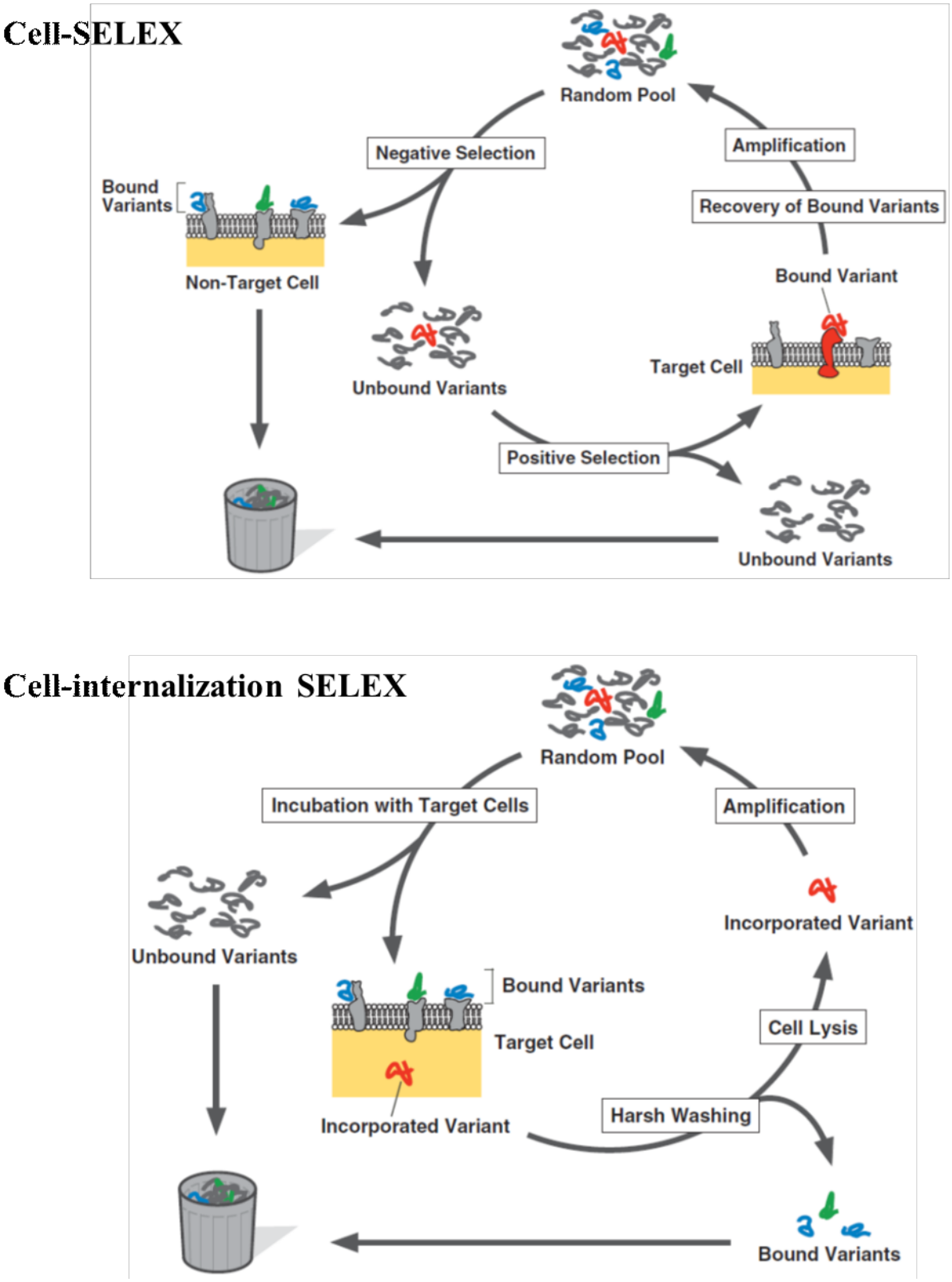

Figure 6. Schematic representation of Cell-SELEX and Cell-internalization SELEX. Both use whole cells as target but with Cell-SELEX (top) selected aptamers are those ones which specifically bound the membrane surface receptors, instead with Cell-internalization SELEX (bottom) selected aptamers are those ones which, after the binding with the cognate target, internalize into the cell cytoplasm [modified from Ohuchi, 2012].

2.3 Aptamers and small RNAs in plant defence response

Nowadays, the research work concerning Cell-SELEX and Cell-internalization SELEX focuses on human therapeutics and diagnostic fields. Due to the relative novelty of the interest in developing aptamers for applications in the plant field, Cell-SELEX and Cell-internalization SELEX have never been applied to plant cells (to our knowledge).

Nevertheless, as stated above, therapeutic aptamers may find relevant applications in the plant field, helping plants in facing biotic and abiotic stresses, which may seriously impair their productivity.

So far, therapeutic oligonucleotides in plants are based on small non-coding RNA molecules, including miRNA and siRNA, which trigger the host RNA interference machinery to regulate the expression of genes in a sequence-specific manner by ultimately cleaving or inhibiting translation of the target mRNA [Islam et al., 2018]. Various groups of plant small RNAs play vital roles in plant defence against pathogens. Small RNAs are involved in plant defence processes via different pathways include both siRNA and miRNA that actively regulate immunity in response to pathogenic attack via tackling PAMPs (Pathogen Associated Molecular Patterns) important for the PTI (PAMPs Triggered Immunity) and effectors relevant for the ETI (Effector Triggered Immunity) [Islam et al., 2018].

AtlsiRNA-1 belongs to a rather new class of endogenous small RNAs in *Arabidopsis thaliana*, which is called long siRNAs (lsiRNAs), and their lengths range from 30 to 40 nucleotides [Katiyar-Agarwal et al., 2007]. Katiyar-Agarwal and colleagues showed that one of these lsiRNAs, namely AtlsiRNA-1, was strongly induced in Arabidopsis plants infected with *Pseudomonas syringae* pv. *tomato* carrying the effector a*vrRpt2*. They found that this small RNA was complementary to the 3′ untranslated region of the antisense gene *AtRAP*, and promoted the *AtRAP* mRNA decapping and its 5′ to 3′ degradation [Katiyar-Agarwal et al., 2007]. AtlsiRNA-1 may be responsible to confer resistance against *Pseudomonas syringae* pv. *tomato* (*avrRpt2*) thanks to the downregulation of a negative regulator of the basal plant defence responses [Katiyar-Agarwal et al., 2007].

Furthermore, small non-coding RNAs triggering the RNA interference machinery could also be exogenously applied to protect plants from pests. In this view, RNAi-based bioproducts could represent an innovative and environmentally sustainable approach to crop protection. Since they are natural biological molecules they are degraded in nature and biological systems [Mezzetti et al., 2020]. There are many reports of genetically modified plants which express dsRNAs to protect them from pests, but the commercialization of transgenic crops producing pest-specific dsRNAs still has

many restrictions and hence, the transformation of many crop species is not applicable [Fletcher et al., 2020; Zotti et al., 2018].

A more recent innovation is the use of topical applications of dsRNA by foliar spray or root drenching to induce gene silencing as a new strategy for plant protection [Fletcher et al., 2020; Mezzetti et al., 2020; Zotti et al., 2018]. A clear example of efficient foliar spray of dsRNAs was applied by Mitter and colleagues, which explored the use of dsRNA complexed with layered double hydroxide nanosheets, also termed BioClay, which conferred 20 or more days of plant protection from viral infections [Mitter et al., 2017].

As consequence, lots of work concerning the production of dsRNA and its formulation to improve the efficacy, stability and persistence is required. The potential hazards posed by RNAi-based pesticides can be categorized as off-target gene silencing, silencing genes in non-target species, saturation of RNAi machinery and immune stimulation [Zotti et al., 2018].

Moreover, the efficient delivery of small therapeutic RNAs into target cells is still a challenge in the development of small RNA-based therapeutics [Sivakumar et al., 2019; Thiel and Giangrande, 2010]. One major drawback is that being oligonucleotides, they are polyanionic molecules and cannot penetrate cells because of poor transit across lipid bilayers [Kruspe and Giangrande, 2017; McNamara et al., 2006]. As stated above, another critical aspect regarding small therapeutic RNAs concerns the specificity. Small therapeutic RNAs must target particular cell types limiting side effects resulting from nonspecific delivery [McNamara et al., 2006]. Cell-specificity can be enhanced by conjugation of specific oligonucleotides, such as aptamers, that enable active binding to a cell-surface protein and internalization on the target cell.

In this view, aptamer and small therapeutic RNAs could be integrated to form chimeras which represent interesting molecular tools to efficiently deliver therapeutic oligonucleotides and stimulate the RNA interference machinery at cell-specific level [Kruspe and Giangrande, 2017; McNamara et al., 2006; Thiel and Giangrande, 2010] (Figure 7).

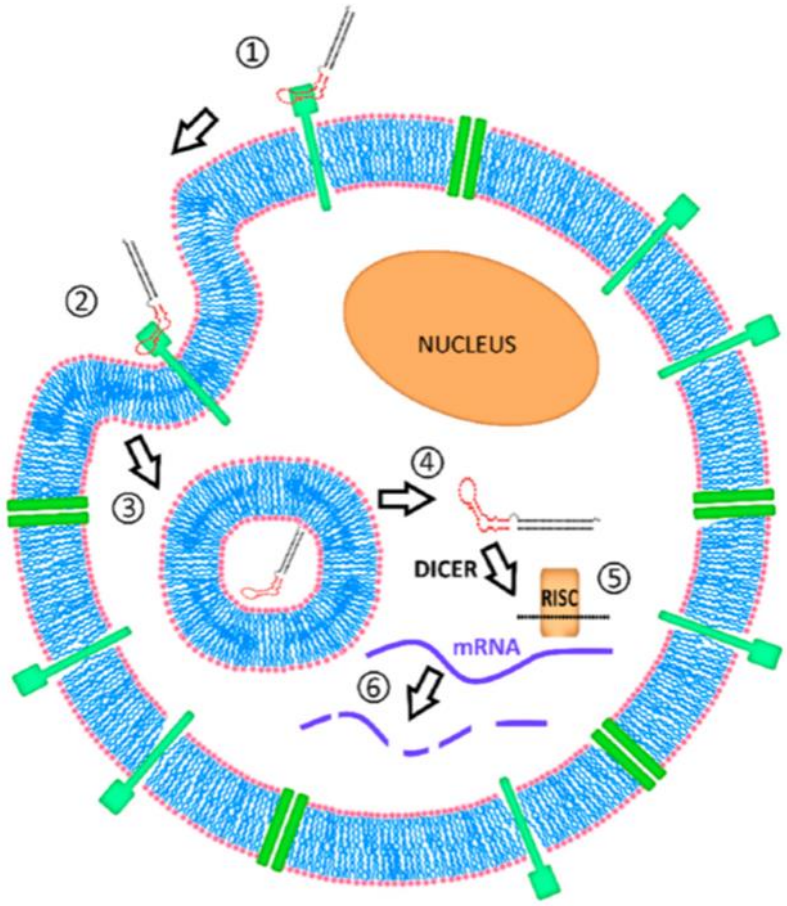

Figure 7. Schematic representation of an aptamer-small therapeutic RNA chimera delivery into a target cell. The chimera is constituted by an aptamer (red) and a small therapeutic RNA (black) which specifically binds (1) to a cell-surface protein (green). After the molecular recognition, the chimera is internalized by endocytosis (2-3) and released into the cell cytoplasm to stimulate the RNA interference machinery. The ribonuclease Dicer (4) binds the small therapeutic RNA part, cuts off the aptamer and loads (5) the RNA guide-strand into the RNA-induced silencing complex (RISC) which degrades the mRNA target (6) [modified from Kruspe and Giangrande, 2017].

In the following research work, for the first time we applied the Cell-SELEX and the Cell-internalization SELEX strategies on cells of *Arabidopsis thaliana* in order to select for aptamers which specifically internalize into plant cells and provide a molecular delivery tool that could be applied in plant biotechnology.

The main goal of the work was to design and select a switchable synthetic biosensor which in presence of a specific plant pathogen biomarker, namely the flagellin of *Pseudomonas syringae* pv. *tomato* DC3000, exhibits both an aptamer to specifically internalize into plant cells and a peculiar small RNA, namely AtlsiRNA-1, to readily *in vivo* stimulate the *Arabidopsis thaliana* defence mechanism in a pathogen-specific manner.

2.4 *Pseudomonas syringae* pv. *tomato*

Pseudomonas syringae is a rod-shaped, Gram-negative bacterium with polar flagella. As a plant-pathogen it can infect a wide variety of plants and causes necrotic symptoms in leaves, stems and fruits [Rico and Preston, 2008].

Pseudomonas syringae enters the host tissues by exploiting natural openings such as stomata or via mechanical wounds [Katagiri et al., 2002; Rico and Preston, 2008].

Pseudomonas syringae is a hemi-biotrophic pathogen, this indicates that at early infection stage it adsorbs the nutrients from the host cells without killing them [Nomura et al., 2005; Rico and Preston, 2008]. While at late stages of pathogenesis *Pseudomonas syringae* multiplies to high population levels which provoke massive host cell death [Nomura et al., 2005].

Molecular analyses of the *Pseudomonas syringae* pathogenicity reveal that its virulence depends on the coordinated expression of the hypersensitive reaction and pathogenicity (hrp) genes, which encode the type III protein secretion system (TTSS) [Buell et al., 2003; Jin et al., 2003; Nomura et al., 2005; Preston, 2000; Rico and Preston, 2008]. The secretion of avirulence- and effector-proteins by the TTSS is necessary to trigger the host disease, since they induce the release of nutrients and water and they suppress the plant defence response [Jin et al., 2003; Preston, 2000].

Pseudomonas syringae pv. *tomato* DC3000 is a model strain for investigating plant-microbe interactions due to its genetic tractability and pathogenicity on tomato, *Arabidopsis* and *Brassica* spp. [Uppalapati et al., 2008; Whalen et al., 1991].

Plant-pathogen interactions, especially those ones concerning biotrophs, are ruled by the plant resistance genes (*R*) which specifically recognize the pathogen avirulence (*avr*) genes. When corresponding *R* and *avr* genes, or their protein versions, like resistance proteins and effectors respectively, are present in both host and pathogen, the result is disease resistance [Dangl and Jones, 2001]. If *R* genes are inactive or absent, disease results.

In the proposed research work, the adopted strategy to stimulate the plant immune system was based on a highly shared molecule among pathogens, as the flagellin, in order to readily and efficiently stimulate the defense response.

3. PROJECT PLAN

In this work, my goal was to select two specific DNA aptamers, one which targets the plant cell and one which targets a plant pathogen biomarker, such as the flagellin from *Pseudomonas syringae* pv. *tomato* DC3000. These two aptamers would then be combined *in silico* to originate a switchable synthetic biosensor, which, when properly activated by the pathogen, would be able to stimulate the defence response through the cell-internalization of AtlsiRNA-1, which is known to be involved in the plant defence mechanism [Katiyar-Agarwal et al., 2007].

The switchable synthetic biosensor is being built so that the plant cell-internalization of AtlsiRNA-1 occurs only upon previous binding of the flagellin specific aptamer to its target. Once that the flagellin is specifically recognized, the structure of the chimeric changes so that the aptamer which specifically internalized into plant cells becomes able to interact with the cell surface and, as consequence, the internalization of AtlsiRNA-1 is accomplished (Figure 8).

During the selection of aptamers which internalize the plant cells, I also focused on potential aptamers which specifically bind the membrane cells.

A Cell-SELEX based approach was adopted to select for specific DNA aptamers targeting the cell surface receptors and/or internalize into the cell cytoplasm.

The SELEX strategy was also adopted to select DNA aptamers which were highly specific for pathogen biomarkers. Aptamers were selected against the flagellin of *Pseudomonas syringae* pv. *tomato* DC3000 and the best putative candidates were integrated *in silico* into the synthetic biosensor for the plant defence activation.

With a similar goal, cubane-modified DNA aptamers or cubamers were selected to specifically bind *Plasmodium falciparum* lactate dehydrogenase (*Pf*LDH), the most virulent agent of malaria. An efficient diagnostic tool should be able to specifically distinguish the same molecular biomarker among the different *Plasmodium spp.*, but canonical DNA aptamers were not so sensitive to reach this goal [Cheung et al., 2020]. Moreover, cubamers were also introduced since a cubamer highly specific for *Plasmodium vivax* LDH (*Pv*LDH) was recently isolated [Cheung et al., 2020].

SELEX in presence of cubane and against *Pf*LDH was used to learn how to menage chemically-modifications on aptamers, in the future perspective of selecting specific cubamers against the flagellin from *Pseudomonas syringae* pv. *tomato* DC3000.

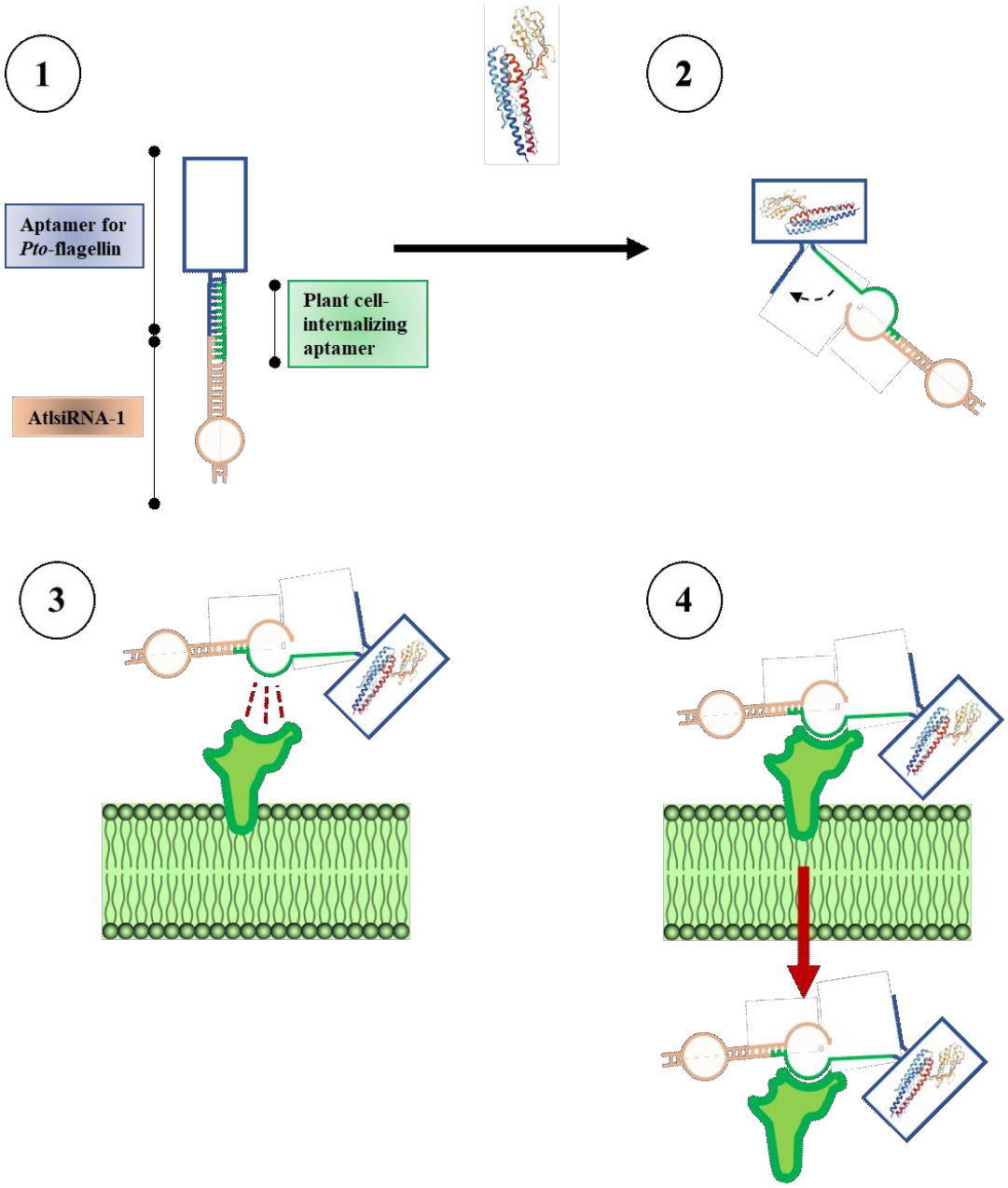

Figure 8. Schematic representation about the functioning of the switchable synthetic biosensor. (1-2) The specific recognition of the *Pto*-flagellin by its specific aptamer, here the blue portion, destabilizes the molecule and (3-4) the plant cell-internalizing aptamer, here the green portion, becomes able to interact with the cell surface and, as consequence, the internalization of AtlsiRNA-1, here the pink portion, is accomplished.

4. MATERIAL and METHODS

4.1 Protoplast isolation from *Arabidopsis thaliana* mesophyll

4.1.1 Plant growth conditions

Arabidopsis thaliana plants (Columbia-0 ecotype) were grown in an environment-controlled growth chamber. Plants were grown with a short photoperiod (10 hours light at 23 °C / 14 hours dark at 20 °C), low intensity light (50 - 75 µmol/m^2s = 1650 - 2475 lux) and 40 - 65 % relative humidity [Yoo et al., 2007]. Healthy young leaves of *A. thaliana* plants of 6- / 8- weeks-old before flowering were used.

4.1.2 Buffers and solutions

Stock solutions for protoplast extraction and Cell-SELEX experiments:

- 1 M $CaCl_2$ (Prolabo, Paris, France).
- 2 M KCl (Merck, Darmstadt, Germany).
- 0.8 M D-Mannitol (Carlo Erba AnalytiCals, Milan, Italy).
- 10 % (w/v) BSA (Bovine Serum Albumin, Sigma Aldrich, Steinheim, Germany).
- 1 M $MgCl_2$ (Sigma Aldrich).
- MES monohydrate 0.2 M pH 5.7 (4-Morpholineethanesulfonic acid, Fluka Biochemika, Buchs, Switzerland).
- W5 buffer: 2 mM MES pH 5.7, 154 mM NaCl (Sigma Aldrich), 125 mM $CaCl_2$ and 5 mM KCl; to sustain protoplasts during and after extraction [Yoo et al., 2007].
- Enzyme solution: 1.5 % (w/v) Cellulase Onozuka R-10 (Duchefa Biochemie, Harlem, Netherlands), 0.4 % (w/v) Macerozyme Onozuka R-10 (Duchefa Biochemie), 20 mM MES pH 5.7, 0.4 M D-Mannitol, 20 mM KCl, 10 mM $CaCl_2$ and 0.1 % (v/v) BSA; to digest leaf strips and release protoplasts [Yoo et al., 2007].
- WI buffer: 4 mM MES pH 5.7, 0.5 M D-Mannitol and 20 mM KCl; to sustain and to perform the viability assay on protoplasts [Lionetti et al., 2015] and in Cell-SELEX washing procedures.

4.1.3 Protoplast isolation

Protoplast isolation was performed according to Yoo et al. [2007] and Lionetti et al. [2015].

The Enzyme solution (10 ml of 20 mM MES pH 5.7, 0.4 M D-Mannitol and 20 mM KCl) was heated at 70 °C for 3 minutes then cooled to approximatively 35 °C on ice. 1.5 % (w/v) Cellulase Onozuka R-10 and 0.4 % (w/v) Macerozyme Onozuka R-10 were added. The pH was adjusted to 5.7 then the solution was heated to 55 °C for 10 minutes to completely dissolve the enzymes. The solution was snap-cooled on ice to reach room temperature, then 10 mM $CaCl_2$ and 0.1 % (v/v) BSA were added from the previously prepared stock solutions. Finally, the solution was filtered with a 0.45 µm syringe filter (EuroClone, Milan, Italy) and a 10 ml needleless syringe.

Twenty healthy leaves for 10 ml of Enzyme solution were collected from *A. thaliana* plants of 4- / 6- weeks-old. The leaves gross weight was calculated immediately after washing the leaves from the soil. Middle parts of the leaves were cut into tiny strips discarding the apex and the base. These strips were weighed, and the gross weight was subtracted to the strip weight yielding the net or fresh weight. This net weight was used to calculate the protoplasts on leaf grams ratio.

Leaves were cut to make strips of 0.5 - 1 mm of the middle part of the leaves avoiding wounding. Leaf strips were transferred in the Enzyme solution being careful to completely soak the strip and to separate strips whenever they touched each other.

Before digestion, a gentle vacuum infiltration was applied for 30 minutes. Digestion occurred at room temperature in the dark at least for 3 hours without shaking. The release of protoplasts in the solution was checked by the optical microscopy (ZEISS Axio Observer.Z1, Carl Zeiss, Milan, Italy).

After digestion, a nylon mesh of 90 µm was prepared as a filter and wetted with W5 buffer to filter the protoplasts from leaf debris. W5 buffer was added to the protoplasts at the same volume as the Enzyme solution and the mixture was slightly shaken.

The around 20 ml of the mixture were recovered and centrifuged at 200 g for 2 minutes at 4 °C to pellet the protoplasts. The supernatant was discarded. Protoplasts were gently resuspended in W5 buffer and counted with a Bürker chamber.

4.1.4 FDA viability assay

FDA (Fluorescein diacetate, Sigma Aldrich) is a cell-permeant esterase substrate that can serve as a viability probe that measures both enzymatic activity, which is required to activate its fluorescence, and cell-membrane integrity, which is required for intracellular retention of their fluorescent products.

The FDA viability assay was performed on released protoplasts according to Lionetti et al. [2015]. FDA working solution was prepared as a 1:100 dilution in WI buffer of the stock solution (5 mg/ml in acetone). To determine the viability of protoplasts, 50 000 - 100 000 cells were used and an equal volume of FDA working solution was added. Solution was incubated for 5 minutes at room temperature and it was visualized by fluorescence microscopy. The fluorescence images were taken with the GFP Filter Set 38 HE (excitation: 470/40 nm, emission: 525/50 nm). A second photograph was taken using the bright field setting.

4.2 Determination of PCR annealing temperature of LIB1.0 library

Random single stranded DNA (ssDNA) library and relative primers were purchased from Sigma Aldrich. LIB1.0 oligonucleotide library was 80 nucleotides long with sequence: 5′-AGCATAGAGACATCTGCTATTGGTAGCACA(N)$_{20}$TGTGCAACCGTAGACTCCAGACTTC AGGTA-3′ where N indicates an equimolar distribution of A, T, G and C nucleotides at each position into the random region. LIB1.0 library will be used for two Cell-SELEXs on *Arabidopsis thaliana* protoplasts and for the SELEX on the flagellin from *Pseudomonas syringae* pv. *tomato* DC3000. LIB1.0 library primers for PCR amplifications were:

- AMP1.0 forward 5′-AGCATAGAGACATCTGCTAT-3′
- AMP1.0 reverse 5′-TACCTGAAGTCTGGAGTCTA-3′

Several dilutions were carried out, as reported in Table 1.

Table 1. LIB1.0 library dilutions.

Solution	Quantity (per µl)	Molar concentration	Dilution
Dilution 4.1	20 pg	0.8 nM	1:125000
Dilution 4.2	4 pg	0.16 nM	1:625000
Dilution 4.3	0.8 pg	32 pM	1:3125000
Dilution 4.4	0.16 pg	6.4 pM	1:15625000
Dilution 4.5	32 fg	1.28 pM	1:78125000

PCR conditions were optimized using standard gradient PCR to determine the optimal annealing temperature. Gradient PCR was performed using Q5® High Fidelity DNA Polymerase (New England Biolabs, Ipswich, MA, U.S.) and a PCR thermal cycler (Bio-Rad, Milan, Italy). Q5® High Fidelity DNA Polymerase Buffer had already 2 mM Mg^{2+} which was within the acceptable concentration range as reported by Tolle and colleagues for a good PCR product yield [Tolle et al., 2014]. Temperature range was set between 52 °C - 60 °C and 52 °C, 54.1 °C, 56 °C, 58 °C and 60 °C were screened to determine the optimal annealing temperature. LIB1.0 library concentration was 2 473.49 ng/µl (100 µM) and it was diluted to 10 and 100 ng/µl in water for molecular biology (Sigma Aldrich).

The gradient standard PCR Master mix is reported in Table 2.

Table 2. Gradient standard PCR Master mix to determine the optimal annealing temperature for LIB1.0 library.

Master mix	**× 1 Reaction**
H_2O for molecular biology	15.5 µl
5× Buffer Q5®	5 µl
dNTPs 2.5 mM - 0.2 mM (Sigma Aldrich)	2 µl
AMP1.0 forward 20 µM - 0.5 µM	0.625 µl
AMP1.0 reverse 20 µM - 0.5 µM	0.625 µl
Q5® High Fidelity DNA Polymerase	0.25 µl
LIB1.0 10 - 100 ng	1 µl
Total volume	25 µl

The gradient standard PCR program is reported in Table 3.

Table 3. Gradient standard PCR program to determine the optimal annealing temperature for LIB1.0 library.

1. 98 °C (Initial denaturation)	0:30
2. 98 °C (Denaturation)	0:10
3. 52 °C ÷ 62 °C (Annealing)	0:15
4. 72 °C (Extension)	0:20
5. GO TO 2	34 cycles
6. 72 °C (Final extension)	5:00

4.2.1 Gel electrophoresis of gradient PCR

Gel electrophoresis of gradient standard PCR was performed using a common electrophoresis apparatus (PeqLab Biotechnologie, Erlangen, Germany; power supply from Bio-Rad). Agarose (CondaLab, Madrid, Spain) gel was prepared at 3 % in 1× TBE buffer (89 mM Tris base (Sigma Aldrich), 89 mM boric acid (Sigma Aldrich) and 2 mM EDTA pH 8 (Sigma Aldrich)) and run at 120 V for 80 minutes. Five µl of PCR product with 1 µl of 6× Blue Loading Dye were loaded into the gel. Afterwards, gel was stained with ethidium bromide 1 µg/ml (Sigma Aldrich) and it was visualized via UV-light with a Trans-UV apparatus (Doc-ItLS software). Marker used for the gel runs was ΦX174 DNA BsuRI (HaeIII) 0.5 µg/µl (Thermo Scientific, Milan, Italy).

4.3 Real Time PCR – HRM analysis of LIB1.0 library

A preliminary test was performed with Q5® High Fidelity DNA Polymerase (New England Biolabs) to check for the melting peaks of LIB1.0 library prior to selection by Real Time PCR amplification and HRM analysis. LIB1.0 library dilutions 4.1, 4.2 and 4.3 were tested (Table 1).

The Real Time PCR Master mix is reported in Table 4.

Table 4. Real Time PCR Master mix for monitoring LIB1.0 library prior to selection.

Master mix	**× 1 Reaction**
H_2O for molecular biology	14.25 µl
5× Buffer Q5®	5 µl
dNTPs 2.5 mM - 0.2 mM (Sigma Aldrich)	2 µl
AMP1.0 forward 20 µM - 0.5 µM	0.625 µl
AMP1.0 reverse 20 µM - 0.5 µM	0.625 µl
EvaGreen® 20× (Biotium, CA, U.S.)	1.25 µl
Q5® High Fidelity DNA Polymerase	0.25 µl
LIB1.0 library 4.1, 4.2 and 4.3 dilutions	1 µl
Total volume	25 µl

The Real Time PCR - HRM program is reported in Table 5.

Table 5. Real Time PCR - HRM program for monitoring LIB1.0 library prior to selection.

1. 98 °C (Initial denaturation)	0:30
2. 98 °C (Denaturation)	0:10
3. 56 °C (Annealing)	0:15
4. 72 °C (Extension)	0:20
5. GO TO 2	34 cycles
6. 95 °C (Denaturation)	1:00
7. 65 °C (Renaturation)	1:00
8. HRM analysis (65 °C ÷ 95 °C)	ΔT = 0:10 / 0.2 °C

4.4 Cell-SELEX I

Two Cell-SELEX experiments with LIB1.0 library were performed on plant protoplasts to select for potential aptamers that binding membrane cell and/or internalizing into cell cytoplasm.

4.4.1 Optimization of Cell-SELEX steps for plant cells

The first part of the work was dedicated to adjusting the buffers used to sustain the protoplasts [Yoo et al., 2007], to fulfil the Cell-SELEX requirements as washing and binding buffers. Cell-SELEX protocol was adapted from Sefah et al. [2010]. Buffers for Cell-SELEX, namely WI and MMg buffers, were prepared fresh for every new Cell-SELEX round.

- WI buffer (described above in 4.1.2)
- MMg buffer: 4 mM MES pH 5.7, 0.4 M D-Mannitol, 15 mM $MgCl_2$, 10 g/l BSA, 1 g/l DNA from herring sperm, (Sigma Aldrich), 1 g/l RNA from calf liver Type IV (Sigma Aldrich); as binding buffer for Cell-SELEX and blocking solution for unspecific sites on protoplasts.
- Protoplast Lysis buffer: WI buffer supplemented with 1 % (v/v) Triton X-100 (Sigma Aldrich); to lyse protoplasts before the DNA extraction procedure.

4.4.1.1 Optimization of blocking and washing steps

In order to evaluate the efficiency of both washing and blocking procedures, the number of washing steps was increased to seven, compared to Sefah's protocol [Sefah et al., 2010], and then all recovered washing fractions were quantified by Qubit® 2.0 Fluorometer dsDNA High Sensitivity Assay kit (Thermo Fisher, Milan, Italy). The washes were applied in duplicates: the first one was done with 100 µl (to detect the DNA concentration by fluorometer), the second one with 3 ml, according to Sefah et al. [2010].

4.4.1.2 Optimization of the elution temperature

The Cell-SELEX protocol was also designed to recover potential aptamers binding the protoplast membrane and/or internalizing into cell cytoplasm. Thus, the elution temperature was chosen as a compromise between the maximum elution efficiency and the need to preserve the integrity of cell membranes. Room temperature, 30 °C, 45 °C, 60 °C and 70 °C were used as elution temperatures, then the protoplast integrity was evaluated by optical microscopy.

4.4.1.3 Optimization of protoplast lysis

The protoplast lysis was also optimised, to ensure the recovering of potential aptamers that internalized into cell cytoplasm. Protoplasts were mixed with Protoplast Lysis buffer and observed by optical microscopy.

4.4.1.4 Checking the accuracy of the Cell-SELEX experiment

To guarantee that eluted and cell-extracted oligonucleotides contained the potential aptamers coming from LIB1.0 library, Cell-SELEX protocol was performed in presence of a negative control of the LIB1.0 library. One aliquot of protoplasts was incubated with LIB1.0 library and another one with a water sample and all Cell-SELEX steps were carried out in duplicates. In the end, Real Time PCR analysis was conducted for both eluted and cell-extracted oligonucleotides in presence of the LIB1.0 library and the negative control, the differences of the threshold cycles (ΔCt) were evaluated as $Ct_{water} - Ct_{LIB1.0}$.

The Real Time PCR Master mix is the same as reported above in 4.3 in Table 4. Real Time PCR - HRM program is the same as descripted above in 4.3 in Table 5.

4.4.2 Cell-SELEX protocol

Cell-SELEX was performed immediately after protoplast extraction from *A. thaliana* leaves because plant protoplasts tend to regrow their cell wall [Yokoyama et al., 2016].

One µl (100 pmol) of 100 µM LIB1.0 library was added to 350 µl of MMg buffer. The solution was mixed, heated at 95 °C for 5 minutes and snapped cool on ice until ready to use. For each Cell-SELEX round, 10^6 protoplasts were used as target.

Protoplasts were centrifuged at 200 g for 3 minutes at 4 °C and the supernatant was discarded. The pellet was resuspended in 3 ml of WI buffer by pipetting or mild vortexing. Cells were pelleted again at the same speed and duration. The washing step was repeated once more.

Cells were resuspended in 330 µl of MMg buffer and incubated for 30 minutes at room temperature to block unspecific sites on cell surface. Afterwards, all the 351 µl of snap-cooled on ice LIB1.0 library in MMg buffer were added to the 330 µl of cell-MMg suspension and incubated on a horizontal shaker for 1 hour at room temperature.

After incubation, cells were centrifuged at 200 g for 3 minutes at 4 °C. Supernatant containing unbound sequences was discarded. The pellet was resuspended in 3 ml of WI buffer, shaken for about 30 seconds and centrifuged again using the same conditions. The supernatant was removed carefully without touching the pelleted cells. The washing procedure was repeated two more times, collecting in the end the cell pellet.

The recovery of specifically bound sequences was performed by resuspending the pelleted cells in 500 µl of WI buffer and transferring the suspension in one 1.5 ml tube. The mixture was then heated at 45 °C for 10 minutes, centrifuged at 200 g for 5 minutes at room temperature and its supernatant was harvested.

To recover the internalized sequences into the protoplasts, a DNA extraction was performed according to Sambrook and Russell [2001].

The pelleted cell mixture was resuspended in 500 µl of Protoplast Lysis buffer and mixed thoroughly. One volume of 24:1 chloroform:isoamyl alcohol (Sigma Aldrich) was added and the mixture was vortexed thoroughly.

The mixture was centrifuged at 13,000 rpm for 15 minutes at 4 °C and the aqueous phase was recovered. Afterwards, 1/10 volume of 3 M NaOAc pH 5.2 (Sigma Aldrich) was added followed by 2 volumes of ethanol 95 % (Sigma Aldrich). $MgCl_2$ was also added to the solution with a final concentration of 10 mM to promote precipitation of short length- and small amount- DNA.

The solution was incubated at -20 °C for 1 hour and centrifuged at 13,000 rpm for 15 minutes at 4 °C. The supernatant was discarded, the tube was filled half-way with 70 % ethanol and the DNA pelleted was washed. The sample was centrifuged at 13,000 rpm for 15 minutes at 4 °C.

The supernatant was discarded, and the DNA pellet was vacuum dried and resuspended in 100 µl of TE buffer (10 mM Tris pH 8 (Sigma Aldrich) and 1 mM EDTA pH 8 (Sigma Aldrich)).

4.4.3 Real Time PCR - HRM analysis to check for the selection progress

After each Cell-SELEX round, Real Time PCR and HRM analysis were performed to monitor the enrichment of the selection pool [Luo et al., 2017; Mencin et al., 2014; Vanbrabant et al., 2014] of the eluted and cell-extracted DNA samples. An actual aptamer class selection from the library is expected to be associated with a peak fluorescence shift from lower to higher melting temperatures, implying that convergence of aptamer species is occurring [Luo et al., 2017].

The Real Time PCR Master mix for eluted and cell-extracted oligonucleotides is the same as reported above in 4.3 in Table 4. The Real Time PCR - HRM program is the same as descripted above in 4.3 in Table 5.

4.4.4 PCR of the entire selected pool after round 1

Standard PCR was performed on eluted and cell-extracted oligonucleotides after the first round of Cell-SELEX I according to Sefah et al. [2010].

Standard PCR was performed with GoTaq® Flexy G2 DNA Polymerase (Promega, Milan, Italy). The standard PCR Master mixes for eluted and cell-extracted oligonucleotides are reported in Table 6.

Table 6. Standard PCR Master mixes to amplify the entire first round selected pool, for both eluted and cell-extracted oligonucleotides.

Master mixes	**× 1 Reaction**
5× Buffer	20 µl
dNTPs 2.5 mM - 0.2 mM (Sigma Aldrich)	8 µl
H_2O for molecular biology	11.5 µl
AMP1.0 forward 20 µM - 0.4 µM	2 µl
AMP1.0 reverse 20 µM - 0.4 µM	2 µl
$MgCl_2$ 25 mM - 1.5 mM	6 µl
GoTaq® FLEXI G2 DNA Polymerase	0.5 µl
Eluted / Cell-extracted oligonucleotides	50 µl

Total volume	100 µl

The standard PCR program is reported in Table 7.

Table 7. Standard PCR program to amplify the entire first round selected pool, for both eluted and cell-extracted oligonucleotides.

1. 95 °C (Initial denaturation)	2:00
2. 95 °C (Denaturation)	0:30
3. 56 °C (Annealing)	0:30
4. 72 °C (Extension)	1:00
5. GO TO 2	8 cycles
6. 72 °C (Final extension)	5:00

4.4.5 PCR to determine the optimum number of amplification cycles

A standard PCR was performed on eluted and cell-extracted oligonucleotides previously amplified to determine the optimum number of amplification cycles before to proceed with the ssDNA generation.

Standard PCR was performed with GoTaq® Flexy G2 DNA Polymerase (Promega) and PCR products were check by gel electrophoresis as described above in 4.2.1. As DNA template, 10 % of the previously amplified pool volume was used for this PCR. Once that optimum number of amplification cycles had been determined, the PCR was performed in larger volumes (1 000 µl).

The standard PCR Master mixes for eluted and cell-extracted oligonucleotides are reported in Table 8.

Table 8. Standard PCR Master mixes to optimize the number of amplification cycles, for eluted and cell-extracted oligonucleotides.

Master mixes	**× 1 Reaction**
5× Buffer	5 µl
dNTPs 2.5 mM - 0.2 mM (Sigma Aldrich)	2 µl
H_2O for molecular biology	12.875 µl
AMP1.0 forward 20 µM - 0.4 µM	0.5 µl
AMP1.0 reverse 20 µM - 0.4 µM	0.5 µl
$MgCl_2$ 25 mM - 1.5 mM	1.5 µl

GoTaq® FLEXI G2 DNA Polymerase	0.125 µl
Eluted / Cell-extracted oligonucleotides	2.5 µl
Total volume	25 µl

The standard PCR program for eluted and cell-extracted oligonucleotides is the same as reported above in 4.4.4 in Table 7, with the only exception for the number of amplification cycles which was optimized to avoid PCR by-products.

4.4.6 Asymmetric-PCR and λ-exonuclease digestion for ssDNA generation

The generation of ssDNA was carried out by coupling the asymmetric-PCR technique to the subsequent digestion of the 5′-phosphate ssDNA with λ-exonuclease [Civit et al., 2012; Marimuthu et al., 2012; Svobodová et al., 2012].

Asymmetric-PCR was performed on both eluted and cell-extracted oligonucleotides with GoTaq® Flexy G2 DNA Polymerase (Promega). The asymmetric-PCR required the optimization of the number of amplification cycles and the primer ratio to increase the ssDNA synthesis, avoiding unspecific and smeared DNA bands [Marimuthu et al., 2012].

The asymmetric-PCR was performed with a phosphorylated, at 5′ position, AMP1.0 reverse primer (5′-[Phos]TACCTGAAGTCTGGAGTCTA-3′) synthesized by Sigma Aldrich, which was required for subsequent λ-exonuclease digestion.

The asymmetric-PCR Master mixes for eluted and cell-extracted oligonucleotides are reported in Table 9.

Table 9. Asymmetric-PCR Master mixes with different primer ratios for eluted and cell-extracted oligonucleotides. *The forward primer to reverse primer concentration ratio ranged from 20, 30, 40 and 50 to 1.

Master mixes	**× 1 Reaction**
5× Buffer	5 µl
dNTPs 2.5 mM - 0.2 mM (Sigma Aldrich)	2 µl
H_2O for molecular biology	14.375 - X µl
AMP1.0 forward 20 µM - X* µM	X µl
[Phos]AMP1.0 reverse 1 µM - 0.04 µM	1 µl
$MgCl_2$ 25 mM - 1.5 mM	1.5 µl
GoTaq® FLEXI G2 DNA Polymerase	0.125 µl
Eluted / Cell-extracted oligonucleotides	1 µl

Total volume	25 µl

The asymmetric-PCR program for eluted and cell-extracted oligonucleotides is the same as reported above in 4.4.4 in Table 7, with the only exception for the number of amplification cycles which was optimized to avoid PCR by-products.

Asymmetric-PCR products were verified by gel electrophoresis as described above in 4.2.1, with GelRed® (Biotium) staining. DNA samples were recovered and quantified with Qubit® 2.0 Fluorometer dsDNA High Sensitivity Assay kit to calculate the lambda exonuclease enzyme volume necessary for the digestion.

DNA digestions were performed with λ-exonuclease (5 U/µl, New England Biolabs), starting from 100 µl of asymmetric-PCR product and adding 10× λ-exonuclease buffer and a variable volume of λ-exonuclease to reach the final ratio of 5 U per µg estimated of dsDNA, to digest both eluted and cell-extracted oligonucleotides. Digestions were performed for 1 hour at 37 °C. λ-exonuclease digestions were verified by gel electrophoresis as described above in 4.2.1, with GelRed® staining. The obtained ssDNAs were quantified by loading and comparing on the same gel with 1 µl of 10 ng/µl, 25 ng/µl, 50 ng/µl and 100 ng/µl of LIB1.0 library.

4.4.7 Round 2 and subsequent rounds up to round 5

After ssDNA quantification, the recovered sequences were diluted to 200 nM in MMg buffer. Each following round of Cell-SELEX I was carried out according to the procedure hereafter described. For each selection round, the same procedure was applied using 10^6 protoplasts.

Real Time PCR - HRM analysis was performed on eluted and cell-extracted oligonucleotides to monitor the progression of the selection.

Standard PCR was performed to determine the optimum number of amplification cycles to maximize the yield of recovered sequences for the subsequent asymmetric-PCR.

The number of amplification cycles and the primer ratio of asymmetric-PCR were carefully optimized to increase ssDNA yield for the following λ-exonuclease digestion. The resulting ssDNA both eluted and cell-extracted oligonucleotides were used for round 3. The following rounds of selection were repeated as the first one.

4.4.8 Cloning and sequencing

Selected sequences from cell-extracted oligonucleotides of Cell-SELEX I round 2 were cloned in JM109 High Efficiency Competent Cells of *Escherichia coli* (Promega) using pGEM®-T Easy Vector System (Promega), as described by the protocol provided by Promega.

A quantity of 3.3 ng of the cell-extracted oligonucleotides (1:2.5 molar ratio between plasmid vector and insert) was used for the ligation reaction. The ligation mix was then incubated at 16 °C for 15 – 16 hours.

Two µl of ligation reaction were added to a 15 ml tube together with 50 µl of JM109 cells. The mixture was gently flicked and placed on ice for 20 minutes, heated shocked at 42 °C for 45 seconds and put back on ice for 2 minutes. Four-hundred-and-fifty µl of S.O.C. medium (Invitrogen Corporation, CA, U.S.) were added to the mixture, which was then incubated at 37 °C with shaking for 1.5 hours. One hundred µl of transformed cells and the transformation control were plated on Luria Bertani plates: 10 g/l tryptone, 10 g/l NaCl, 5 g/l yeast extract, pH 7 (Sigma Aldrich) and Bacto™ agar 15 g/l (Serlabo Technologies, France), supplemented with 100 µg/ml ampicillin (Sigma Aldrich), 0.5 mM IPTG (Isopropyl β-D-1-thiogalactopyranoside, Promega) and 80 µg/ml X-gal (5-Bromo-4-chloro-3-indolyl β-D-galactopyranoside, Promega). To determine the transformation efficiency, pUC19 plasmid vector (Promega) was used.

After 16 – 24 hours of incubation at 37 °C, white bacteria colonies were plated in LB replica plates supplemented with 100 µg/ml ampicillin. Colony-PCR with GoTaq® Flexy G2 DNA Polymerase (Promega) was performed on boiled white-bacteria using AMP1.0 primers. PCR products were verified by gel electrophoresis as described above in 4.2.1.

The Colony-PCR Master mix is the same as reported above in 4.4.5 in Table 8, with the only exception of 1 µl of DNA template. The Colony-PCR program is the same as reported above in 4.4.4 in Table 7, with the only exception of 30 amplification cycles.

After colony-PCR, 8 positive clones to the library amplification were inoculated on 5 ml of LB liquid cultures (10 g/l tryptone, 10 g/l NaCl, 5 g/l yeast extract, pH 7) supplemented with 100 µg/ml ampicillin and incubated at 37 °C with shaking for 15 – 16 hours. Plasmid DNAs were then isolated from the overnight bacterial liquid cultures by Wizard® *Plus* SV Minipreps DNA Purification System kit (Promega) and quantified by measuring UV absorbance at 260 nm.

Potential aptamers were sequenced at Genechron s.r.l. using the Sanger method and the random regions of the sequenced potential aptamers were aligned using Clustal Omega leaving the default program parameters.

4.5 Cell-SELEX II

The Cell-SELEX II experiment was conducted similarly to Cell-SELEX I (described above in 4.4), except for the methodology used to regenerate the ssDNA. In this second experiment according to Sefah et al. [2010], Streptavidin-Sepharose Beads (BioVision, CA, U.S.) were introduced to reach this goal.

Moreover, for rounds 7 and 8, for the elution step WI buffer was supplemented with NaCl and acetic acid [Hernandez et al., 2013].

4.5.1 PCR of the entire selected pool after round 1

Standard PCR was performed on eluted and cell-extracted oligonucleotides after the first round of Cell-SELEX according to Sefah et al. [2010] as described above in 4.4.4. PCR amplification was performed with a biotinylated, at 5′ position, AMP1.0 reverse primer synthesized by Sigma Aldrich which was required for the subsequent DNA attachment to the Streptavidin-Sepharose Beads (AMP1.0 reverse primer sequence with biotin at 5′ position was: 5′-[Btn]TACCTGAAGTCTGGAGTCTA-3′).

The standard PCR Master mixes for eluted and cell-extracted oligonucleotides are the same as reported above in 4.4.4 in Table 6, with the only exception of the [Btn]AMP1.0 reverse primer. The standard PCR program is the same as described above in 4.4.4 in Table 7.

4.5.2 PCR to determine the optimum number of amplification cycles

Standard PCR was performed on eluted and cell-extracted oligonucleotides previously amplified to determine the optimum number of amplification cycles for both samples as described above for the experiment I in 4.4.5. PCR amplification was performed with a biotinylated, at 5′ position, AMP1.0 reverse primer. Once the optimum number of amplification cycles had been determined, the PCR was performed in larger volumes (1 000 µl).

The standard PCR Master mixes for eluted and cell-extracted oligonucleotides are the same as reported above in 4.4.5 in Table 8, with the only exception of the [Btn]AMP1.0 reverse primer. The standard PCR program is the same as described above in 4.4.4 in Table 7, with the only exception of the number of amplification cycles which was optimized to avoid PCR by-products.

4.5.3 Preparation of ssDNA from PCR product

ssDNA synthesis was performed according to Sefah et al. [2010] with modifications for both eluted and cell-extracted oligonucleotides.

A filter (Glen Research, VA, U.S.) was inserted at one end of an empty DNA synthesis column (Glen Research). Then the plunger was removed from a needleless 10 ml syringe and the empty syringe was inserted at the other end of the column. Two hundred µl of Streptavidin-Sepharose Beads were added to the column, the plunger was inserted and the storage buffer was drained.

Beads were washed with 2.5 ml of WI buffer, afterwards the PCR product was being slowly passed three times through the column. A second wash was applied with 2.5 ml of WI buffer. At this point 0.5 ml of 0.2 M NaOH (Sigma Aldrich) were added to the column, to break hydrogen bonds between the DNA strands, and the eluate was collected.

Eluted ssDNA was desalted by using NAP-5 column (GE Healthcare, Buckinghamshire, U.K.) and eluted in 1 ml of water for molecular biology.

Eluted ssDNA in water was vacuum dried and then quantified by measuring UV absorbance at 260 nm.

4.5.4 Round 2 and subsequent rounds up to round 8

After the ssDNA quantitation, 40 pmol of eluted and cell-extracted oligonucleotides were resuspended in 200 µl of MMg buffer. For the selection, the same procedure was applied using 10^6 protoplasts.

Real Time PCR and HRM analysis were performed on eluted and cell-extracted oligonucleotides to monitor the progression of the selection.

Standard PCR was performed to determine the optimum number of amplification cycles and to prepare for the ssDNA synthesis. The ssDNA resulting from both eluted and cell-extracted oligonucleotides were used for round 3. The following rounds of selection were repeated as the first one up to round 6.

For rounds 7 and 8, only cell-extracted oligonucleotides were used. Before the elution step the protoplasts were resuspended in WI buffer supplemented with 0.5 M NaCl and 0.2 M acetic acid (pH 2.6) and then incubated at 4 °C for 5 minutes. After incubation, cells were centrifuged at 200 g for 5 minutes at 4 °C, then the pellet was treated to recover internalizing oligonucleotides as described above in 4.4.2.

4.5.5 Sequencing of putative aptamers and alignment of random regions

Selected sequences from cell-extracted oligonucleotides of Cell-SELEX II round 6 were sequenced by Nanopore technology (MinION Mk1B, MIN-101B, Oxford Nanopore Technologies, Oxford, U.K.). Putative aptamers were amplified by standard PCR, purified and 89.36 ng were used to generate the library necessary to start the sequencing procedure. It has been followed the sequencing protocol provided by the manufacturing company (GDE_9063_v109_revT_14Aug2019) with real time low accuracy data processing. At the end of the run, each sequence read obtained was submitted to BLASTN analysis using the PCR primers as the query sequences and a word size of 14. The fast5 files corresponding to the sequences that produced significant hits for both primers were selected and re-processed for high accuracy with the aid of the MinKNOW software. The resulting sequence set was processed with a custom PERL script to align the primer sequences and identify the random regions. The sequences of the random regions were subsequently extracted and processed with another custom PERL script which provides the enumeration of the k-mers taking into account all two-positions possible variants. Only octamers, including two-positions possible variants, which were shared by at least 29-30 random regions were considered into the analysis.

4.5.6 Assessment of aptamer internalization into plant cells *via* Real Time PCR assay

Before to proceed with the Real Time PCR assay, putative aptamer sequences were chemically synthesized by Thermo Scientific.

A negative control oligonucleotide represented by a poly A sequence as random region (5′-AGCATAGAGACATCTGCTATTGGTAGCACAAAAAAAAAAAAAAAAAAAATGTGCAACCGTAGACTCCAGACTTCAGGTA-3′) was also synthesized.

To perform the assay, it was followed the protocol adopted by Civit et al. [2017] with modifications.

One µl (10 pmol) of 10 µM of each putative aptamer and the negative control was added to 199 µl of MMg buffer and heated at 95 °C for 5 minutes and snapped cool on ice until ready to use. For each sequence, 10^6 protoplasts were used as target.

Protoplasts were centrifuged at 200 g for 3 minutes at 4 °C and the supernatant was discarded. The pellet was resuspended in 3 ml of WI buffer by pipetting or mild vortexing. Cells were pelleted at the same speed and duration. Washing step was repeated once more.

Cells were resuspended in 200 µl of MMg buffer and incubated for 30 minutes at room temperature to block unspecific sites on cell surface. Afterwards, all the 200 µl snap-cooled on ice putative aptamers were added to the 200 µl of cell-MMg suspension and incubated on a horizontal shaker for 1 hour at room temperature.

After incubation, cells were centrifuged at 200 g for 3 minutes at 4 °C. Supernatant containing unbound sequences was discarded. The pellet was resuspended in 3 ml of WI buffer, shaken for about 30 seconds and centrifuged again using the same conditions. The supernatant was removed carefully without touching the pelleted cells. Washing procedure is repeated two times more, collecting in the end the cell pellet.

The elution step was performed by resuspending the pelleted cells in 500 µl of WI buffer and transferring the suspension in one 1.5 ml tube. The mixture was then heated at 45 °C for 10 minutes, centrifuged at 200 g for 5 minutes at room temperature and its supernatant was harvested.

Pelleted cells were then resuspended in 1 ml of WI buffer and counted by Bürker chamber. After that, they were centrifuged at 200 g for 5 minutes at room temperature, resuspended in 200 µl of WI buffer and heated at 95 °C for 5 minutes.

Cell-lysates were diluted to around 1860 cells/µl and one µl was analysed *via* Real Time PCR with Q5® High Fidelity DNA Polymerase. DNA standards were included; 10^{-4} – 10^{-7} fmol in 1 to 10 dilutions. Each sample and standard were run in duplicates.

The Real Time PCR Master mix for putative aptamer internalization and DNA standards is the same as described above in 4.3 in Table 4, scaling down all reagent concentrations accordingly to 12 µl of reaction volume. The Real Time PCR program is the same as reported above in 4.3 in Table 5, with the only exceptions of 30 amplification cycles and the removal of the steps for HRM analysis.

4.6 Cloning, expression, purification and refolding of flagellin from *Pseudomonas syringae* pv. *tomato* DC3000 (*Pto*), *Pseudomonas syringae* pv. *tabaci* (*Pta*) and *Pseudomonas fluorescens-4* (*Pf4*)

4.6.1 Preparation of genomic DNA from bacteria

The following protocol was used to isolate genomic DNA (gDNA) from *Pseudomonas syringae* pv. *tomato* DC3000 (reference genome NCBI GenBank: AE016853.1) [Buell et al., 2003], *Pseudomonas syringae* pv. *tabaci* (reference genome *Pseudomonas amygdali* pv. *lachrymans*, NCBI GenBank: CP020351.1) and *Pseudomonas fluorescens-4* [Moruzzi et al., 2017] (reference genome assembly NCBI GenBank GCA_002891555.1) and was adapted from Wilson [1997].

One single colony was picked from the plate with the bacterial strain of interest and was used to inoculate 5 ml of LB liquid culture. Liquid cultures were grown at 28 °C with shaking until saturation.

When the cultures were ready, 1.5 ml were centrifuged for 5 minutes at 20 °C and at 10,000 rpm and the supernatants were discarded. Bacterial pellets were resuspended in 567.4 µl of TE buffer, and 2.6 µl of 23 mg/ml proteinase K (Sigma Aldrich) and 30 µl of 10 % (w/v) SDS (Sigma Aldrich) were added to give a final concentration of 100 µg/ml proteinase K in 0.5 % SDS. The mixtures were incubated for 1 hour at 37 °C, becoming clear and viscous as the detergent lysed the bacterial cell walls.

Afterwards, 100 µl of 5 M NaCl were added and mixed, then 80 µl of CTAB (Cetyltrimethylammonium Bromide, Sigma Aldrich) / NaCl solution (0.274 M CTAB, 0.701 M NaCl) were added and mixed well again. The solutions were incubated at 65 °C for 10 minutes.

Seven-hundred-and-fifty µl of 24:1 chloroform:isoamyl alcohol were added, solutions were mixed well and centrifuged for 5 minutes, at 20 °C at 8,000 rpm. The aqueous phases were recovered to fresh microcentrifuge tubes, leaving the interphases behind. Last two steps were repeated if necessary.

Isopropanol (Sigma Aldrich) in 0.6 volumes was added to precipitate the nucleic acids, the tubes were shaken back and forth until white DNA precipitates were become clearly visible. The tubes were centrifuged for 5 minutes at 4 °C at 14,000 rpm and the supernatants were discarded.

The DNA pellets were washed with 1 ml of ethanol 70 %, centrifuged for 3 minutes at 4 °C at 14,000 rpm and the supernatants were discarded. The DNA pellets were vacuum dried and

resuspended in 100 µl of TE buffer. Genomic DNAs were quantified by measuring UV absorbance at 260 nm.

4.6.2 16S rDNA identification

Analysis of rRNA sequences is used to study the phylogenesis and evolutionary relationships among the organisms [Weisburg et al., 1991]. The 16S rDNA gene is a powerful tool to characterize strains belonging to the *Pseudomonas* genus [Lu et al., 2017; Mulet et al., 2010; Yamamoto et al., 2000].

4.6.2.1 PCR amplification of 16S rDNA genes for sequencing

To proceed with the analysis of 16S rDNA sequences, a standard PCR was performed for all gDNAs with Q5® High Fidelity DNA Polymerase (New England Biolabs). Standard PCR was carried out on gDNAs previously extracted from *Pseudomonas* spp., with the universal primers fD1 (5′-AGAGTTTGATCCTGGCTCAG-3′) and rP1 (5′-ACGGTTACCTTGTTACGACTT-3′) [Weisburg et al., 1991].

All gDNAs were diluted to 2 ng/µl and 4 ng were used as template.

The standard PCR Master mix is reported in Table 10.

Table 10. Standard PCR Master mix for the amplification of 16S rDNA genes of *Pto*, *Pta* and *Pf4*.

Master mix	**× 1 Reaction**
5× Buffer Q5®	10 µl
dNTPs 2.5 mM - 0.2 mM (Sigma Aldrich)	4 µl
H_2O for molecular biology	31.5 µl
fD1 20 µM - 0.4 µM (Sigma Aldrich)	1 µl
rP1 20 µM - 0.4 µM (Sigma Aldrich)	1 µl
Q5® High Fidelity DNA Polymerase	0.5 µl
gDNA (4 ng)	2 µl
Total volume	50 µl

The standard PCR program is reported in Table 11.

Table 11. Standard PCR program for the amplification of 16S rDNA genes of *Pto*, *Pta* and *Pf4*.

1. 98 °C (Initial denaturation)	0:30
2. 98 °C (Denaturation)	0:10
3. 60 °C (Annealing)	0:15
4. 72 °C (Extension)	0:20
5. GO TO 2	39 cycles
6. 72 °C (Final extension)	2:00

PCR products were recovered and prepared for gel electrophoresis with agarose 1 % in 1× TAE buffer (40 mM Tris base, 0.114 % (v/v) acetic acid (Sigma Aldrich) and 1 mM EDTA pH 8), run at 100 V for 60 minutes. Five µl of PCR product were loaded in gel with 1 µl of 6× Loading dye. Marker was GeneRuler^{TM} 1 Kb DNA Ladder 0.5 µg/µl. Agarose gel was stained with ethidium bromide and observed by trans-UV.

After checking DNA bands, PCR products were purified by Wizard® SV Gel and PCR Clean-Up System kit (Promega) following producer's instructions. Purified PCR products were quantified by measuring UV absorbance at 260 nm and they were confirmed by gel electrophoresis. Purified PCR products were sequenced at BMR Genomics s.r.l. using the Sanger method.

BLASTN was performed between the sequenced PCR products and the 16S rDNA sequences provided by NCBI for *Pto* and *Pf4* and Pseudomonas Genome Database for *Pta*.

4.6.3 Flagellin gene amplification

The gene coding the flagellin was *fliC* for both *Pseudomonas syringae* pv. *tomato* DC3000 (NCBI Gene ID: 1183594; [Buell et al., 2003]) and *Pseudomonas syringae* pv. *tabaci* (NCBI GenBank: AB061230.2). The closest relative to *Pseudomonas fluorescens-4* was *Pseudomonas protegens* CHAO^{T} (AJ278812) [Moruzzi et al., 2017], and the gene coding the flagellin was *hag* (NCBI Gene ID: 15559583).

Flagellin gene amplifications by standard PCR were performed with F0 – R0, F1 – R1 and F2 – R2 primers. Each primer was designed thanks to Primer3 software, purchased from Sigma Aldrich and listed at Table 12. Specifically, F1 – R1 and F2 – R2 primer amplifications were used to prepare the amplified DNA fragments for cloning by including in the products the cleavage sites and the accessory sequences as reported in Figure 9.

Table 12. Primer list to amplify flagellin genes from *Pto*, *Pta* and *Pf4*.

Primer name	Sequence (5′ – 3′)	Strain
PsF0	ATGGCTTTAACAGTAAACAC	*Pto*, *Pta*
PsR0	AAGCAGTTTCAGTACAGC	*Pto*, *Pta*
PsF1	TTAAGAAGGAGATATACCATGGCTTTAACAGTAAACAC	*Pto*, *Pta*
PsR1	TGATGCTTGTAGCTGCCACGCGGAACCAAAAGCAGTTTCAGTACAGC	*Pto*, *Pta*
PsF2	CACAACGGTTTCCCTCTAGAAATAATTTTGTTTAACTTTAAGAAGGAGATAT	*Pto*, *Pta*
PsR2	CTTTGTTAGCAGCCGGATCCTCAGTGATGGTGATGATGATGCTTGTAGCTGCC	*Pto*, *Pta*
Pf4F0	ATGGCTTTAACAGTAAACACT	*Pf4*
Pf4R0	AAGCAGCTTCAGTACAGC	*Pf4*
Pf4F1	TTAAGAAGGAGATATACCATGGCTTTAACAGTAAACACT	*Pf4*
Pf4R1	TGATGCTTGTAACTGCCACGCGGAACCAAAAGCAGCTTCAGTACAGC	*Pf4*
Pf4F2	CACAACGGTTTCCCTCTAGAAATAATTTTGTTTAACTTTAAGAAGGAGATAT	*Pf4*
Pf4R2	CTTTGTTAGCAGCCGGATCCTCAGTGATGGTGATGATGATGCTTGTAACTGCC	*Pf4*

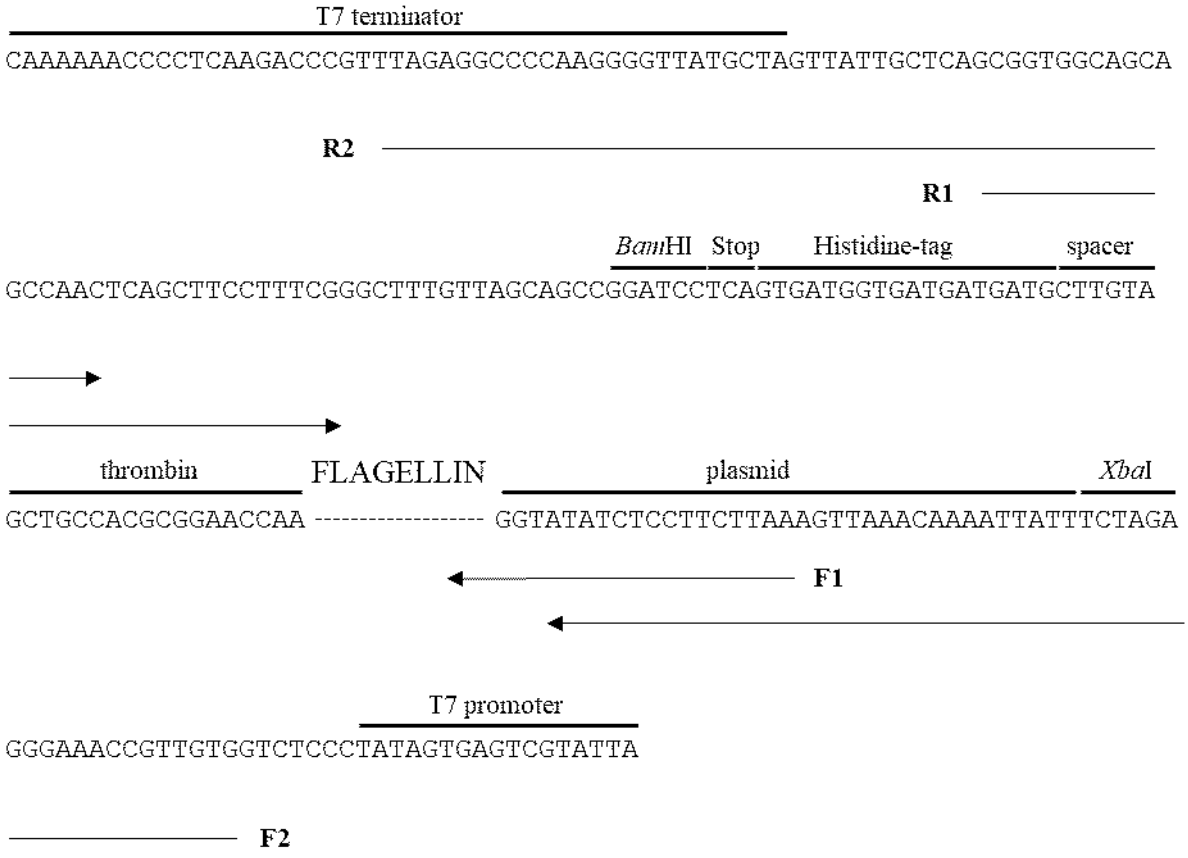

Figure 9. Schematic representation of the preparation of flagellin genes for the cloning with pET-14b plasmid vector, here represented from the T7 terminator to the T7 promoter sequences. Flagellin genes were amplified with F1 – R1 primers in order to incorporate a part of the sequence which regulated gene transcription and translation on pET-14b plasmid vector at the 5′ position, and the thrombin cleavage site, the spacer and a part of the Histidine-tag at the 3′ position. F2 – R2 amplifications were performed to incorporate the remaining part of the sequence which regulated gene transcription and translation on pET-14b plasmid vector and *Xba*I cleavage site at the 5′ position, and the remaining part of the Histidine-tag, the stop codon and *Bam*HI cleavage site at the 3′ position.

4.6.3.1 F0 - R0 primer amplification

Gradient PCR with F0 - R0 primers and GoTaq® Flexy G2 DNA Polymerase (Promega) on gDNAs of *Pto*, *Pta* and *Pf4* previously extracted, was performed to check for the optimum annealing temperature for flagellin gene amplifications.

The gradient PCR Master mixes for both PsF0 / PsR0 and Pf4F0 / Pf4R0 primers are reported in Table 13.

Table 13. Gradient PCR Master mixes for the amplification of flagellin genes.

Master mixes	**× 1 Reaction**
5× Buffer	5 µl
dNTPs 2.5 mM - 0.2 mM (Sigma Aldrich)	2 µl
H_2O for molecular biology	14.375 µl
(PsF0, Pf4F0) 20 µM - 0.4 µM	0.5 µl
(PsR0, Pf4R0) 20 µM - 0.4 µM	0.5 µl
$MgCl_2$ 25 mM - 1.5 mM	1.5 µl
GoTaq® FLEXI G2 DNA Polymerase	0.125 µl
gDNA (2 ng)	1 µl
Total volume	25 µl

The gradient PCR programs for both PsF0 / PsR0 and Pf4F0 / Pf4R0 primers are reported in Table 14.

Table 14. Gradient PCR programs for the amplification of flagellin genes.

1. 95 °C (Initial denaturation)	2:00
2. 95 °C (Denaturation)	1:00
3. 54 °C, 53 °C, 52 °C (Annealing)	0:30
4. 72 °C (Extension)	1:00
5. GO TO 2	29 cycles
6. 72 °C (Final extension)	5:00

PCR products were verified by gel electrophoresis as described above in 4.6.2.1.

4.6.3.2 F1 - R1 primer amplification

Standard PCR with F1 - R1 primers is performed as described above in 4.6.3.1 in Table 13, with the only exception of PsF1 / PsR1 and Pf4F1 / Pf4R1 primers. The standard PCR programs for both PsF1 / PsR1 and Pf4F1 / Pf4R1 primers are the same as reported above in 4.6.3.1 in Table 14, with the only exceptions of 10 amplification cycles and the usage of 54 °C as annealing temperature for Ps-primers and 52 °C for Pf4-primers.

Standard PCRs with F1 - R1 primers were also performed with 30 cycles as positive controls of DNA amplification. PCR products were verified by gel electrophoresis as described above in 4.6.2.1.

4.6.3.3 F2 - R2 primer amplification

Standard PCR with F2 - R2 primers was performed with Advantage® HD Polymerase (Takara Bio USA, CA, U.S.). Before to proceed with the amplification, the PCR products from the PCR with F1 - R1 primers were diluted 1:10 in water for molecular biology.

The standard PCR Master mixes for both PsF2 / PsR2 and Pf4F2 / Pf4R2 primers are reported in Table 15.

Table 15. Standard PCR Master mixes for the amplification of flagellin genes.

Master mixes	**× 1 Reaction**
5× Advantage® HD Buffer	10 µl
dNTPs 2.5 mM - 0.2 mM (Sigma Aldrich)	4 µl
H_2O for molecular biology	32 µl
(PsF2, Pf4F2) 20 µM - 0.3 µM	0.75 µl
(PsR2, Pf4R2) 20 µM - 0.3 µM	0.75 µl
Advantage® HD DNA Polymerase	0.5 µl
F1 - R1 PCR product 1:10 diluted	2 µl
Total volume	50 µl

The standard PCR programs for both PsF2 / PsR2 and Pf4F2 / Pf4R2 primers are reported in Table 16.

Table 16. Standard PCR programs for the amplification of flagellin genes.

1. 98 °C (Initial denaturation)	0:30
2. 98 °C (Denaturation)	0:10
3. 43 °C (Annealing)	0:15
4. 72 °C (Extension)	1:00
5. GO TO 2	29 cycles
6. 72 °C (Final extension)	2:00

PCR products were verified by gel electrophoresis, purified and quantified as described above in 4.6.2.1.

4.6.4 Cloning of flagellin genes into pET-14b plasmid vector and sequencing

4.6.4.1 Preparation of competent JM101, BL-21 *Escherichia Coli* cells

Competent cells were necessary to store (JM101) and express (BL-21) the ligation products between the flagellin genes and pET-14b plasmid vector. Competent cells were prepared following Chang et al. [2017] with modifications.

One single colony was picked from the plates with the bacterial strains of interest and used to inoculate 2 ml of LB liquid culture. The cultures were grown for 12 - 16 hours at 37 °C with shaking.

The overnight bacterial liquid cultures were diluted 1:100 in 50 ml of LB and grown at 37 °C with shaking until they reached 0.3 - 0.4 O.D. at 600 nm (OD_{600}).

Cells were chilled on ice for 1 hour then centrifuged at 4,000 rpm for 10 minutes at 4 °C. The supernatants were discarded, and the pellets were resuspended in ¼ volume of ice cold 0.1 M $CaCl_2$ and left them on ice for at least 1 hour.

Cells were centrifuged at 4,000 rpm for 10 minutes at 4 °C and the supernatants were discarded. The pellets were resuspended in ice cold 0.1 M $CaCl_2$ supplemented with 10 % (w/v) glycerol (Sigma Aldrich) at a final concentration of 15 OD_{600} units/ml. Competent cells were stored in 50 µl aliquots at -80 °C.

To check the cell competency, both strains were transformed with pUC19 control plasmid vector (0.1 ng/µl, Takara Bio USA). One competent cell aliquot for both strains was thawed on ice and 1 ng of pUC19 was added. The mixtures were incubated on ice for 30 minutes, then heat-shock

was applied at 42 °C for 30 seconds and put back on ice for 2 minutes. One ml of pre-warmed LB was added for both mixtures and they were grown at 37 °C with shaking for 1 hour. One to ten dilutions of the cultures were plated on warm selective screening LB plates supplemented with 100 µg/ml ampicillin. The plates were incubated at 37 °C for 12 - 16 hours and then inspected.

4.6.4.2 Digestion of pET-14b plasmid vector and flagellin genes with *Xba*I and *Bam*HI restriction enzymes, ligation and transformation of JM101 cells

One aliquot of 100 µl of MAX Efficiency® Stbl2™ competent cells (Invitrogen) was transformed with 2.5 ng of pET-14b plasmid vector following the producer's instructions. The grown colonies were used to inoculate 5 ml of LB liquid cultures supplemented with 100 µg/ml ampicillin. The overnight bacterial liquid cultures were used to isolate the plasmid DNA as described above in 4.4.8 and to generate glycerol-stocks of the bacteria. Purified plasmid DNAs were quantified by measuring UV absorbance at 260 nm.

The purified pET-14b plasmid vector is double-digested with *Xba*I (Thermo Scientific) and *Bam*HI (Thermo Scientific) restriction enzymes at 37 °C for 15 – 16 hours as reported by Table 17. Digestions were stopped by heating at 80 °C for 20 minutes.

Table 17. Digestion mix for purified pET-14b plasmid vector.

Digestion mix	**× 1 Reaction**
pET-14b plasmid vector (1 µg)	3.58 µl
10× Buffer *Bam*HI	5 µl
H_2O for molecular biology	38.42 µl
*Bam*HI 10 U/µl	1 µl
*Xba*I 10 U/µl	2 µl
Total volume	50 µl

All digested pET-14b mixtures were prepared for gel electrophoresis as described above in 4.6.2.1. The expected size of linearized pET-14b plasmid vector was approximatively of 4,500 bp. The DNA bands of interest were extracted and purified by NucleoSpin® Gel and PCR Clean-up kit (MACHEREY-NAGEL, Düren, Germany), the linearized and purified pET-14b plasmid vector was quantified by measuring UV absorbance at 260 nm.

F2 - R2 primer amplified and purified flagellin genes are double-digested with *Xba*I and *Bam*HI restriction enzymes at 37 °C for 15 – 16 hours as reported by Table 18. Digestions were stopped by heating at 80 °C for 20 minutes.

Table 18. Digestion mixes for purified flagellin genes.

Digestion mixes	**× 1 Reaction**
Flagellin genes (250 ng)	5.5 µl (*Pto*), 4.94 µl (*Pta*), 10.7 µl (*Pf4*)
10× Buffer *Bam*HI	5 µl
H_2O for molecular biology	36.5 µl (*Pto*), 37.06 µl (*Pta*), 31.3 µl (*Pf4*)
*Bam*HI 10 U/µl	1 µl
*Xba*I 10 U/µl	2 µl
Total volume	50 µl

Digested flagellin genes are ligated to linearized and purified pET-14b plasmid vector with a molar ratio of 3:1 respectively, in presence of T4 DNA ligase (Thermo Scientific) at 16 °C for 15 – 16 hours as reported by Table 19.

Table 19. Ligation mixes for linearized purified pET-14b plasmid vector and digested flagellin genes.

Ligation mixes	**× 1 Reaction**
pET-14b plasmid vector (50 ng)	7.82 µl
Flagellin genes (30.74 ng)	6.12 µl
H_2O for molecular biology	3.06 µl
10× Buffer T4 DNA ligase	2 µl
T4 DNA ligase 5 U/µl	1 µl
Total volume	20 µl

JM101 competent cells were transformed with the ligation reactions. Two µl of each ligation reaction were added into a 15 ml tube together with 50 µl of JM101 competent cells on ice. The tubes were gently mixed and left them on ice for 20 minutes. Cells were heated shock at 42 °C for 45 seconds, then put back on ice for 2 minutes. Nine-hundred-and-fifty µl of room temperature S.O.C. medium were added to each tube and mixtures were incubated at 37 °C for 1.5 hours with shaking. One hundred µl of each transformation culture were plated as: undiluted, diluted 1:10 in S.O.C.

medium and all the remaining on LB plates supplemented with 100 µg/ml ampicillin. Plates were incubated at 37 °C for 16 – 24 hours and then inspected.

4.6.4.3 Screening of JM101 colonies

Sixty colonies for *Pto*-transformation and fifty colonies for *Pta*- and *Pf4*- transformations were transferred in new LB plates supplemented with 100 µg/ml ampicillin. Colony-PCRs with F0 - R0 primers and GoTaq® Flexy G2 DNA Polymerase (Promega) were performed.

Colony-PCR Master mixes and colony-PCR programs for both PsF0 / PsR0 and Pf4F0 / Pf4R0 primers are the same as described above in 4.6.3 in Table 13 and Table 14, respectively. PCR products were verified by gel electrophoresis as described above in 4.6.2.1. The expected amplicon sizes were 846 bp for *Pto* and *Pta*, 849 bp for *Pf4*.

Six positive clones to the flagellin amplification for each transformation, were picked and inoculated in 5 ml of LB liquid culture supplemented with 100 µg/ml ampicillin. Cells were grown at 37 °C with shaking for 15 – 16 hours. The overnight bacterial liquid cultures were used to isolate the plasmid DNA as described above in 4.4.8 and to generate glycerol-stocks of the bacteria. Purified plasmid DNAs were quantified by measuring UV absorbance at 260 nm and were sequenced at BMR Genomics s.r.l. using the Sanger method.

After checking the accuracy of the flagellin coding sequence and the proper orientation of the gene, one ligation product of pET-14b plasmid vector and flagellin for each transformation was used to transform BL-21 competent cells.

DNA was diluted to 10 ng/µl and 10 ng were added into a 15 ml tube together with 50 µl of BL-21 competent cells on ice. The tubes were gently mixed and left them on ice for 20 minutes. Cells were heated shock at exactly 42 °C for 45 seconds, then put back on ice for 2 minutes. Nine-hundred-and-fifty µl of room temperature S.O.C. medium were added to each tube and mixtures were incubated at 37 °C for 1.5 hours with shaking. One hundred µl of each transformation culture were plated as: undiluted, diluted 1:10 in S.O.C. medium and all the remaining on LB plates supplemented with 100 µg/ml ampicillin. Plates were incubated at 37 °C for 16 – 24 hours and then inspected.

One colony from each transformation was picked and inoculated on 5 ml of LB liquid culture supplemented with 100 µg/ml ampicillin and incubated at 37 °C for 15 – 16 hours. The overnight bacterial liquid cultures were used to prepare glycerol-stocks of the bacteria.

4.6.5 Expression, purification and refolding of *Pto*-flagellin

Pto-flagellin was *in vitro* expressed and purified with a histidine tag localized at C′ position which enabled its immobilization onto Ni-NTA column and was carried out in collaboration with the research groups of: "Bioorganic Chemistry of Nucleic Acids" and the "Technological Platform for Production and Purification of Recombinant Proteins" both of Institut Pasteur of Paris, France.

4.6.5.1 Expression of the flagellin

One BL-21 colony previously transformed with the ligation product of pET-14b plasmid vector and *Pto*-flagellin was picked and inoculated on 5 ml of LB liquid culture supplemented with 100 µg/ml ampicillin and incubated at 37 °C for 15 – 16 hours. The overnight bacterial liquid culture was used to prepare glycerol-stock of the bacteria and to isolate plasmid DNA by QIAprep Spin Miniprep kit (QIAGEN, Hilden, Germany). Plasmid DNA was quantified by measuring the absorbance at 260 nm.

Plasmid DNA was diluted to 3 ng/µl and 3 ng were added into the tube containing 100 µl of BL 21 Star^{TM} (DE 3) *E. coli* competent cells (Invitrogen) on ice. The tube was gently mixed and left on ice for 30 minutes. Cells were heated shock at 42 °C for 30 seconds, then put back on ice for 2 minutes. Four-hundred-and-fifty µl of room temperature LB medium were added to the tube and it was incubated at 37 °C for 1.5 hours with shaking. One hundred µl of the transformation culture were plated as: undiluted, diluted 1:10 in LB medium and all the remaining on LB plates supplemented with 100 µg/ml ampicillin. Plates were incubated at 37 °C for 16 – 24 hours and then inspected.

One single colony was picked and inoculated in 15 ml of LB liquid culture supplemented with 100 µg/ml ampicillin. The bacterial liquid culture was incubated at 30 °C with shaking (200 rpm) for 15 – 16 hours.

Five ml of the overnight liquid culture were used to inoculate 50 ml of NZY Auto-induction LB medium (NZYTech, Lda., Lisbon, Portugal) supplemented with 100 µg/ml ampicillin. The medium was constituted of glucose to sustain the first bacterial growth to reach high OD_{600} values and of lactose to induce the expression of the protein of interest during the second growth [Studier, 2005]. The liquid culture was being grown at 37 °C for 5 hours with shaking (180 rpm) and then at 20 °C for 16 hours with shaking (180 rpm).

The induced bacterial culture was centrifuged at 6,000 rpm for 15 minutes at 4 °C, the supernatant was discarded, and the pellet was stored at -80 °C.

4.6.5.2 Purification, refolding and quantitation of the flagellin

The purification of *Pto*-flagellin was performed under denatured conditions according to Behrouz et al. [2016] and Goudarzi et al. [2009] with modifications.

The bacterial pellet was resuspended in 8 ml of Lysis Buffer: 50 mM NaH_2PO_4 (Sigma Aldrich), 300 mM NaCl, pH 7.4. The mixture was evenly homogenized and 1 mM PMSF (Phenylmethylsulfonyl fluoride, Sigma Aldrich) was added as protease inhibitor. The complete breakage of the bacterial pellet was performed by sonication with 5 pulses of 10 seconds at high intensity and 30 seconds of rest in ice in between each pulse.

The suspension was centrifuged at 11,000 rpm for 30 minutes at 4 °C, the supernatant was recovered as soluble fraction of *E. coli* and stored at 4 °C.

The pellet was resuspended in 8 ml of Urea Buffer: 8 M Urea (Sigma Aldrich), 20 mM NaH_2PO_4, 500 mM NaCl, pH 7.4; and incubated at room temperature for 2 hours with shaking until complete dissolving of inclusion bodies. The suspension was centrifuged at 11,000 rpm for 30 minutes at 20 °C and the supernatant was recovered as insoluble fraction of *E. coli*.

Protein purification under denatured conditions was performed at room temperature by using HisPur™ Ni-NTA Spin Column of 1 ml resin bed (Thermo Scientific). Ten column volumes of Binding Buffer: 20 mM NaH_2PO_4, 500 mM NaCl, 8 M urea, pH 7.8; were used to equilibrate the resin before to apply the sample. Then the insoluble fraction of *E. coli* was added to the resin and incubated on rotatory shaker for 30 minutes. Twenty column volumes of Wash Buffer: 20 mM NaH_2PO_4, 500 mM NaCl, 8 M urea, 20 mM imidazole (Sigma Aldrich), pH 8; were used to wash away unspecific proteins and weak-bound proteins to the resin. Ten column volumes of Elution Buffer: 20 mM NaH_2PO_4, 500 mM NaCl, 250 mM imidazole, pH 8; were used to elute the protein of interest.

All the purification steps, the flow-through, the wash and the elution were analyzed by 12 % SDS-PAGE denaturing gel. Ten µl of each sample were mixed with 9.5 µl of 2× SDS-PAGE Sample Buffer: 62.5 mM Tris-HCl (Sigma Aldrich) pH 6.8, 25 % glycerol, 0.01 % Bromophenol blue (Sigma Aldrich), 2 % SDS; and with 0.5 µl of 2-mercaptoethanol (Sigma Aldrich) and boiled at 99 °C for 10 minutes. Twenty µl of each sample and 7 µl of mPAGE Unstained Protein Standards (Sigma Aldrich) were loaded on SDS-PAGE gel and run for 40 minutes at 200 V.

Detection of protein bands was performed with Coomassie Brilliant Blue R-250 staining solution: 0.1 % (w/v) Coomassie Brilliant Blue R-250 (Sigma Aldrich), 40 % (v/v) methanol (Sigma Aldrich) and 10 % (v/v) acetic acid (Sigma Aldrich). After the run, the gel was rinsed in water and 50 ml of Coomassie Brilliant Blue R-250 staining solution were added. The gel was shaken for 1 hour

and rinsed with water, then destaining solution: 40 % (v/v) methanol and 10 % (v/v) acetic acid, was added to remove the background signal. Stained gel was stored in water.

Soluble and insoluble fractions of *E. coli* before purification were analyzed by Western Blot with mouse anti Histidine tag monoclonal antibody conjugated with Horseradish Peroxidase (HRP) (Bio-Rad).

Elution aliquots from the protein purification were pooled together and the removal of the denaturing agent from the protein sample was performed by dialysis with a decreasing linear gradient of urea from 8 to 0 M in 20 mM Tris pH 9 (Sigma Aldrich) buffer. Around 15 ml of sample were added to a Slide-A-Lyzer^{TM} G2 Dialysis Cassette (10K MWCO) (Thermo Scientific) and dialysed against 930 ml of 20 mM Tris pH 9 buffer supplemented with 7, 6, 5, 4, 3, 2, 1 and 0 M of urea. Each dialysis step was conducted at 4 °C and lasted 24 hours. The dialysis with 0 M of urea was performed two consecutive times.

Protein concentration was determined by Bradford assay in microplate format using 1.25, 2.5, 5, 7.5 and 10 µg/ml of BSA as standards. One-hundred-and-fifty µl of Bradford reagent (Sigma Aldrich) were added to the same volume of the blank, the BSA standards and the protein and, after 5 minutes of incubation at room temperature, the absorbance was recorded at 570 nm. Each sample was measured in duplicates. The protein concentration was determined by comparison to the BSA standard curve.

4.7 SELEX on *Plasmodium falciparum* lactate dehydrogenase (*Pf*LDH)

Also this part of the work was developed in collaboration with the research group of "Bioorganic Chemistry of Nucleic Acids" of the Institut Pasteur of Paris, France.

SELEX was performed to select cubane-modified aptamers or cubamers with *Pf*LDH as target. Cubamers included a chemical modification where instead of dTTP they bear dUTP functionalized at the 5′ position with protein-like benzyl/2-napthyl/3-indolyl-carboxamide (dU^{C}TP) [Cheung et al., 2020].

*Pf*LDH was *in vitro* expressed and purified with a histidine tag which facilitated immobilization onto magnetic beads for aptamer selection and was carried out at the "Technological Platform for Production and Purification of Recombinant Proteins" of Institut Pasteur of Paris, France.

MH35 ssDNA library and relative MH36 (forward) and MH37 (reverse) primers were synthesized at Microsynth AG, Balgach, Switzerland. Oligonucleotide MH35 library sequence was 71 nucleotides long with the 5′ position phosphorylated and its sequence: 5'-[Phos]CGTACGGTCGACGCTAGC(N)$_{35}$CACGTGGAGCTCGGATCC-3'. MH35 library primers for PCR amplifications were:

- MH36 5′-CGTACGGTCGACGCTAGC-3′
- MH37 5′-[Phos]GGATCCGAGCTCCACGTG-3′

4.7.1 Real Time PCR - HRM analysis of MH35 library

A preliminary test was performed with Q5® High Fidelity DNA Polymerase (New England Biolabs) to check for the Real Time PCR amplification and the melting peaks of MH35 library prior to selection.

MH35 library concentration was 2 198.32 ng/µl (100 µM) and it was diluted to 100 nM, 10 nM, 1 nM and 0.1 nM. MH36 and MH37 primers were concentrated 1 mM and were diluted to 10 µM. dATP, dCTP and dGTP (New England Biolabs) were premixed and diluted to 10 mM. dTTP (New England Biolabs) was diluted to 5 mM.

The Real Time PCR Master mix is reported in Table 20.

Table 20. Real Time PCR Master mix for MH35 library amplification prior to selection.

Master mix	**× 1 Reaction**
H_2O for molecular biology	10.6 µl
5× Buffer Q5®	4 µl
(dATP - dCTP - dGTP) 10 mM - 0.2 mM	0.4 µl
dTTP 5 mM - 0.2 mM	0.8 µl
MH36 10 µM - 0.5 µM	1 µl
MH37 10 µM - 0.5 µM	1 µl
EvaGreen® 20× (Biotium)	1 µl

Q5® High Fidelity DNA Polymerase	0.2 µl
MH35 library 100 nM, 10 nM, 1 nM and 0.1 nM	1 µl
Total volume	20 µl

The Real Time PCR - HRM program is reported in Table 21.

Table 21. Real Time PCR - HRM program for monitoring MH35 library prior to selection.

1.	98 °C (Initial denaturation)	0:30
2.	98 °C (Denaturation)	0:10
3.	69 °C (Annealing)	0:20
4.	72 °C (Extension)	0:30
5.	GO TO 2	19 cycles
6.	95 °C (Denaturation)	1:00
7.	65 °C (Renaturation)	1:00
8.	HRM analysis (65 °C ÷ 95 °C)	5 acquisitions / °C

4.7.2 Introducing dU^{C}TP into the MH35 library sequence

Before to proceed with the SELEX experiment, in order to expand the chemical repertoire of the oligonucleotide library, dU^{C}TP was introduced into the random region of MH35 library sequence.

Standard PCR was performed using Q5® High Fidelity DNA Polymerase (New England Biolabs) and ProFlex PCR System thermal cycler (Thermo Scientific). dTTP was exploited as negative control.

The standard PCR Master mixes are reported in Table 22.

Table 22. Standard PCR Master mixes for MH35 library amplification.

Master mixes	**× 1 Reaction**
H_2O for molecular biology	14.75 µl
5× Buffer Q5®	5 µl
(dATP - dCTP - dGTP) 10 mM - 0.2 mM	0.5 µl
(dU^{C}TP / dTTP) 5 mM - 0.2 mM	1 µl
MH36 10 µM - 0.5 µM	1.25 µl

MH37 10 µM - 0.5 µM	1.25 µl
Q5® High Fidelity DNA Polymerase	0.25 µl
MH35 library 100 nM, 10 nM and 1 nM	1 µl
Total volume	25 µl

The standard PCR program is reported in Table 23.

Table 23. Standard PCR program for MH35 library amplification.

1. 98 °C (Initial denaturation)	0:30
2. 98 °C (Denaturation)	0:10
3. 69 °C (Annealing)	0:30
4. 72 °C (Extension)	1:00
5. GO TO 2	19 cycles
6. 72 °C (Final extension)	2:00

Five µl of PCR products were mixed with 5 µl of 1× E-Gel™ Sample Loading Buffer (Invitrogen), load in E-Gel™ Agarose Gels 2 % (Invitrogen) and run with E-Gel™ Power Snap Electrophoresis System (Invitrogen) together with Low Molecular Weight DNA Ladder (New England Biolabs) for 10 minutes. DNA detection was allowed by SYBR™ Safe DNA stain. Gel image was taken by E-Gel™ Power Snap Camera (Invitrogen). Expected amplicon sizes were of 71 bp. PCR products were then purified as described above in 4.6.4.2 and quantified by measuring the absorbance at 260 nm.

Purified PCR products were digested with λ-exonuclease to regenerate the single stranded structure of the MH35 library. The exonuclease digestion was performed for 1 hour at 37 °C in 50 µl of reaction volume: 1 µl of λ-exonuclease (5 U/µl) (New England Biolabs), 5 µl of 10× λ-exonuclease buffer and up to 5 µg of dsDNA. λ-exonuclease digestion products were purified as described above in 4.6.4.2 using NTC (MACHEREY-NAGEL) as binding buffer for ssDNA. ssDNA was quantified by measuring the absorbance at 260 nm. Approximatively 89 pmol of MH35 library were used to start the SELEX experiment. ssDNA pool was completely vacuum dried and stored at -20 °C.

4.7.3 SELEX protocol

One hundred µl of Ni-NTA Magnetic Agarose Beads (Jena Bioscience GmbH, Jena, Germany) were added to two 1.5-ml microcentrifuge tubes and located to the magnetic support to remove the storage buffer. Magnetic beads were washed twice with 500 µl of protein buffer: 25 mM Tris pH 8, 100 mM NaCl; one tube was for the Negative Selection and the other one was for the Positive Selection.

Three hundred µl of *Pf*LDH (100 µg) were added to the Positive Selection tube and incubated at 23 °C for 30 minutes with shaking (900 rpm). The tube was located to magnetic support and the supernatant was discarded. *Pf*LDH proteins linked to the magnetic beads were washed three times with 500 µl of protein buffer.

MH35 ssDNA pool (89 pmol) was resuspended in 300 µl of protein buffer, added to the magnetic beads of the Negative Selection tube and incubated at 23 °C for 30 minutes with shaking (900 rpm). The tube was located to the magnetic support, the supernatant was recovered, added to the Positive Selection tube and incubated at 23 °C for 1 hour with shaking (900 rpm). The tube was located to the magnetic support and the supernatant was discarded. Three washing steps were carried out with 500 µl of protein buffer. Two hundred µl of water for molecular biology were added and ssDNA was eluted by heating at 95 °C for 20 minutes. The tube was located to the magnetic support and the supernatant was recovered and stored at -20 °C.

From round 4 to round 10 the selection stringency is increased as described by Table 24.

Table 24. Increasing of the selection stringency among SELEX rounds.

Round	Selection stringency
4, 5	Reduce incubation time between *Pf*LDH and MH35 ssDNA to 45 minutes
6, 7	Introduce *Plasmodium vivax* LDH (*Pv*LDH) as target for the Negative Selection
8, 9	Reduce incubation time between *Pf*LDH and MH35 ssDNA to 30 minutes
10	Introduce *Pv*LDH as target for the Negative Selection

4.7.4 Real Time PCR - HRM analysis to check the selection progress

After each SELEX round, Real Time PCR and HRM analysis were performed to monitor the enrichment of the ssDNA selected pool [Luo et al., 2017; Mencin et al., 2014; Vanbrabant et al., 2014].

The Real Time PCR Master mix is the same as reported above in 4.7.1 in Table 20. Real Time PCR - HRM program is the same as described above in 4.7.1 in Table 21.

4.7.5 Preparation of DNA sequences for consecutive rounds

The standard PCR Master mix is performed as described above in 4.7.2 in Table 22, with only $dU^{C}TP$. The standard PCR program is the same as reported above in 4.7.2 in Table 23, with the only exception of the number of amplification cycles which was optimized to avoid PCR by-products. PCR products were checked as described above in 4.7.2. Once that optimum number of amplification cycles had been determined, the PCR was performed in larger volumes. PCR products were then purified as described above in 4.6.4.2 and quantified by measuring the absorbance at 260 nm.

Purified PCR products were digested with λ-exonuclease and the originated ssDNA was purified as described in 4.7.2. Approximatively 89 pmol of ssDNA selected pool were used to start each SELEX round. ssDNA pool was completely vacuum dried and stored at -20 °C.

4.7.6 Aptamer cloning system and sequencing

Selected potential aptamers from round 10 were prepared for the cloning with TOPO® TA Cloning® kit (Invitrogen).

Standard PCR with Taq DNA Polymerase (New England Biolabs) was performed on ssDNA sequences to produce single adenine overhangs at the 3′ positions necessary for the ligation with pCR™2.1-TOPO® plasmid vector. dTTP was used instead of $dU^{C}TP$ and MH37 reverse primer was without the phosphorylation at the 5′ position ([no phos]MH37, Microsynth AG).

The standard PCR Master mix is reported in Table 25.

Table 25. Standard PCR Master mix for the cloning of potential aptamers.

Master mix	**× 1 Reaction**
H_2O for molecular biology	17.375 µl
10× ThermoPol Reaction Buffer	2.5 µl
(dATP - dCTP - dGTP) 10 mM - 0.2 mM	0.5 µl
dTTP 5 mM - 0.2 mM	1 µl
MH36 10 µM - 0.5 µM	1.25 µl
[no phos]MH37 10 µM - 0.5 µM	1.25 µl
Taq DNA Polymerase	0.125 µl
ssDNA selected pool	1 µl
Total volume	25 µl

The standard PCR program is reported in Table 26.

Table 26. Standard PCR program for the cloning of potential aptamers.

1. 95 °C (Initial denaturation)	0:30
2. 95 °C (Denaturation)	0:30
3. 55 °C (Annealing)	0:30
4. 72 °C (Extension)	0:30
5. GO TO 2	19 cycles
6. 72 °C (Final extension)	7:00

PCR products were checked as described above in 4.7.2. PCR products were then purified as described above in 4.6.4.2 and quantified by loading and comparing on the same gel with DNA Ladder. PCR products were diluted to approximatively 1 ng/µl before to proceed with cloning.

Purified and amplified sequences from round 10 are ligated with pCR™2.1-TOPO® plasmid vector with a molar ratio of 11:1, respectively, for 15 minutes at room temperature as reported in Table 27.

Table 27. Ligation mix for pCR™2.1-TOPO® plasmid vector and amplified sequences from round 10.

Ligation mix	**× 1 Reaction**
pCR™2.1-TOPO® plasmid vector (10 ng)	1 µl
Sequences of round 10 (2 ng)	2 µl
H_2O for molecular biology	2 µl
Salt Solution (1.2 M NaCl, 60 mM $MgCl_2$)	1 µl
Total volume	6 µl

Two µl of the Ligation mix were added to a vial of One Shot® DH5α™ competent cells (Thermo Scientific) on ice. The mixture was gently flicked, incubated for 30 minutes, heated shock at 42 °C for 30 seconds and put back on ice. Two-hundred-and-fifty µl of room temperature S.O.C. medium were added to the mixture and incubated at 37 °C for 1 hour with shaking. One hundred and 200 µl were plated on LB selective plates supplemented with 100 µg/ml ampicillin and spreaded with 40 µl of 40 mg/ml X-gal. The plates were incubated at 37 °C for 16 – 24 hours and then inspected.

One hundred white bacteria colonies were plated in LB replica plates supplemented with 100 µg/ml ampicillin. Colony-PCR was performed with Taq DNA Polymerase (Invitrogen) on boiled white-bacteria using MH36 and MH37 primers, followed by standard gel electrophoresis with 2.5 % agarose, run in 1× TBE buffer (Sigma Aldrich) at 120 V for 30 minutes. Ethidium bromide was the DNA intercalant. Expected amplicon sizes were of 71 bp.

The colony-PCR Master mix is reported in Table 28.

Table 28. Colony-PCR Master mix for insert screening in pCR™2.1-TOPO® plasmid vector.

Master mix	**× 1 Reaction**
H_2O for molecular biology	17.375 µl
10× PCR Buffer	2.5 µl
(dATP - dCTP - dGTP) 10 mM - 0.2 mM	0.5 µl
dTTP 5 mM - 0.2 mM	1 µl
$MgCl_2$ 50 mM - 1.25 mM	0.625 µl
MH36 10 µM - 0.125 µM	0.3125 µl
MH37 10 µM - 0.125 µM	0.3125 µl
Taq DNA Polymerase	0.1 µl
White bacteria DNA sample	1 µl
Total volume	25 µl

The colony-PCR program is reported in Table 29.

Table 29. Colony-PCR program for insert screening in pCR™2.1-TOPO® plasmid vector.

1. 94 °C (Initial denaturation)	4:00
2. 94 °C (Denaturation)	0:30
3. 55 °C (Annealing)	0:30
4. 72 °C (Extension)	1:00
5. GO TO 2	24 cycles
6. 72 °C (Final extension)	5:00

After colony-PCR, 50 positive clones to the library amplification were inoculated on 5 ml of LB liquid cultures supplemented with 100 µg/ml ampicillin and incubated at 37 °C with shaking for

15 – 16 hours. Plasmid DNAs were then isolated from the overnight bacterial liquid cultures as described above in 4.6.5.1 and quantified by measuring UV absorbance at 260 nm. Potential aptamers were sequenced at Eurofins Genomics using the Sanger method. The alignment of the random regions of potential aptamers was performed with MUSCLE of SnapGene® software, leaving the default program parameters.

4.7.7 Checking the specificity of selected potential aptamers

Potential aptamers from round 10 with similar motives, G-rich sequences forming putative quadruplex structures and T-rich sequences among the random regions, were labelled with the fluorescein tag [6FAM] and their specificity for the target was evaluated by Typhoon fluorescence scanning.

Potential aptamers were chemically synthesized with the 5′ position phosphorylated and in the reverse complement conformation by Microsynth AG. The sequences were then amplified by primer extension in presence of MH36 primer labelled at 5′ position with fluorescein (5′-[6FAM]CGTACGGTCGACGCTAGC-3′) (Microsynth AG).

The hybridization Master mix is reported in Table 30.

Table 30. Hybridization Master mix to hybridize potential aptamers with [6FAM]MH36 primer.

Master mix	**× 1 Reaction**
H_2O for molecular biology	0.5 µl
[6FAM]MH36 10 µM	1 µl
Potential aptamers 10 µM	1.5 µl
Total volume	3 µl

Hybridization Master mix was incubated at room temperature for 1 hour in boiling water to hybridize the primer to the template.

The primer extension Master mix was performed with Vent® (exo-) DNA Polymerase (New England Biolabs) and is reported in Table 31.

Table 31. Primer extension Master mix of potential aptamers.

Master mix	**× 1 Reaction**
10× ThermoPol Reaction Buffer	1 µl
(dATP - dCTP - dGTP) 1 mM - 0.2 mM	2 µl
$dU^{C}TP$ 5 mM - 0.2 mM	0.4 µl
H_2O for molecular biology	1.6 µl
Hybridization mix	3 µl
Vent® (exo-) DNA Polymerase	2 µl
Total volume	10 µl

Primer extension Master mix was incubated at 60 °C for 3 hours to synthesize the DNA complement strand.

Primer extension products are digested with λ-exonuclease and ssDNA purified as reported in 4.7.2. Approximatively 15 pmol of the selected sequences from round 10 were used to check the specificity for *Pf*LDH.

The binding assay, to check the specificity for the target, was performed as a typical SELEX round. The selected fluorescent sequences from round 10 were incubated with *Pf*LDH at 23 °C for 1 hour with shaking (900 rpm). Then, the flow-through and the washing steps were recovered. Selected sequences were eluted in 200 µl of water for molecular biology at 95 °C for 20 minutes.

Flow-through, wash and elution steps were purified as described above in 4.6.4.2, using NTC as binding buffer for ssDNA. Purified ssDNAs were vacuum dried. The pellets were resuspended in 2 µl of water for molecular biology and 2 µl of Loading buffer Blue were added, the mixtures were boiled at 95 °C for 5 minutes. The samples were loaded on 20 % polyacrylamide denaturing gel in presence of 7 M urea and run in 1× TBE buffer at 40 W for 3.5 hours. Detection of the fluorescent signal was performed by Typhoon fluorescence scanning.

4.8 SELEX on *Pseudomonas syringae* pv. *tomato* DC3000 (*Pto*) flagellin

4.8.1 SELEX protocol

Fifty µl of Ni-NTA Magnetic Agarose Beads (Cube Biotech, Monheim, Germany) were added to two 1.5-ml microcentrifuge tubes and located to the magnetic support to remove the storage buffer. Magnetic beads were washed twice with 250 µl of protein buffer: 20 mM Tris pH 9; one tube was for the Negative Selection and the other one was for the Positive Selection.

Fifty µg of *Pto*-flagellin were added to the Positive Selection tube and incubated at room temperature for 30 minutes with shaking. The tube was located to the magnetic support and the supernatant was discarded. *Pto*-flagellin proteins linked to the magnetic beads were washed three times with 250 µl of protein buffer.

LIB1.0 ssDNA pool (50 pmol) was resuspended in 1 ml of protein buffer, added to the magnetic beads of the Negative Selection tube and incubated at room temperature for 30 minutes with shaking. The tube was located to the magnetic support, the supernatant was recovered, added to the Positive Selection tube and incubated at room temperature for 1 hour with shaking. The tube was located to the magnetic support and the supernatant was discarded. Three washing steps were applied with 250 µl of protein buffer. One hundred µl of water for molecular biology were added and ssDNA was eluted by heating at around 88 °C for 20 minutes. The tube was located to the magnetic support and the supernatant was recovered and stored at -20 °C.

From round 3 to round 6 the selection stringency was increased by reducing the incubation time between LIB1.0 ssDNA pool and the target to 45 minutes for rounds 3 and 4 and to 30 minutes for rounds 5 and 6. While for rounds 7 and 8 the protein amount was reduced to 37.5 µg, maintaining 30 minutes for the incubation between LIB1.0 ssDNA pool and the target.

4.8.2 Real Time PCR - HRM analysis to check the selection progress

After each SELEX round, Real Time PCR and HRM analysis were performed to monitor the enrichment of the ssDNA selected pool [Luo et al., 2017; Mencin et al., 2014; Vanbrabant et al., 2014].

The Real Time PCR Master mix for checking the selection progress is the same as described above in 4.3 in Table 4, scaling down all reagent concentrations accordingly to 12 µl of reaction

volume. The Real Time PCR program is the same as reported above in 4.3 in Table 5, with the only exception of 30 amplification cycles.

4.8.3 DNA preparation for consecutive rounds, sequencing and alignment

Standard PCRs were performed on eluted sample after the first round of SELEX according to Sefah et al. [2010] as described above in 4.5.1 and 4.5.2.

ssDNA synthesis was performed according Sefah et al. [2010] as described above in 4.5.3, with the only exception of 20 mM Tris pH 9 as wash buffer.

After the ssDNA quantitation, 50 pmol of eluted sample were resuspended in protein buffer (20 mM Tris pH 9) in order to start the second round. Round 2 was performed as the number one.

Real Time PCR and HRM analysis were performed on eluted samples to monitor the progression of the selection as described in 4.8.2.

Standard PCR was performed to determine the optimum number of amplification cycles and to prepare for the ssDNA synthesis.

After the round 8 selected potential aptamers were sequenced as described above in 4.5.5, using 35.42 ng of purified PCR product and NBE_9065_v109_revY_14Aug2019 sequencing protocol.

After recovery of the PCR fragment sequences using custom scripts, as described above, alignment of the random regions of the sequences was performed by SnapGene® software.

4.9 Switchable synthetic biosensor design

The switchable synthetic biosensor was designed with the aid of the NUPACK 4.0 software [Zadeh et al., 2011]. Both aptamers were assumed to consist by DNA alone, as the chimera switch is localized in the DNA region. The sequences of both aptamers were obtained after the SELEXs which were performed in this work, while the sequence of AtlsiRNA-1 was provided by Katiyar-Agarwal et al. [2007]. The dTTP at the 3′ position of Int_AtlsiRNA-1 is intended to be modified with chemical groups such as 2′-NH_2, 2′-F or 2′-O-CH_3, to impair the nuclease degradation.

According to the design, the switchable synthetic biosensor is formed following hybridization between the two oligonucleotides, to be performed with both PtoflagAptamer and Int_AtlsiRNA-1 at 10 mM concentration, in presence of 1 M NaCl and 200 mM $MgCl_2$ and at 25 °C.

5. RESULTS

5.1 Plant Cell-SELEX

Two Cell-SELEX experiments with LIB1.0 library were performed on *A. thaliana* protoplasts to recover potential aptamers that bind membrane cell and/or internalize into cell cytoplasm.

5.1.1 Preliminary tests on LIB1.0 library

Before to proceed with the selection, preliminary tests on LIB1.0 library were performed, such as the determination of the optimal annealing temperature for PCR amplification and the determination of the melting peaks to follow the progression of the selection.

Fifty-six °C was chosen as the optimal annealing temperature being the highest temperature which gave optimal yields as shown in Figure 10- A and B. The chosen annealing temperature gave good amplification rates of LIB1.0 library for all the PCR- and Real Time PCR- experiments, with both GoTaq® G2 Flexi and Q5® High Fidelity DNA Polymerases. The full gel images are reported in Figure S10- A and B in the Supplementary Materials section.

Real Time PCR - HRM analysis was performed on LIB1.0 library to determine the melting peaks. All LIB1.0 library dilutions showed very similar melting peaks of the same height, at the same temperature of 73.80 °C. Thus, this melting temperature was associated to the condition where the LIB1.0 library showed the highest diversity among the random regions of the sequences (Figure 10- C).

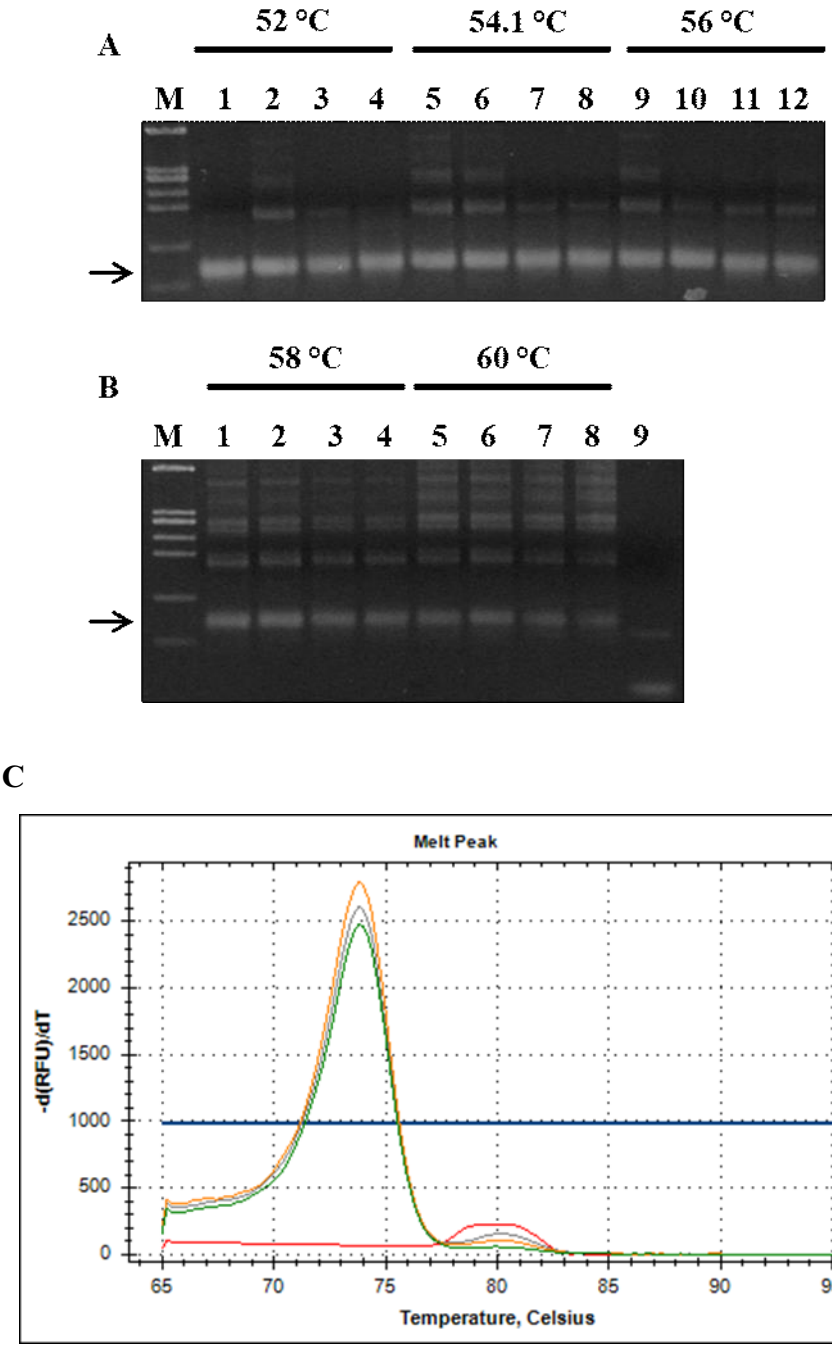

Figure 10- A, B and C. (A-B) Gradient PCR of LIB1.0 library with 52 °C, 54.1 °C, 56 °C, 58 °C and 60 °C as annealing temperatures. **(A)** M is ΦX174 DNA BsuRI (HaeIII) marker (310 bp, 281 bp, 271 bp, 234 bp, 194 bp, 118 bp and 72 bp). Lanes 1, 2, 5, 6, 9 and 10 are 10 ng of LIB1.0 library. Lanes 3, 4, 7, 8, 11 and 12 are 100 ng of LIB1.0 library. **(B)** M is ΦX174 DNA BsuRI (HaeIII) marker (310 bp, 281 bp, 271 bp, 234 bp, 194 bp, 118 bp and 72 bp). Lanes 1, 2, 5 and 6 are 10 ng LIB1.0 library. Lanes 3, 4, 7 and 8 are 100 ng LIB1.0 library. Lane 9 is the negative control. Expected amplicon sizes are of 80 bp (black arrows). **(C)** HRM analysis of LIB1.0 library dilutions 4.1, 4.2 and 4.3. Dilution 4.1 is the green curve, dilution 4.2 is the orange curve, dilution 4.3 is the grey curve and the negative control is the red curve.

5.1.2 Optimization of Cell-SELEX steps for plant cells

In order to evaluate the efficiency of both washing and blocking procedures of Cell-SELEX, the number of washing steps was increased to seven, compared to the three adopted by Sefah et al. [2010], and then in all fractions the DNA was quantified. The measurements of DNA concentrations from the first to the last wash were: 16.1 ng/µl, 0.456 ng/µl, 0.0928 ng/µl, 0.204 ng/µl, 0.233 ng/µl, 0.0448 ng/µl and 0.0596 ng/µl. Starting from the third wash the DNA concentration detected was similar and low (Figure 11).

Figure 11. Graph representing the values of the measured DNA concentration during the washing steps of Cell-SELEX.

Up to round 6, the Cell-SELEX protocol was designed to select potential aptamers binding the protoplast membrane and/or internalizing into cell cytoplasm. The first group of potential aptamers was recovered by heat-eluting the protoplasts while for the second one, the membrane cells were subsequently lysed. Thus, the elution temperature had to be chosen as a compromise between the maximum elution efficiency and the need to preserve the integrity of cell membranes. The integrity of almost all the protoplasts was preserved at room temperature (Figure 12- A) and 30 °C (Figure 12- B), at 45 °C (Figure 12- C) was partially preserved but not at 60 °C (Figure 12- D) and 70 °C (Figure 12- E) where only few protoplasts appeared undamaged. The temperature of 45 °C was chosen as the optimal elution temperature.

Cell lysis was carried out to recover the potential aptamers which internalized into the protoplasts. Protoplasts were resuspended in Protoplast Lysis buffer, mixed and observed by optical microscopy to evaluate cell rupture (Figure 12- F, G and H).

For rounds 7 and 8, an elution buffer based on WI buffer and supplemented with NaCl and acetic acid was designed in order to more efficiently remove the oligonucleotides that were specifically or unspecifically bound to the cell membrane. Protoplast incubations with WI buffer alone (Figure 12- I) and with WI supplemented with NaCl and acetic acid (Figure 12- J) were observed by optical microscopy and did not show remarkable differences. Moreover, protoplast integrity was maintained for both tested conditions.

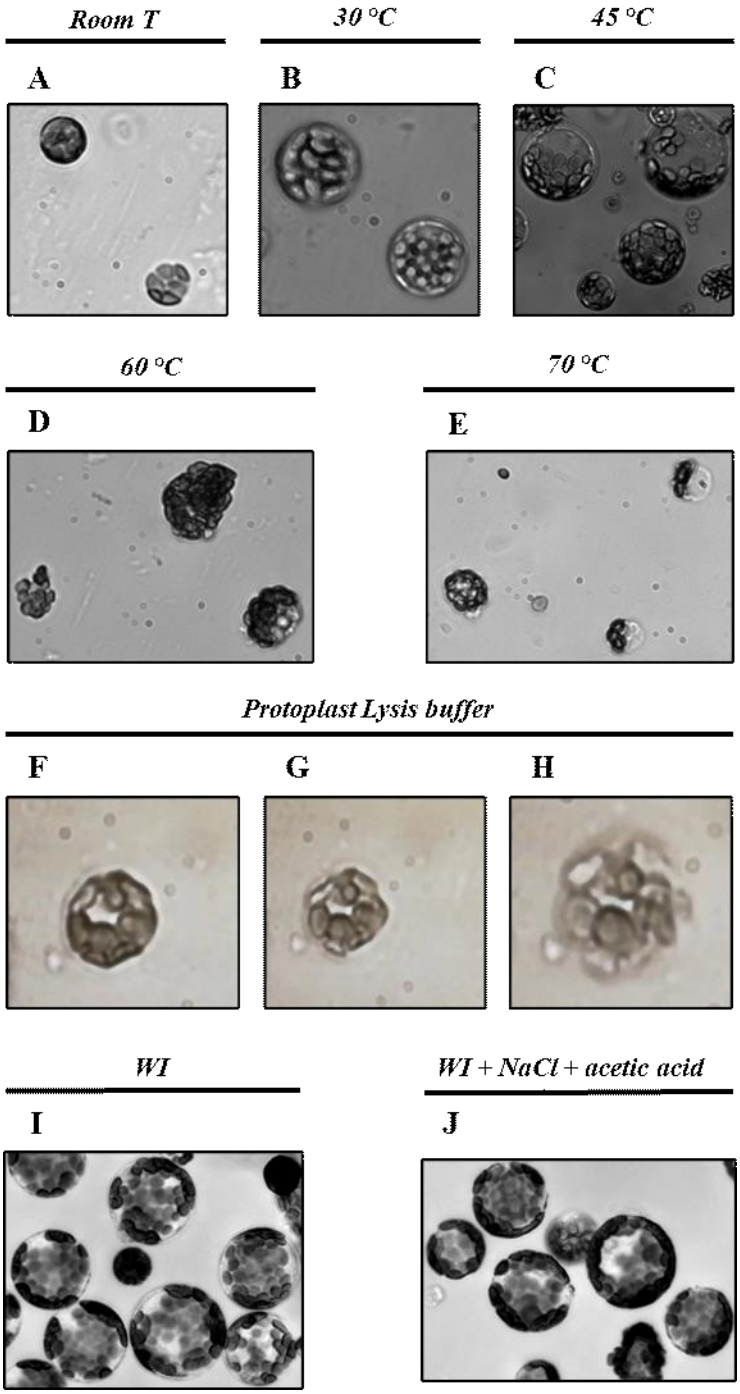

Figure 12- A, B, C, D, E, F, G, H, I and J. (A-B-C-D-E) Screening of the most suitable elution temperature to keep the protoplast viability. Room temperature **(A)**, 30 °C **(B)**, 45 °C **(C)**, 60 °C **(D)** and 70 °C **(E)** were evaluated. **(F-G-H)** Sequence from F to H shows a protoplast when exposed to Protoplast Lysis buffer. As the membrane is disrupted, the cell loses the structural integrity and eventually all its content is released outside. **(I-J)** Effect of WI buffer alone **(I)** and WI supplemented with NaCl and acetic acid **(J)** on protoplast integrity.

The results of the Real Time PCR analysis of LIB1.0 and negative control, carried out on both the eluted and cell-extracted oligonucleotides are displayed in Figure 13 and Table 32. The ΔCt between the amplification curves of the eluted oligonucleotides was of 15.81 cycles: $Ct_{LIB1.0}$ was 1.26

and Ct_{water} was 17.07. The ΔCt between the amplification curves of the cell-extracted oligonucleotides was of 2.72 cycles: $Ct_{LIB1.0}$ was 14.42 and Ct_{water} was 17.14. LIB1.0 library incubations showed lower Ct values compared the water, confirming the specificity of the Cell-SELEX assay.

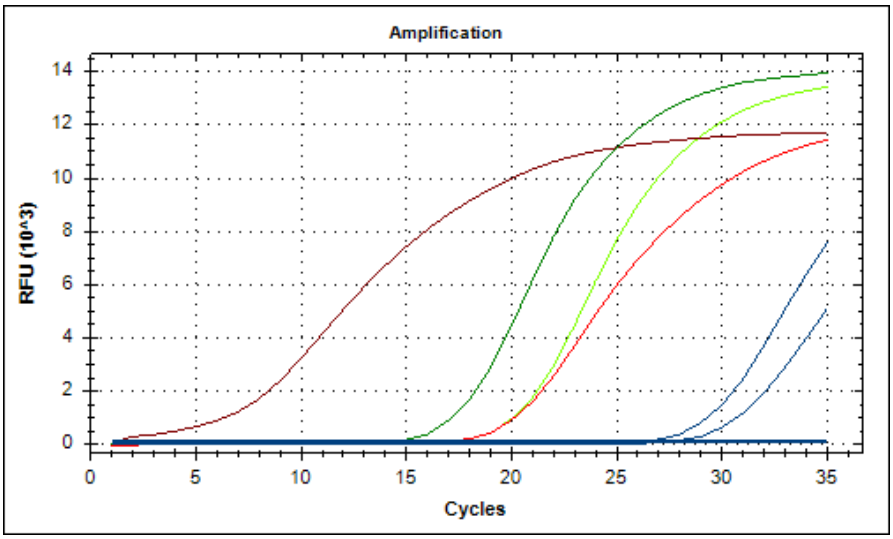

Figure 13. Real Time PCR of eluted and cell-extracted oligonucleotides in presence of the negative control of LIB1.0 library. Red curves are the eluted oligonucleotides following incubation with LIB1.0 (dark red) and water (red). Green curves are the cell-extracted oligonucleotides following incubation with LIB1.0 (dark green) and water (light green). Blue curves are the negative controls of Real Time PCR amplification.

Table 32. Ct values of Real Time PCR analysis of LIB1.0 and negative control (water), carried out on both the eluted and cell-extracted oligonucleotides.

	Eluted oligonucleotides	**Cell-extracted oligonucleotides**
$Ct_{LIB1.0}$	1.26	14.42
Ct_{water}	17.07	17.14

5.1.3 Cell-SELEX

5.1.3.1 Protoplast isolation

Protoplasts of *A. thaliana* appeared under optical microscope with a round shape, rich in green chloroplasts of approximately 10 – 50 µm (Figure 14- A).

The isolation experiment from 20 leaves (0.5 – 0.6 g) in 10 ml of enzymatic mixture usually yielded approximatively 10^6 cells/ml.

Cell-SELEX used live cells as target. The same day, after the extraction, as suggested by Sefah et al. [2010], the cell viability assay was performed on released protoplasts using fluorescein diacetate (FDA). FDA is an esterase substrate which can only be hydrolysed by living cells. The FDA viability assay was performed for each Cell-SELEX round. An example of the FDA viability assay was reported in Figure 14- B, C and D.

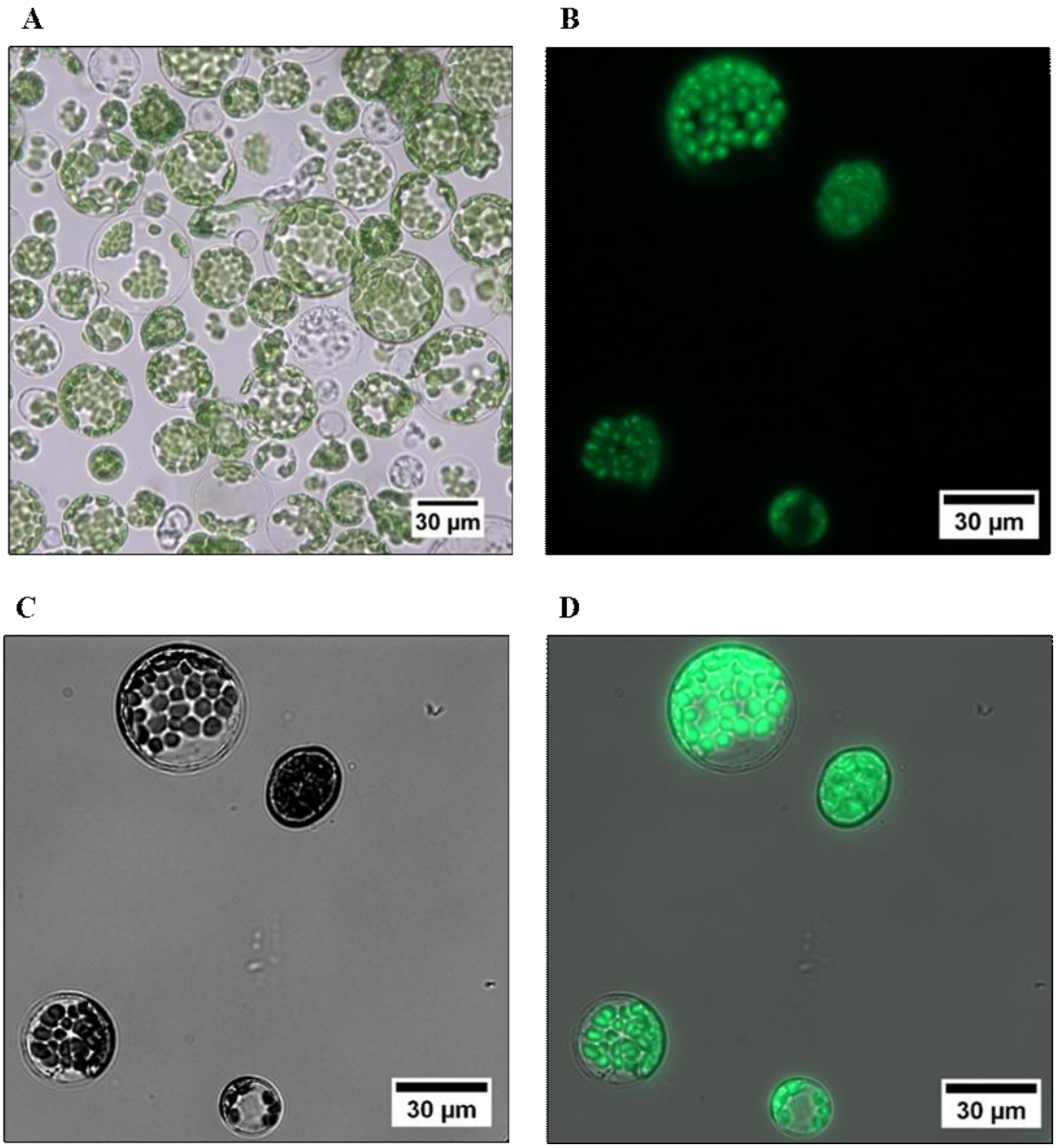

Figure 14- A, B, C and D. (A) Protoplasts released from *A. thaliana* mesophyll and after the washing procedure with W5 buffer. **(B)** GFP Filter Set 38 HE visualized protoplasts. **(C)** Bright field visualized protoplasts. **(D)** The merge of B and C photos.

5.1.3.2 Real Time PCR – HRM analysis

In the first Cell-SELEX round (Figure 15- A) eluted and cell-extracted oligonucleotides showed a melting peak at 74.20 °C and 74.40 °C, respectively, which were very similar to the result obtained by the Real Time PCR - HRM of the starting LIB1.0 library prior selection (Figure 10- C), hence a reduction of aptamer diversity was not detected.

In the second round, as compared to the first round, a second melting peak at 81 °C was detected for the cell-extracted oligonucleotides (Figure 15- B). Eluted oligonucleotides did not show any difference when compared to the first round.

The second melting peak of the cell-extracted oligonucleotides at 81 °C indicated a decrease in the diversity of the sequences.

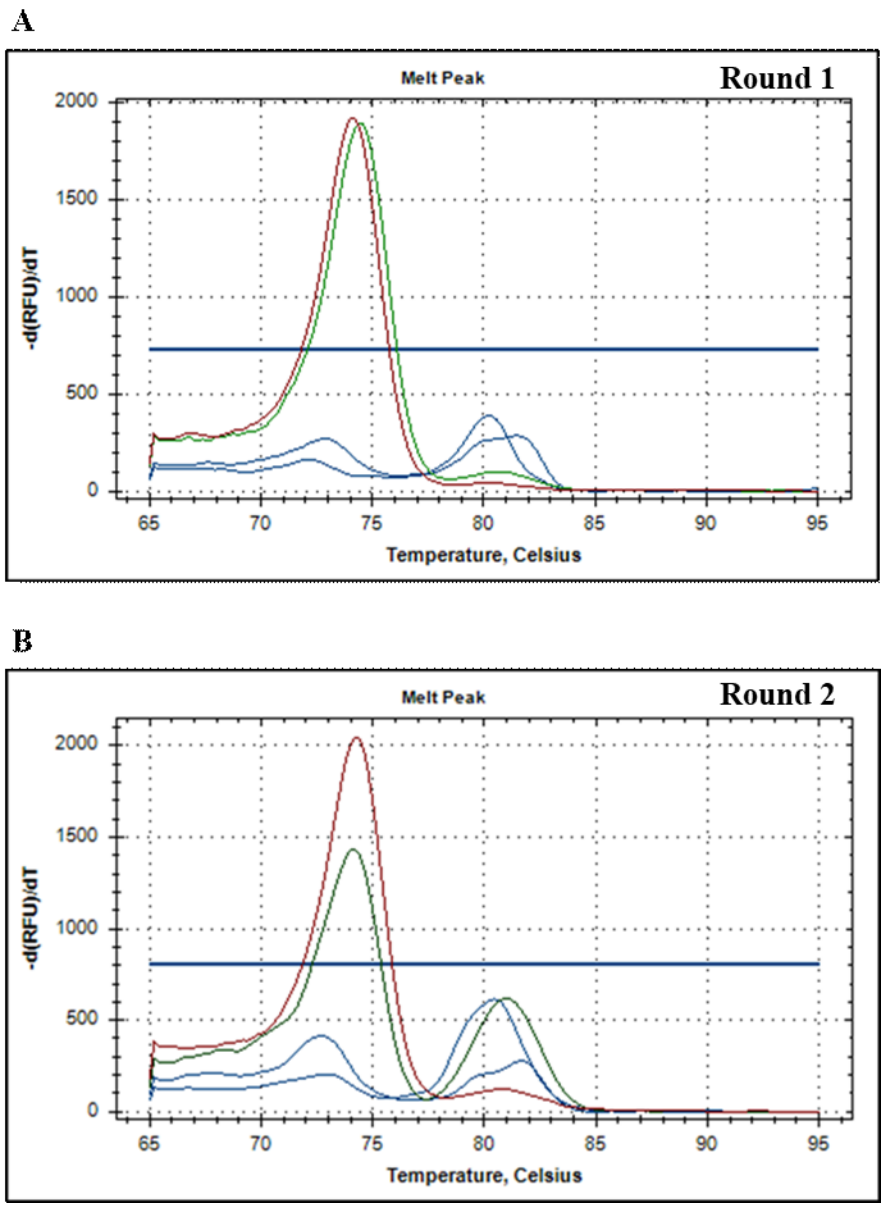

Figure 15- A and B. (A) HRM analysis of Cell-SELEX round 1 and **(B)** HRM analysis of Cell-SELEX round 2, of selected eluted and cell-extracted oligonucleotides. Eluted oligonucleotides are the dark red curve, cell-extracted oligonucleotides are the dark green curve and negative controls are the blue curves.

As the selection progressed up to the fifth round, when compared to the other rounds, also for the eluted oligonucleotides a fluorescence drop in the melting peak at 74 °C and the appearance of a second melting peak at 81 °C were observed. This melting peak at 81 °C for the diluted eluted oligonucleotides was observed in the HRM graph for the 1:10 and 1:100 dilutions but not for the undiluted eluted oligonucleotides (Figure 16- A and B). The fluorescence intensity of the melting peak at 74 °C of the diluted eluted oligonucleotides was lower than of the undiluted eluted oligonucleotides, presumably due to the additional melting peak at 81 °C. Cell-extracted

oligonucleotides did not show a significant difference when compared to the previous rounds in the pattern of melting peaks (Figure 16- C).

The gel electrophoresis of the Real Time PCR products (Figure 16- D) revealed single DNA bands in between the marker bands of 72 bp and 118 bp, which is congruent with the expected amplicon sizes of 80 bp. This meant that the two detected melting peaks originated from the selected sequences amplified by Real Time PCR and no PCR by-products were generated. The full gel image is reported in Figure S16 in the Supplementary Materials section.

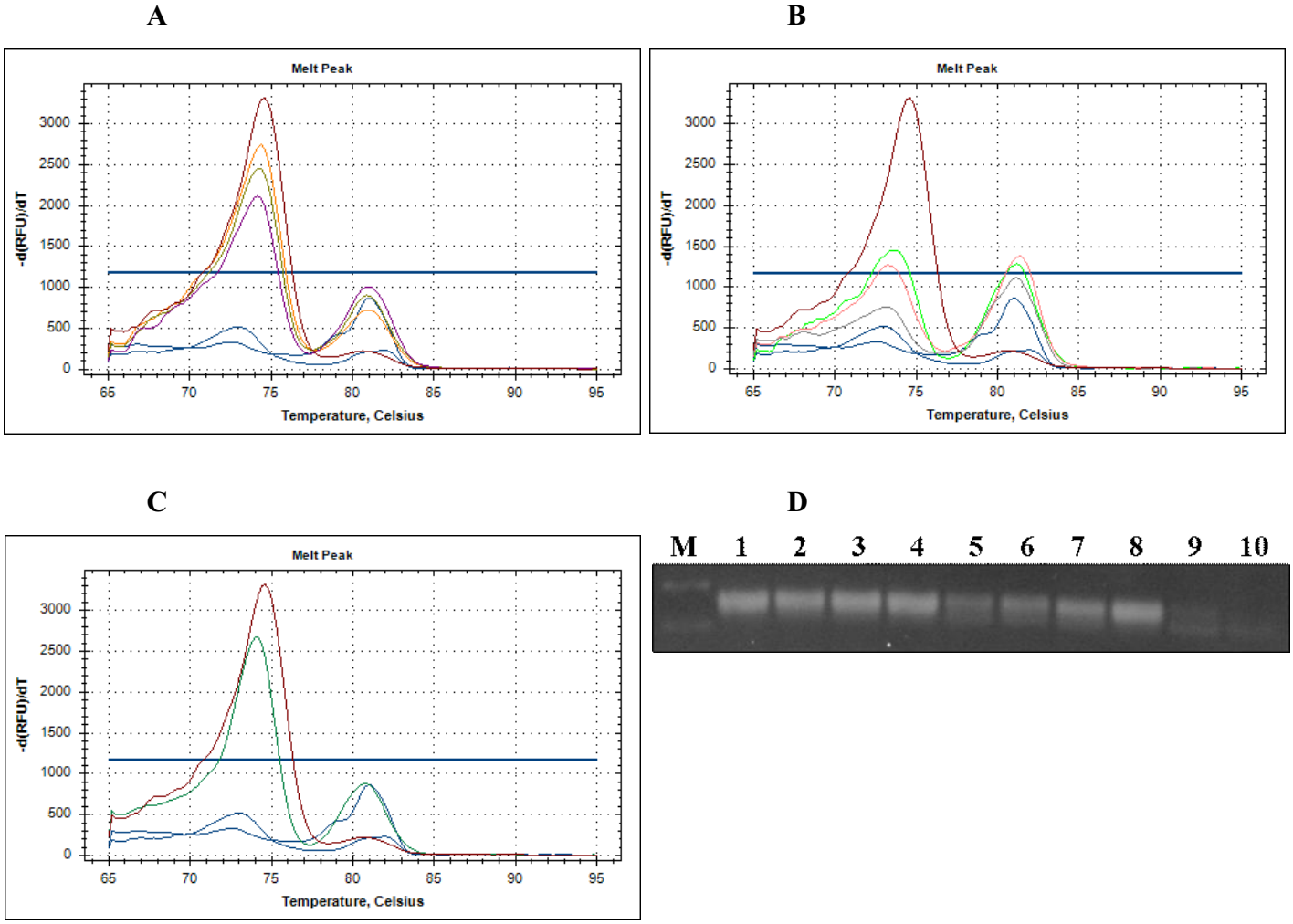

Figure 16- A, B, C and D. (A-B-C) Real Time PCR - HRM analysis of Cell-SELEX round 5. **(A)** Eluted oligonucleotides 1 µl (dark red). Eluted oligonucleotides and 1:10 diluted: 1 µl (violet), 2.5 µl (olive) and 5 µl (orange). **(B)** Eluted oligonucleotides 1 µl (dark red). Eluted oligonucleotides and 1:100 diluted: 1 µl (grey), 2.5 µl (pink) and 5 µl (light green). **(C)** Eluted oligonucleotides 1 µl (dark red) and cell-extracted oligonucleotides 1 µl (dark green). Blue are the negative controls. **(D)** Gel electrophoresis of Real Time PCR products. M is ΦX174 DNA BsuRI (HaeIII) marker (118 bp and 72 bp). Lane 1 is eluted oligonucleotides 1 µl. Lanes 2, 3 and 4 are the eluted oligonucleotides 1:10 diluted, of 1 µl, 2.5 µl and 5 µl, respectively. Lanes 5, 6 and 7 are the eluted oligonucleotides 1:100 diluted, of 1 µl, 2.5 µl and 5 µl, respectively. Lane 8 is the cell-extracted oligonucleotides 1 µl. Lanes 9 and 10 are the negative controls.

Cell-extracted oligonucleotides recovered from Cell-SELEX round 8 showed a melting profile that was very similar to the round fifth (Figure 16- C), with a main melting peak registered at around 74 °C and a second melting peak registered at a higher temperature of around 80 °C (Figure 17- A).

Also for round 8, as shown previously for round 5, the gel electrophoresis of the Real Time PCR products (Figure 17- B) showed one DNA band in between the marker bands of 50 and 100 bp, which was congruent with the expected amplicon size of 80 bp. Notwithstanding, an extra DNA band was also present at lower molecular weight and probably it was due to primer-dimers formation. The full gel image is reported in Figure S17 in the Supplementary Materials section.

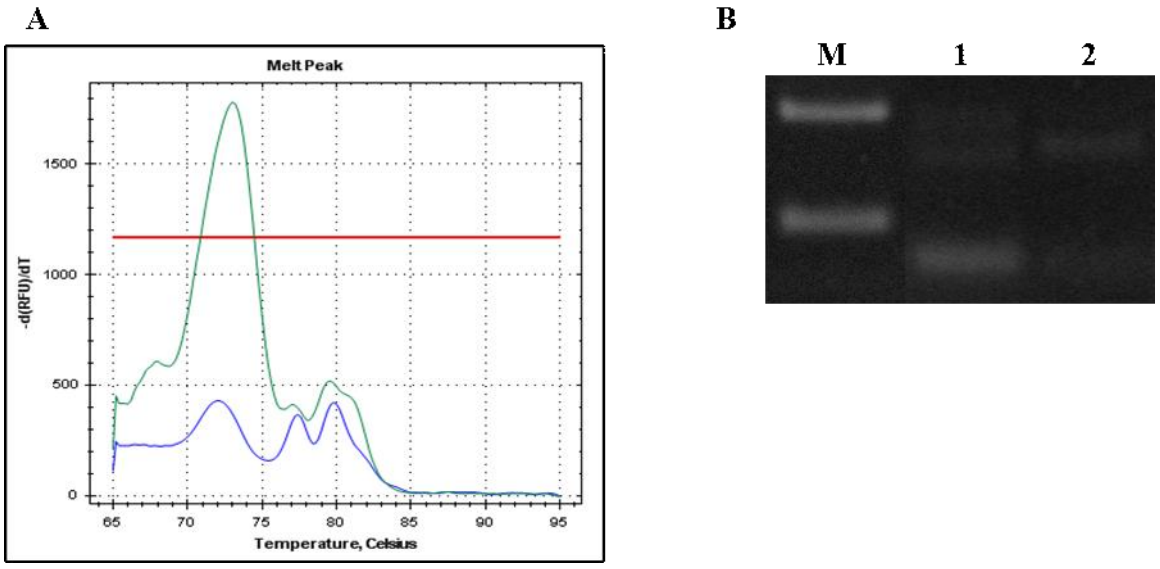

Figure 17- A and B. (A) Real Time PCR - HRM analysis of Cell-SELEX round 8. Cell-extracted oligonucleotides are the green curve. Negative control is the blue curve. **(B)** Gel electrophoresis of Real Time PCR products. M is *SHARPMASS*™ 50 marker (100 bp and 50 bp). Lane 1 is cell-extracted oligonucleotides. Lane 2 is the negative control.

5.1.4 Sequencing of potential aptamers

Selected internalizing aptamers from round 2 of Cell-SELEX I, were cloned and sequenced. From the cloning experiment all 29 picked colonies resulted positive to the colony-PCR amplification (Figure 18- A and B) and the sequence of the cloned insert of 8 positive clones are reported in Table 33. Full gel images are reported in Figure S18- A and B at Supplementary Materials section.

Table 34 reported the alignment of the random regions which showed some shared sequences. The AAACTACAG motif was detected in potential aptamers 2 and 5 while the potential aptamer 8 showed a similar motif, AxCTxACAG. Potential aptamers 3 and 5 shared AGAGT and AACTA motifs. Potential aptamers 3 and 4 shared a TxTCAACxxxAT motif.

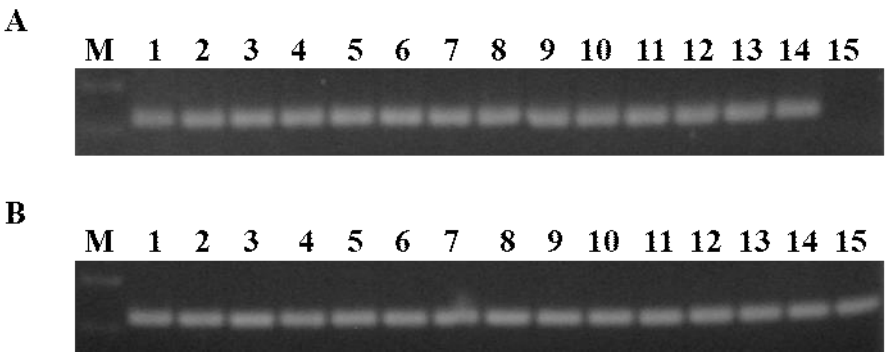

Figure 18- A and B. Colony-PCR on cells transformed with the cell-extracted oligonucleotides of Cell-SELEX I round 2. **(A)** M is ΦX174 DNA BsuRI (HaeIII) marker (118 bp and 72 bp). Lanes 1 to 14 are the screened colonies from number 1 to number 14. Lane 15 is the negative control. **(B)** M is ΦX174 DNA BsuRI (HaeIII) marker (118 bp and 72 bp). Lanes 1 to 15 are the screened colonies from number 15 to number 29.

Table 33. Potential aptamer sequences of Cell-SELEX I round 2. Random regions are highlighted in bold.

N°	Sequence (5′ - 3′)
1	AGCATAGAGACATCTGCTATTGGTAGCACA**CTTTAGAGTGACTCGCGGAG**TGTGCAACCGTAGACTCCAG ACTTCAGGTA
2	AGCATACAGACATCTGCTATTGGTAGCACA**TACGAAACTACAGCATCAGT**TGTGCAACCGTAGACTCCAG ACTTCAGGTA
3	AGCATCCAGACATCTGCTATTGGTAGCACA**AGAGTTGTTTTCAACTAGAT**TGTGCAACCGTAGACTCCAGA CTTCAGGTA
4	AGCATACAGACATCTGCTATTGGTAGCACA**TGTCAACACTATACGTCAGA**TGTGCAACCGTAGACTCCAG ACTTCAGGTA
5	AGCATACAGACATCTGCTATTGGTAGCACA**AGAGTGACCAAAACTACAGG**TGTGCAACCGTAGACTCCAG ACTTCAGGTA
6	TACCTGAAGTCTGGAGTCTACGGTTGCACA**TCAGACTGAAAGACAGCCCC**TGTGCTACCAATAGCAGATG TCTCTATGCT
7	AGCATACAGACATCTGCTATTGGTAGCACA**TCGTAACGGGGGCTTAGAGC**TGTGCAACCGTAGACTCCAG ACTTCAGGTA
8	AGCATAGAGACATCTGCTATTGGTAGTACA**CTATTGACCTAACAGTACTG**TGTGCAACCGTAGACTCCAG ACTTCAGGTA

Table 34. Alignment of the random regions of the potential aptamer sequences of Cell-SELEX I round 2. Shared motives are highlighted in bold.

N°	Alignment
2	----------TACG**AAACTACAG**--CATCAGT
5	-----**AGAGT**GACCA**AAACTACAG**--G------
8	---------CTATTG**A**C**CT**A**ACAG**TACTG----
3	-----**AGAGT**TGT**TT**TCAACTA**G**AT--------
4	----------**T**G**TCAAC**ACT**AT**ACGTCAGA

A more complete and deeper work was performed for potential internalizing-aptamers coming from round 6 of Cell-SELEX II. Table 35 reports the results of the analysis of the sequences obtained from the total analysed 597 octamers. The table highlights the octamers that, with two miss-matches allowed, occur most frequently within in the random regions of the obtained sequences.

Table 35. Octamers from random regions of potential aptamer of Cell-SELEX II round 6.

Octamer	Frequency	N°
GTGTATGT	30	48-282
TATTAATT	30	35-259
GTTCTGTA	30	98
		132
GGGTATAT	30	24-250
		106
		120
GGATCATT	30	9-239
TGGCAATG	30	21-285
ATCTATTA	29	38-263
TCTTTATT	29	72
		118
GGCAGTTT	29	2-279

5.1.5 Evaluation of internalizing ability of some selected potential aptamers

Some potential aptamers bringing the octamers displayed in Table 35 were assessed for their capability to internalize into plant cells.

The results of the quantification of the potential aptamer amount internalized into plant protoplasts, estimated by quantitative PCR of the cell lysate after repeated washing, are reported in Table 36. For the quantification, a calibration curve was constructed for each potential aptamer. According to the results, the amount of aptamers 132, 118, 120, 35-259 and 106 that was internalized into the protoplasts was of 2.69×10^{-7}, 1.89×10^{-7}, 1.98×10^{-9}, 1.90×10^{-7} and 3.02×10^{-9} fmol/cell, respectively. Id est, for aptamer 132, was about 89 folds higher than aptamer 106 and about 136 folds higher than aptamer 120. While for aptamers 118 and 35-259 was about 63 folds higher than aptamer

106 and about 96 folds higher than aptamer 120. The internalized amount of the poly A oligonucleotide, used as control, was estimated to be of 2.05×10^{-8} fmol/cell.

The octamer GTGTATGT which had one of the highest internalization frequencies was selected for further use in the construction of the chimeric synthetic biosensor.

Table 36. Internalized amounts of potential aptamers of Cell-SELEX II round 6.

Oligonucleotide	Amount (fmol/cell)
poly A	2.05×10^{-8}
132	2.69×10^{-7}
118	1.89×10^{-7}
120	1.98×10^{-9}
35-259	1.90×10^{-7}
106	3.02×10^{-9}

5.2 Development of pathogen specific aptamers

5.2.1 SELEX on *Pf*LDH

5.2.1.1 Preliminary test on MH35 library

As a preliminary experiment, Real Time PCR - HRM analysis was performed on MH35 library to determine the melting peaks of MH35 library.

MH35 library showed a main melting peak that was registered approximatively at 71 °C (Figure 19- A). Thus, this melting temperature was associated to the condition where the MH35 library showed the highest diversity among the random regions of the sequences.

Real Time PCR products were analysed by electrophoresis on agarose gel (Figure 19- B). MH35 library dilutions 100 nM, 10 nM and 1 nM showed a smear immediately above the bands of interest that could be related with the different composition of the random regions. Single stranded DNA portions originated after the HRM analysis could impact the DNA migration. The full gel image is reported in Figure S19 in the Supplementary Materials section.

A

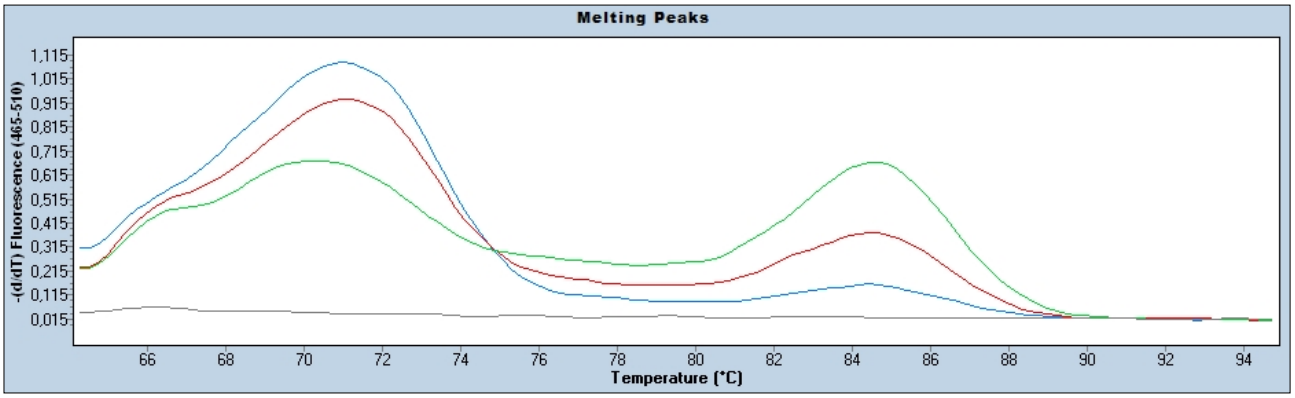

B

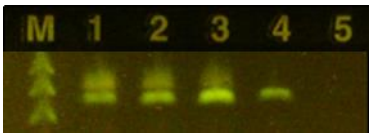

Figure 19- A and B. (A) Real Time PCR - HRM analysis of MH35 library diluted 100 nM (blue curve), 10 nM (dark red curve) and 1 nM (dark green curve) prior to selection. Negative control is the grey curve. **(B)** Electrophoresis on agarose gel of Real Time PCR products. M is Low Molecular Weight DNA Ladder (100 bp, 75 bp and 50 bp). Lanes 1, 2, 3 and 4 are MH35 library 100 nM, 10 nM, 1 nM and 0.1 nM, respectively. Lane 5 is the negative control.

5.2.1.2 Real Time PCR – HRM analysis

Real Time PCR – HRM analysis of SELEX rounds was displayed at Figure 19- A.

Starting from round 3 (Figure 20- A, violet curve) a melting peak was detected at approximatively 89 °C, potentially indicative that the diversity of the sequences may have started to decrease.

By proceeding with the selection until round 6 (Figure 20- A, pink curve), the melting peak reached approximatively the temperature of 90 °C. Compared the Round 3, it suggests that more similar sequences have been selected.

Round 10 (Figure 20- A, light blue curve) showed a very similar melting peak to that one was registered for the Round 6 at 90 °C. This result suggests, after the round 6, the selective pressure on the recovered sequences had reached a stable level.

Real Time PCR products were analysed by electrophoresis on agarose gel (Figure 20- B). All tested conditions showed the DNA band of interest in between the 50 bp and 75 bp bands of the DNA ladder. MH35 library dilutions 1 nM, 0.5 nM and 0.2 nM, together with round 3 and 1:2000 dilutions of round 6 and round 10, showed a smear immediately above the bands of interest that could be related with the different composition of the random regions. The full gel image is reported in Figure S20 in the Supplementary Materials section.

A

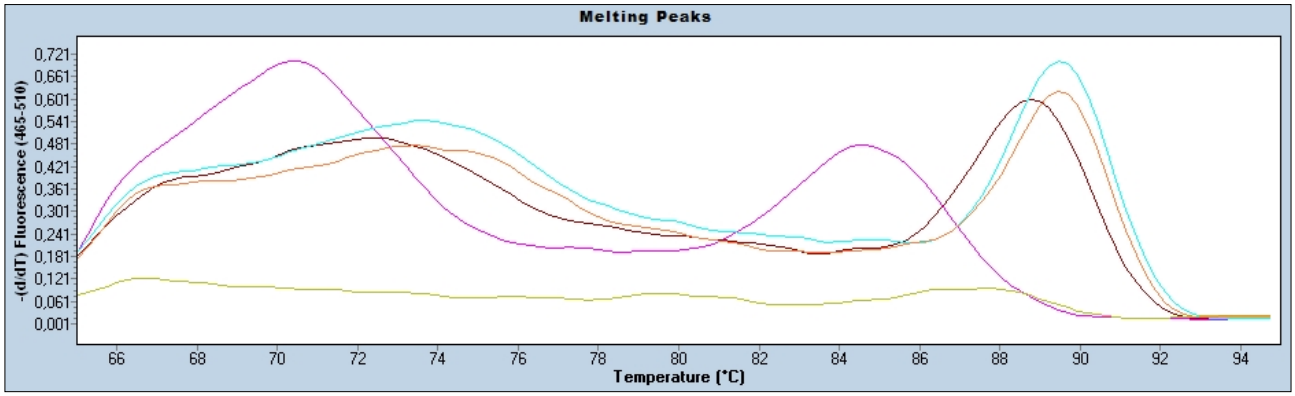

B

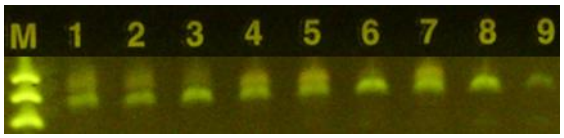

Figure 20- A and B. (A) Real Time PCR - HRM analysis of SELEX rounds 3, 6 and 10. MH35 library diluted 1 nM prior selection (purple curve), round 3 (violet curve), round 6 (pink curve) and round 10 (light blue curve). Negative control is the grey curve. **(B)** Electrophoresis on agarose gel of Real Time PCR products. M is Low Molecular Weight DNA Ladder (100 bp, 75 bp and 50 bp). Lanes 1, 2 and 3 are MH35 library prior selection of 1 nM, 0.5 nM and 0.2 nM, respectively. Lane 4 is round 3. Lanes 5 and 6 are round 6 dilution 1:2000 and dilution 1:10000, respectively. Lanes 7 and 8 are round 10 dilution 1:2000 and dilution 1:10000, respectively. Lane 9 is the negative control.

5.2.1.3 Potential aptamer cloning, sequencing and evaluation of their target-specificity

The results of round 10 of SELEX were cloned and 51 of the screened colonies resulted positive to the colony-PCR amplification.

The sequencing results of fifty potential aptamers of the Round 10 of SELEX are displayed in Table 37.

Table 37. Potential aptamer sequences of the round 10 of SELEX. Random regions are highlighted in bold.

N°	Sequence (5′ - 3′)
2	CGTACGGTCGACGCTAGC**CGGAGGGGGGTCGATGTGTCACGGCTGCAGCTGGG**CACGTGGA GCTCGGATCC
4	CGTACGGTCGACGCTAGC**CCCAGCCGGTCCGGCCCCCTCGGCAGCGGTGGTGC**CACGTGGA GCTCGGATCC
5	CGTACGGTCGACGCTAGC**CGGAGGGCGAGGTGGTACCGCCCCTCAGCCGCTGG**CACGTGGA GCTCGGATCC
8	CGTACGGTCGACGCTAGC**CGGACGGAACCAGCCCGCTCGTGTCCCGGGGCCGC**CACGTGGA GCTCGGATCC
10	CGTACGGTCGACGCTAGC**CAGGGGACGGGCAGCGGTCAAAGGGGCGGGGCTTG**CACGTGGA GCTCGGATCC
11	CGTACGGTCGACGCTAGC**CCACACCGGCGGGCTGAGGGTAGGGCCCCGGTCTG**CACGTGGA GCTCGGATCC
14	CGTACGGTCGACGCTAGC**CAGCGAGGGGGGCACGGGCATGGGGGTGTCTGGCG**CACGTGGA GCTCGGATCC

15	CGTACGGTCGACGCTAGC**CGGAGCGGGGGGGACCCCGTAATCAGCCCCCCTGG**CACGTGGA GCTCGGATCC
16	CGTACGGTCGACGCTAGC**CGCAGGTGGGGGCAAGCTGTAGGTCGGCGCATGGG**CACGTGGA GCTCGGATCC
20	CGTACGGTCGACGCTAGC**CCGTGTGTGGACGGTGGCACCCAGCACCAGGTGCG**CACGTGGA GCTCGGATCC
22	CGTACGGTCGACGCTAGC**CCGGCGGACGGGTCAGGGTCTCACTCCGCGGCTGG**CACGTGGA GCTCGGATCC
24	CGTACGGTCGACGCTAGC**CGGGGAGAGGGCAGGCCTGGGGATGTGCAACGTGG**CACGTGGA GCTCGGATCC
25	CGTACGGTCGACGCTAGC**CCCACGGATCACGCGCAGCTCCGGGTCCATGGTGC**CCACGTGGAG CTCGGATCC
31	CGTACGGTCGACGCTAGC**CCCAGGGTCCCCCGGCGGGTATCGAGTGACGCTGG**CACGTGGA GCTCGGATCC
38	CGTACGGTCGACGCTAGC**CGGCCAGGGTCTCAGGTACGGCTCATCCGGTGGCC**CACGTGGA GCTCGGATCC
40	CGTACGTCGACGCTAGCC**CGGCAGGGTAGCCACAGAGGGACGCGGTGGGTCG**CACGTGGAG CTCGGATCC
42	CGTACGGTCGACGCTAGC**CGGCAGCCAACGGGGCCAAGCCAGGCGGGGTGTGC**CCACGTGGA GCTCGGATCC
44	CGTACGGTCGACGCTAGC**GCTACCTTATGGCGCGCCCTCCAGTCTAATCTCAA**CACGTGGAG CTCGGATCC
49	CGTACGGTCGACGCTAGC**GGATACTGCAGTTGGTCTGGATTAGCAGCATGCAT**CACGTGGAG CTCGGATCC
50	CGTACGGTCGACGCTAGC**CGGGGGACCAACACGTCCACGGGATGCGGGCTTGG**CACGTGGA GCTCGGATCC
51	CGTACGGTCGACGCTAGC**CAGGCGCGTAAACGCTCGGGGCTACCGCTCGGTGG**CACGTGGA GCTCGGATCC
52	CGTACGGTCGACGCTAGC**CCCCACCACCCGATGTCAGCTCGTAGACCGGGGCG**CACGTGGAG CTCGGATCC
53	CGTACGGTCGACGCTAGC**CAGGGGTGGGCAGCTGAGGAGACGGTGGGGCTTGG**CACGTGGA GCTCGGATCC
54	CGTACGGTCGACGCTAGC**CGGGGCGTGCAACACGGAGACAGGCTGCATGTGGG**CACGTGGA GCTCGGATCC
57	CGTACGGTCGACGCTAGC**CCCCAGCACAGCCGCGGATGGGACCCTCCAGCTGC**CACGTGGA GCTCGGATCC
60	CGTACGGTCGACGCTAGC**GGGCCAGGGCACCCCGGCACGGTGCCGCGCATGCG**CACGTGGA GCTCGGATCC
62	CGTACTGTCGACGCTAGC**CGGAGCGGGTGCGAGGGTCAGATCCATCCGGTGGC**CACGTGGA GCTCGGATCC
66	CGTACGGTCGACGCTAGC**CGGCTAGGGACGCAGGGCCACCCACCCGCGCTGTA**CACGTGGA GCTCGGATCC
67	CGTACGGTCGACGCTAGC**CAGCGGGTGCGCCAGGTTCGTCAGTGCATCCGCGGC**CACGTGG AGCTCGGATCC
68	CGTACGGTCGACGCTAGC**CGGATCCCCCCTGCCCCCGATAGACCCCCGGTGGG**CACGTGGAG CTCGGATCC
70	CGTACGGTCGACGCTAGC**CACCCACGCGATAGGGCACAGGCAGCCCGGGTTGC**CACGTGGA GCTCGGATCC
71	CGTACGGTCGACGCTAGC**CGGAGAGCGATGGACACGGCCCCTCCCCGGGTTCG**CACGTGGA GCTCGGATCC
72	CGTACGGTCGACGCTAGC**CCGGCCAGGGACACCTACCCCCGTCCTGCACCCG**CACGTGGAGC TCGGATCC
73	CGTACGGTCGACGCTAGC**AGGGCACGCGGGGGCCGGGGCACACCTAGGCTGGC**CACGTGGA GCTCGGATCC
75	CGTACGGTCGACGCTAGC**CAGGCCGGGGGAGACAGGTCACAGGGTGCGTTGGC**CACGTGGA GCTCGGATCC
76	CGTACGGTCGACGCTAGC**CGGGGGGGAGGAGCGGGTACAGCCAGGGTGGTCCG**CACGTGGA GCTCGGATCC
78	CGTACGGTCGACGCTAGC**TTGGCCCCCGTGAGGGGACTAAAGGGCAGGTACCA**CACGTGGA GCTCGGATCC

79	CGTACGGTCGACGCTAGC**CCACCCCGGCGCCTAGGGGACCCTCATACGCCTGG**CACGTGGAG CTCGGATCC
80	CGTACGGTCGACGCTAGC**CGGGCAGCGGAGTCCAAACCCCGGGTGGCCCCTGG**CACGTGGA GCTCGGATCC
88	CGTACGGTCGACGCTAGC**CCACGGACTCCAGCCGGTCCAGATCCTCCCGTGG**CACGTGGAGC TCGGATCC
92	CGTACGGTCGACGCTAGC**AGGGCGGAGGCGGTCTGGGGAACCCGCTGGGCTCG**CACGTGGA GCTCGGATCC
96	CGTACGGTCGACGCTAGC**CCACGAGGGTCAGCGCATGGAGGGTCGGACGTCGG**CACGTGGA GCTCGGATCC
97	CGTACGGTCGACGCTAGC**CCCGGCGTACATCCGCTACGCCCCCGGCCGCATGC**CCACGTGGAG CTCGGATCC

The alignment of the random regions of potential aptamers showed some interesting similarities (Figure 21- A, B, C, D and E).

Potential aptamers from colonies number 2 and 16 shared CCCA, CTCxG and TGGTGC motives (Figure 21- A).

Potential aptamers from colonies number 10 and 50 shared CxGGGGAC, GTCxAxGGG and GGGCTTG motives. Potential aptamers from colonies number 10 and 53 shared CxGGGG, GGGCAGCxG and GGGCTTG motives. Potential aptamers from colonies number 50 and 53 shared CxGGGG and GGGCTTGG motives (Figure 21- B).

Potential aptamers from colonies number 38 and 62 shared CGG, GGGT, AGG and CATCCGGTGG motives (Figure 21- C).

Potential aptamers from colonies number 70 and 71 shared GCGAT, GGxCAC, CxxCCCGGGTT motives (Figure 21- D).

Potential aptamers from colonies number 62 and 67 shared AGCGGGTGCG, AGG, GTCAG, TxCATCC and GxGGC motives (Figure 21- E).

Interestingly, potential aptamers from colonies number 44 and 49 showed T-rich sequences, which suggests the presence of $dU^{C}TP$ within the random regions. Their sequences were GCTACCTTATGGCGCGCCCTCCAGTCTAATCTCAA with nine thiamines (underlined) and GGATACTGCAGTTGGTCTGGATTAGCAGCATGCAT with ten thiamines (underlined), respectively.

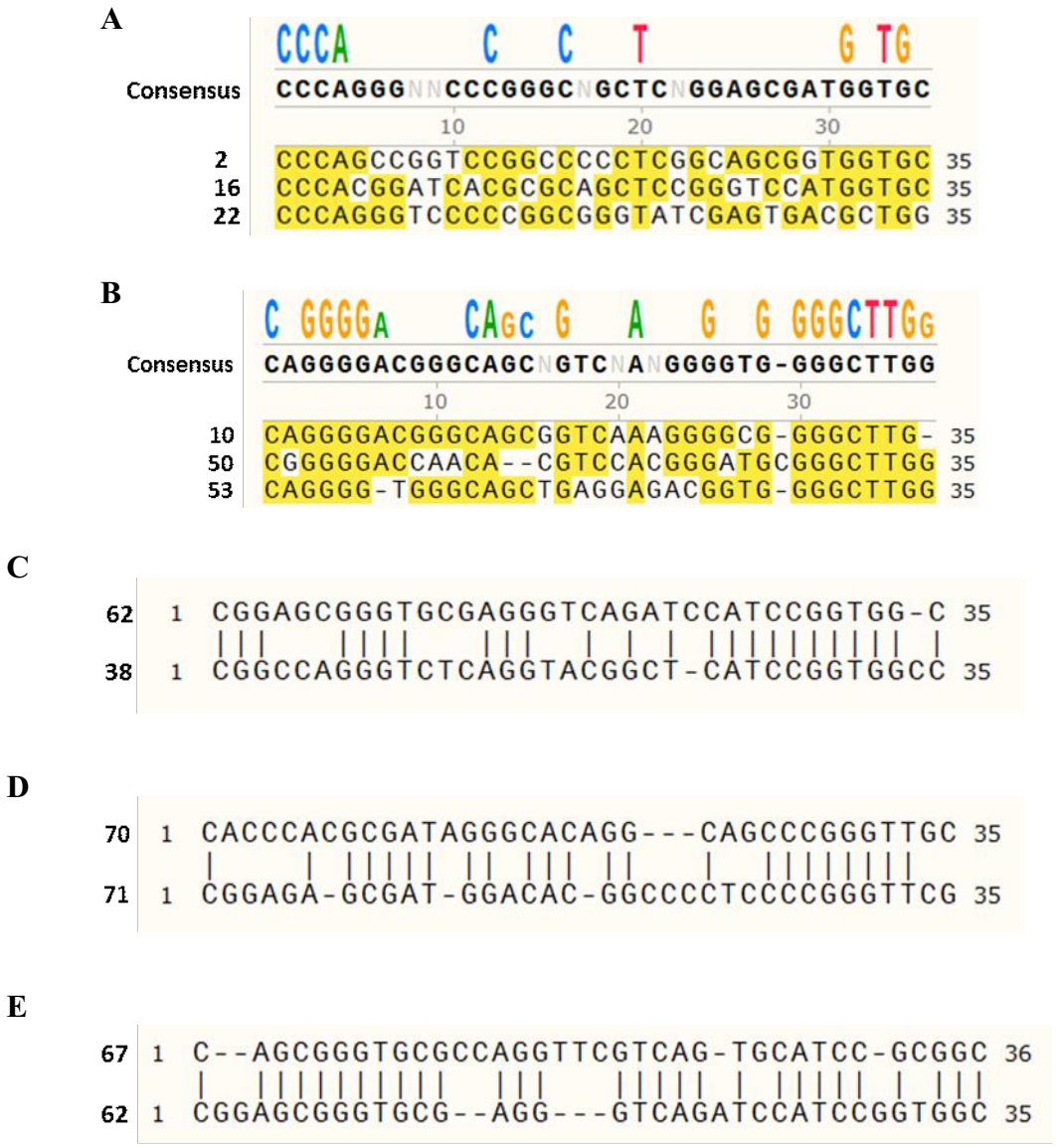

Figure 21- A, B, C, D and E. Alignment of random regions of potential aptamers from colonies n° 2, 10, 16, 22, 38, 50, 53, 62, 67, 70 and 71 of round 10 of SELEX.

The binding assay of potential aptamers which showed important similarities coming from the alignment was reported in Figure 22. The registered fluorescence signals originated from the flow-through, the wash and the elution steps of each binding assay. The gel electrophoresis showed that potential aptamers (black squares) coming from colonies number 2 (lane 1), 10 (lane 2), 16 (lane 3), 22 (lane 4), 38 (lane 5), 49 (lane 7), 50 (lane 8), 53 (lane 9) and 70 (lane 12) had specificity to the target. Especially for colonies number 10, 16, 22, 38 and 49 the signals were quite intense.

Instead, the results of the binding assay for colony 44 was negative, since no bands at the expected size have been detected in all three recovered fractions.

The full gel image is reported in Figure S22 in the Supplementary Materials section.

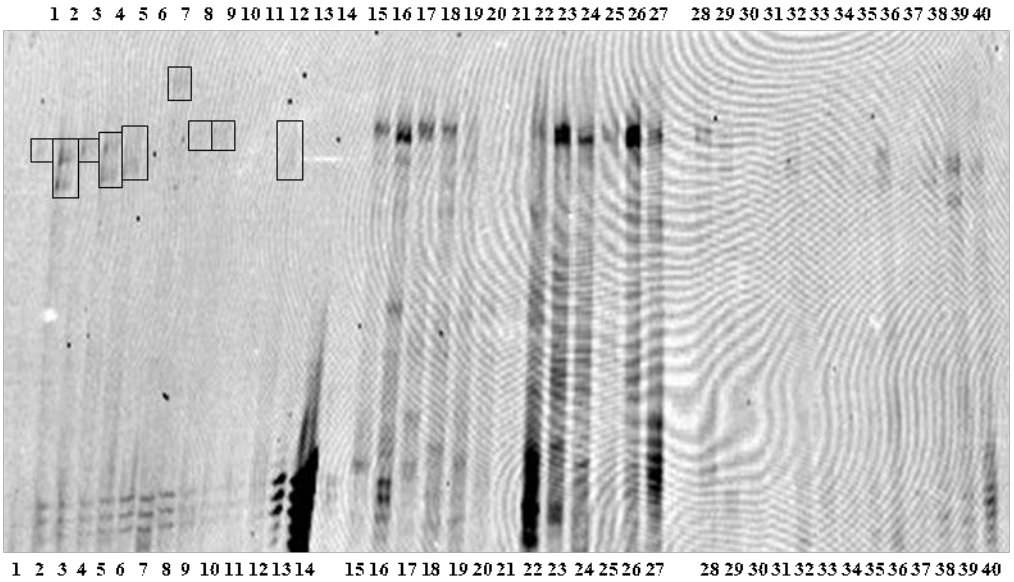

Figure 22. Denaturing polyacrylamide gel of elution (lanes 1 to 13), flow-through (lanes 15 to 27) and wash (lanes 28 to 40) steps of potential aptamers from round 10. Colony n° 2 is lanes 1, 15 and 28; n° 10 is lanes 2, 16 and 29; n° 16 is lanes 3, 17 and 30; n° 22 is lanes 4, 18 and 31; n° 38 is lanes 5, 19 and 32; n° 44 is lanes 6, 20 and 33; n° 49 is lanes 7, 21 and 34; n° 50 is lanes 8, 22 and 35; n° 53 is lanes 9, 23 and 36; n° 62 is lanes 10, 24 and 37; n° 67 is lanes 11, 25 and 38; n° 70 is lanes 12, 26 and 39; n° 71 is lanes 13, 27 and 40. Lane 14 is [6FAM]MH36 primer. Black squares highlight the specificity of some potential aptamers to the target.

5.2.2 Cloning, expression and purification of flagellin from *Pseudomonas syringae* pv. *tomato* DC3000, *Pseudomonas syringae* pv. *tabaci* and *Pseudomonas fluorescens-4* strains

Before to proceed with the cloning of flagellin genes, the identity of the strains as member of the *Pseudomonas* genus was confirmed by 16S rDNA sequencing of the relative PCR products of *Pto*, *Pta* and *Pf4* (Figure 23- A).

After that, suitable annealing temperatures for F0 – R0 primers were screened as reported in Figure 23- B to prepare the flagellin genes for subsequent PCRs and cloning. The best annealing temperature for PsF0 / PsR0 primers was 54 °C (Figure 23- B, lane 1 for *Pto* and lane 4 for *Pta*) and for Pf4F0 / Pf4R0 primers was 52 °C (Figure 23- B, lane 10).

The same annealing temperatures were also adopted for F1 – R1 primers, since their sequences included F0 – R0 primers, as reported by the gel electrophoresis at Figure 23- C.

In the end, Figure 23- D displayed the gel electrophoresis of the standard PCRs with F2 – R2 primers which were the last preparative PCRs before the cloning of flagellin genes.

The full gel images are reported in Figure S23- A, B, C and D in the Supplementary Materials section.

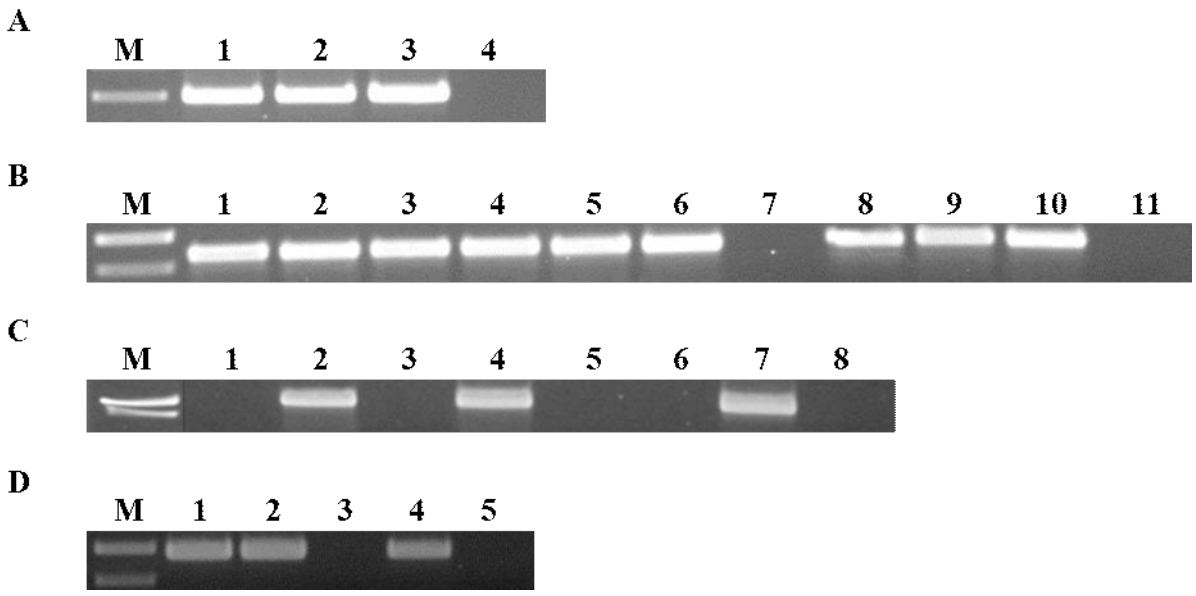

Figure 23- A, B, C and D. (A) Standard PCR amplification of 16S rDNA genes of *Pto*, *Pta* and *Pf4* gDNAs. M is GeneRuler^{TM} 1 Kb DNA Ladder (1 500 bp) marker. Lane 1 is *Pto*. Lane 2 is *Pta*. Lane 3 is *Pf4*. Lane 4 is the negative control. Expected amplicon sizes are of 1 504 bp. **(B)** Gradient PCR amplification with F0 and R0 primers of flagellin genes of *Pto*, *Pta* and *Pf4* gDNAs. M is GeneRuler^{TM} 1 Kb DNA Ladder marker (1 000 bp and 750 bp). Lanes 1, 2 and 3 are *Pto* at 54 °C, 53 °C and 52 °C, respectively. Lanes 4, 5 and 6 are *Pta* at 54 °C, 53 °C and 52 °C, respectively. Lane 7 is PsF0 / PsR0 negative control. Lanes 8, 9 and 10 are *Pf4* at 54 °C, 53 °C and 52 °C, respectively. Lane 11 is Pf4F0 / Pf4R0 negative control. **(C)** Standard PCR amplification with F1 and R1 primers of flagellin genes of *Pto*, *Pta* and *Pf4* gDNAs. M is GeneRuler^{TM} 1 Kb DNA Ladder marker (1 000 bp and 750 bp). Lanes 1 and 2 are *Pto* with 10 and 30 amplification cycles, respectively. Lanes 3 and 4 are *Pta* with 10 and 30 amplification cycles, respectively. Lane 5 is PsF1 / PsR1 negative control. Lanes 6 and 7 are *Pf4* with 10 and 30 amplification cycles, respectively. Lane 8 is Pf4F1 / Pf4R1 negative control. **(D)** Standard PCR amplification with F2 and R2 primers of F1 - R1 PCR products. M is GeneRuler^{TM} 1 Kb DNA Ladder marker (1 000 bp and 750 bp). Lane 1 is *Pto*. Lane 2 is *Pta*. Lane 3 is PsF2 / PsR2 negative control. Lane 4 is *Pf4*. Lane 5 is Pf4F2 / Pf4R2 negative control.

The cloning was performed between the digestion products of pET-14b plasmid vector, displayed at Figure 24- A, and the digested flagellin genes as described in material and methods section.

The transformation of the *Pto*-flagellin gene resulted in 33 positive colonies to the colony-PCR over 60 screened colonies (Figure 24- B, C and D).

A similar trend was shown by the transformations of *Pta*- and *Pf4*- flagellin genes, where 38 (Figure 24- E, F and G) and 37 (Figure 24- H, I and J) colonies were positive to the colony-PCR over 50 screened colonies, respectively.

The full gel images are reported in Figure S24- A, B, C, D, E, F, G, H, I and J in the Supplementary Materials section.

The sequence of the plasmid inserts of the recombinant pET-14b clones containing the flagellin fragment amplified from *Pto* respected the flagellin sequence reported in NCBI (Gene ID: 1183594). Also the sequence of the plasmid inserts of the recombinant pET-14b clones containing

the flagellin fragment amplified from *Pta* respected the flagellin sequence reported in NCBI (GenBank: AB061230.2).

Instead, the sequence of the plasmid inserts of the recombinant pET-14b clones containing the flagellin fragment amplified from *Pf4* showed a single nucleotide polymorphism throughout the flagellin sequence compared to the NCBI accession (Gene ID: 15559583).

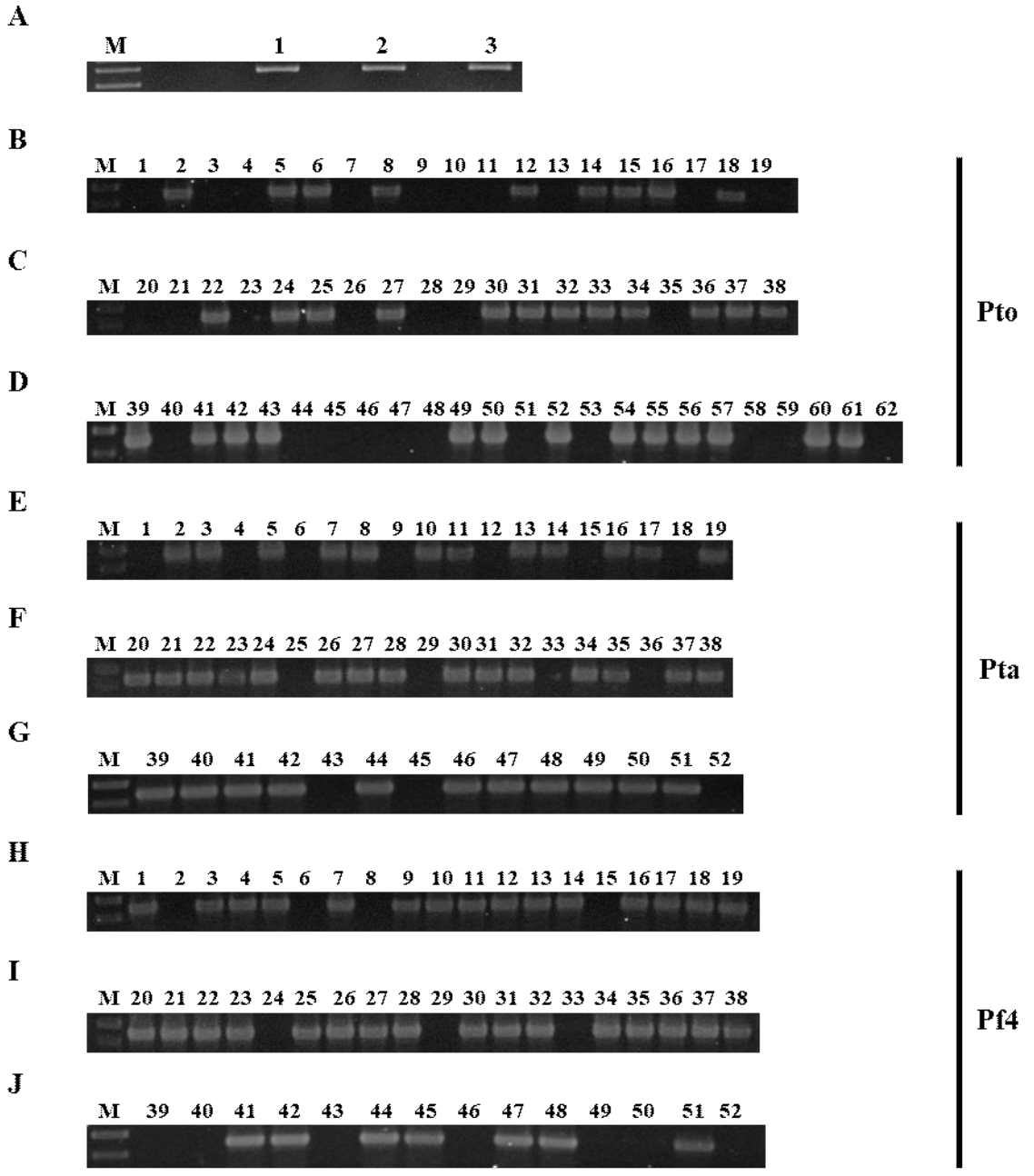

Figure 24- A, B, C, D, E, F, G, H, I and J. (A) pET-14b plasmid vector double-digested with *Xba*I and *Bam*HI restriction enzymes. M is GeneRuler^{TM} 1 Kb DNA Ladder marker (5 000 bp and 4 000 bp). Lanes 1, 2 and 3 are the digestion products. **(B-C-D)** Colony-PCR on JM101 cells transformed with ligation product of pET-14b plasmid vector and *Pto*-flagellin. M is GeneRuler^{TM} 1 Kb DNA Ladder marker (1 000 bp and 750 bp). Lanes 1 to 60 are the screened colonies from number 1 to number 60. Lane 61 is *Pto* gDNA. Lane 62 is the negative control. **(E-F-G)** Colony-PCR on

JM101 cells transformed with ligation product of pET-14b plasmid vector and *Pta*-flagellin. M is GeneRuler^{TM} 1 Kb DNA Ladder marker (1 000 bp and 750 bp). Lanes 1 to 50 are the screened colonies from number 1 to number 50. Lane 51 is *Pta* gDNA. Lane 52 is the negative control. **(H-I-J)** Colony-PCR on JM101 cells transformed with ligation product of pET-14b plasmid vector and *Pf4*-flagellin. M is GeneRuler^{TM} 1 Kb DNA Ladder marker (1 000 bp and 750 bp). Lanes 1 to 50 are the screened colonies from number 1 to number 50. Lane 51 is *Pf4* gDNA. Lane 52 is the negative control.

Expression of *Pto*-flagellin was only detected into the insoluble fraction of *E. coli*, at the expected size of approximatively 30 kDa (Figure 25- C). The full Western Blot image is reported in Figure S25 in the Supplementary Materials section.

Pto-flagellin purification was displayed in Figure 25- A and B, and the flagellin band was clearly detected from the lane 3 to the lane 7 of the elution steps at the height of approximatively 30 kDa according to the protein Standards (Figure 25- B).

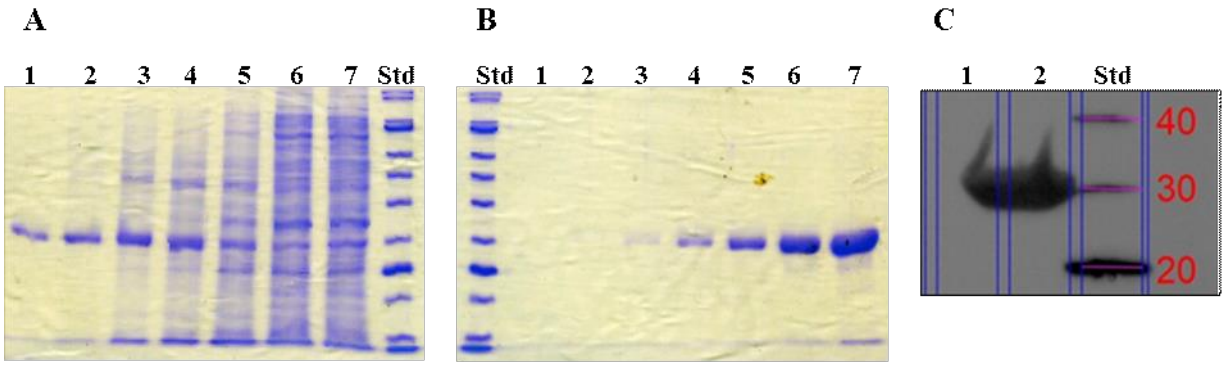

Figure 25- A, B and C. **(A-B)** SDS-PAGE of the purification steps of *Pto*-flagellin. **(A)** Lanes from 1 to 5 are the ninth, seventh, fifth, third and first wash steps, respectively. Lane 6-7 are the flow-through steps. Std is the mPAGE Unstained Protein Standards (200 kDa, 150 kDa, 100 kDa, 85 kDa, 60 kDa, 50 kDa, 40 kDa, 30 kDa, 25 kDa, 20 kDa and 15 kDa). **(B)** Std is the mPAGE Unstained Protein Standards. Lanes from 1 to 7 are the seventh, sixth, fifth, fourth, third, second and first elution steps, respectively. Expected protein size is approximatively of 30 kDa. **(C)** Western Blot of soluble and insoluble fractions of *E. coli* before protein purification. Lane 1 is the soluble fraction. Lane 2 is the insoluble fraction. M are the Protein Standards (40 kDa, 30 kDa and 20 kDa).

5.2.3 SELEX on *Pto*-flagellin

Pto-flagellin was fully expressed into the insoluble fraction of *E. coli* (Figure 25- C), hence the following purification and the refolding, have been challenging since the protein easily precipitated after the removal of the urea. A SELEX against the *Pto*-flagellin was preliminary performed with the low complexity, standard library LIB1.0 to verify that specific aptamers could be selected even if the target was not completely stable. The future goal will be select for cubane-modified aptamers or cubamers using the high complexity MH35 library.

The monitoring of the selection progress by Real Time PCR and HRM analysis showed a melting peak at 81 °C since the first SELEX rounds (Figure 26- A and B). This melting peak was flanking the main melting peak at around 74 °C typical of the LIB1.0 library prior selection, that was already registered during the previous Cell-SELEX experiments (Figure 10- C).

The melting peak registered at a higher melting temperature did not show any change from round 2 to the round 8 of the selection (Figure 26- A and B).

Gel electrophoresis of Real Time PCR products showed a single DNA band in between the marker bands of 50 bp and 100 bp, which is congruent with the expected amplicon sizes of 80 bp. This meant that the two detected melting peaks originated from the selected sequences amplified by Real Time PCR and no PCR by-products were generated (Figure 26- C). The full gel image is reported in Figure S26 in the Supplementary Materials section.

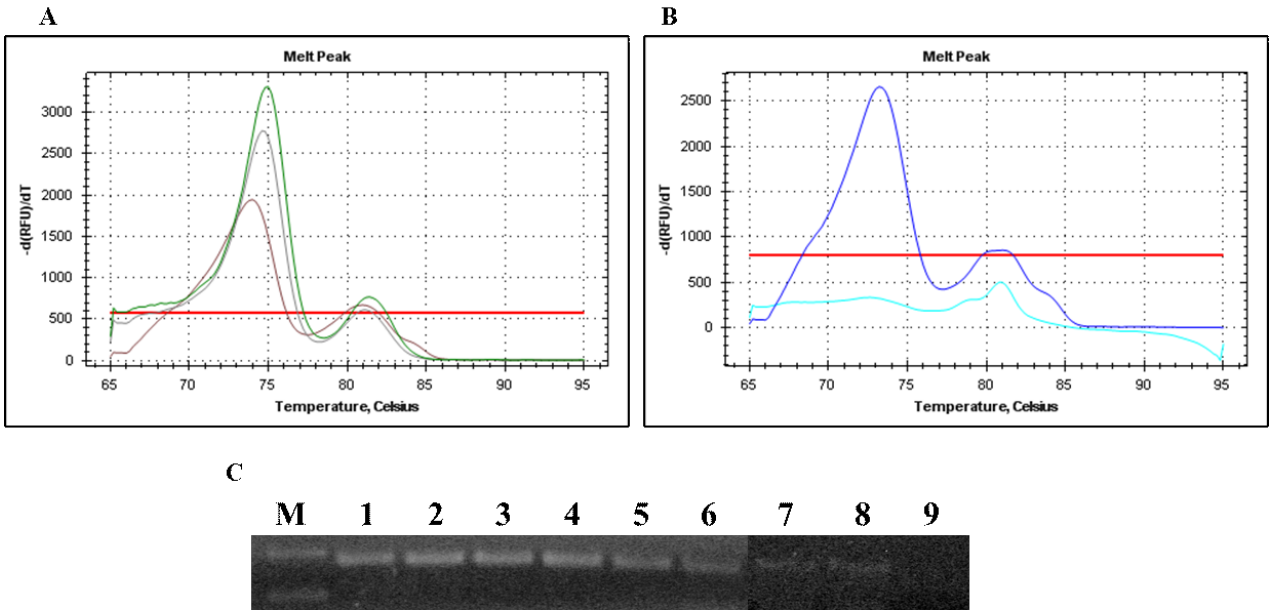

Figure 26- A, B and C. (A) Real Time PCR - HRM analysis of SELEX rounds 2 (green curve), 4 (grey curve) and 6 (brown curve). **(B)** Real Time PCR **-** HRM analysis of SELEX round 8 (blue curve), negative control is the light blue curve. **(C)** Gel electrophoresis of Real Time PCR products. M is *SHARPMASS*^{TM} 50 marker (100 bp and 50 bp). Lanes 1 to 8 are SELEX rounds 1 to 8, respectively. Lane 9 is the Real Time PCR negative control.

5.2.3.1 Sequencing of potential aptamers and alignment

Selected potential aptamers from round 8 were sequenced as reported in Table 38. The alignment of the random regions showed some noticeable similarities among all 80 sequences analysed.

Potential aptamers 1, 3, 8, 10, 12, 14 resulted with the same random region, as also for aptamers 2, 4, 9, 11, 13.

Potential aptamers 53, 54, 60, 66, 74, 76, 87 shared the same following motif, GxACCTTGGCCxxxxxGCxx (Figure 27).

A portion of the random region from aptamers 66, 74 and 76 namely, CCTTGGCCGCTTTGCGC, was selected for further use in the construction of the chimeric synthetic biosensor.

Table 38. Random regions of potential aptamer of round 8 of the SELEX.

N°	Sequence (5′ - 3′)
1	CGCCGCCACCTATAACGGAT
2	TGACGGATAATCGGGTATAC
3	CGCCGCCACCTATAACGGAT
4	TGACGGATAATCGGGTATAC
5	TAAAAAACCATTGAGAAAGT
6	CTTTTGTTGCATCCGCATGG
7	TATGATGTAATGAGCTCTG
8	CGCCGCCACCTATAACGGAT
9	TGACGGATAATCGGGTATAC
10	CGCCGCCACCTATAACGGAT
11	TGACGGATAATCGGGTATAC
12	CGCCGCCACCTATAACGGAT
13	TGACGGATAATCGGGTATAC
14	CGCCGCCACCTATAACGGAT
15	TAAAAAACCATTGAGAAAGT
16	ATAGTCTACGCGATAGTGTT
17	ATGCGTATACATCAGGCTTT
18	ACTCGGTTCCGATTGCCTGT
19	GGGACTTGGGATATCCATTG
20	TGATAAGGTTAGCGAAGAGT
21	CTTTGTCGCAGTCGATCAGC
22	GGTTCCTGGCCGCGTAGCGC
23	ACCTTCTTTTATAGGTGACA
24	AAATTCTCCGCATGGGCTTT

25	GATAATTGTTGGCCATACAT
26	CTTCCAGGTACCATTCTACA
27	GACTCCAGACTTCAGGCAGC
28	GTAAGACTTTCCATGATAGT
29	GTTTGTTAGGATTACATTTG
31	GTTCCCTGGCCGCTTAGCGC
32	GGTCATTTGACGCATTCGCT
37	CTTTTGTTGCATCCGCATGG
38	ACGTTTAGCACGTACTGCAT
39	GATAATTGTTGGCCATACAT
41	GTAAGACTTTCCATGATAGT
46	TAAAAAACCATTGAGAAAGT
48	CCATCCTTTGATTACGT
49	ATGCGTATACATCAGGCTTT
51	ACTCGGTTCCGATTGCCTGT
52	CCATCCTTTGATTACGT
53	GAACCTTGGCCGCATCGC
54	GTACCTTGGCCGCACTGCGC
55	CTAACAGTAGTGGCGAATTC
56	CGTGTGCCGTCCTACGTA
58	ACTAGCCGTTGTATTCTCTT
59	TCTACTGATTTGAGCACACG
60	GGTACCTTGGCCCGAAGGCG
61	TAGGTATAAGGCCATGCT
62	AATCCCTGCCGCTTATTGGT
63	GGTTTACCTCAAGCGTAGTG
64	CGGTTGTACTTCGCCACTAG
65	TCGCGTGTTTTGATTGACCA
66	GTACCTTGGCCGCTTTGCGC
68	GTATAAACGAGCCTAGCGAC
69	AGGTATCTGTAACTACGGTT
70	ATCTAAAAGAACTGACTGCA
72	AGGTATCTGTAACTACGGTT
73	ATCTAAAAGAACTGACTGCA
74	GTACCTTGGCCGCTTTGCGC

75	AGTGAGACTTCGTAGAACATAAG
76	GTACCTTGGCCGCTTTGCGC
77	ACTATGCAAGAACCCCCTAT
78	TCTTGATTATACACACACTG
79	TCTTGATTATACACACACTG
80	GGTCATTTGACGCATTCGCT
81	GAGAGCTTACTGTACAAAAT
82	TATGATGTAATGAGCTCTG
83	GGTCATTTGACGCATTCGCT
84	GAGAGCTTACTGTACAAAAT
85	TATGATGTAATGAGCTCTG
86	GGGACTTGGGATATCCATTG
87	GAACCTTGGCCGCATCGC
88	TGCTCTACTGGGGTTTCTGT
89	GATGAATCGATTCAATATAG
94	CGTCAGCTAGCGTCCTGATC
96	GATGAATCGATTCAATATAG
101	CTTTTGTTGCATCCGCATGG
104	GGTTCCTGGCCGCGTAGCGC
106	GGTTCCTGGCCGCGTAGCGC
108	TGGCAGCGGGTATCGAGCAG

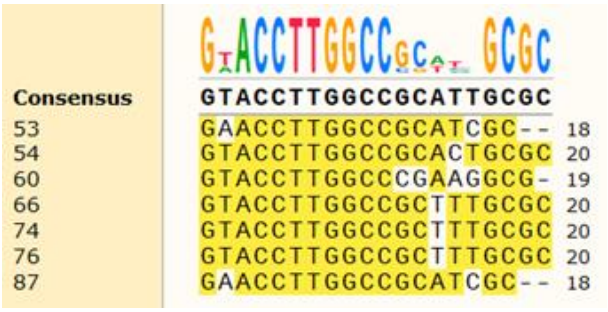

Figure 27. Alignment of random regions of potential aptamers 53, 54, 60, 66, 74, 76 and 87 from round 8 of the SELEX.

5.3 Switchable synthetic biosensor design

A model of a switchable synthetic biosensor was designed to simulate the plant cell-internalization of AtlsiRNA-1 in a pathogen-specific manner (Figure 28). The synthetic designed molecule is a hybrid of two aptamers, the aptamer specific for the *Pto*-flagellin and the aptamer which specifically promotes the plant cell-internalization of its cargo, namely AtlsiRNA-1.

When the specific aptamer for *Pto*-flagellin (Figure 28, pink background) binds its target the hybrid is destabilized and the aptamer for the plant cell-internalization (Figure 28, green background) is exhibited and allows the internalization of AtlsiRNA-1 (Figure 28, blue background).

The design includes the use of the following oligonucleotides: PtoflagAptamer (5′-TACCCTTGGCCGCTTTGCGCA-3′) and Int_AtlsiRNA-1 (5′-CCAAGTGTATGTCGAUGAACAGAUGCUUCUGGUUCUGAAGAUCGCCUGUUACT-3′).

PtoflagAptamer was the aptamer to specifically recognize the *Pto*-flagellin, while Int_AtlsiRNA-1 was the aptamer to allow the plant cell-internalization of AtlsiRNA-1 (above underlined to highlight ribonucleoside residues).

For the design of the switchable synthetic biosensor were chosen the octamer GTGTATGT which had shown one of the highest internalization frequencies and a selected portion of the random region from potential aptamers 66, 74 and 76, 5′-CCTTGGCCGCTTTGCGC-3′, selected against the *Pto*-flagellin.

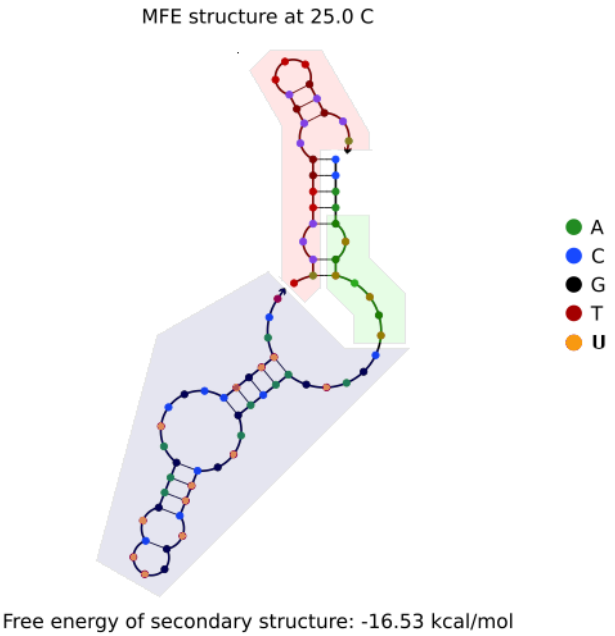

Figure 28. Representation of the model of a switchable synthetic biosensor which allows the plant cell-internalization of AtlsiRNA-1 in a pathogen-specific manner.

6. DISCUSSION

6.1 Aptamers for stimulation of plant defence

A novel strategy was designed to stimulate *in vivo* the plant defence response upon pathogen trigger. Such strategy exploits aptamers, functional nucleic acids oligomers that have found several applications in the scientific field, such as in biosensing and biotechnology, but with very few examples of application in the plant field. This relative novelty was a strong motivation in the development of specific DNA aptamers which modulated the plant defence response, but also a big challenge due the lack of previously developed protocols specifically tailored for the plant field.

A primary challenge for this work was the selection for DNA aptamers which specifically internalised into plant cells. Cell-internalizing aptamers may have wide applications in plant biotechnology, providing an interesting molecular tool to specifically deliver exogenous signals or molecules to plant cells. In this view, my intent was to design and develop a chimera based on a cell-internalizing aptamer which specifically delivers a small oligonucleotide involved in plant defence stimulation, such as AtlsiRNA-1 [Katiyar-Agarwal et al., 2007].

The designed chimera is activated by another aptamer which was selected against the flagellin from *Pseudomonas syringae* pv. *tomato* DC3000, a model pathogen of *Arabidopsis thaliana* [Whalen et al., 1991], making the plant defence stimulation specific to the presence of this microorganism.

Plants respond to pathogen invasions using a two-branched innate immune system. The first branch recognizes and responds to molecules which are common and shared by many classes of microorganisms, including non-pathogens [Jones and Dangl, 2006]. These biomarkers are called PAMPs and stimulate the PTI (PAMPs Triggered Immunity) defence line. At this stage, plants activate generic physiological responses intended for resisting against a pathogen attack [Bigeard et al., 2015]. The second branch is called ETI (Effector Triggered Immunity) and is an accelerated and amplified version of the PTI which responds to specific pathogen virulence factors, also named effectors, usually activating a hypersensitive cell death response at the infection site [Jones and Dangl, 2006]. Effectors act by impairing the PTI response, but thanks to the AtlsiRNA-1 activity, the PTI could be re-established. AtlsiRNA-1 was demonstrated to be a positive regulator of the basal defence response in *Arabidopsis thaliana* by downregulating the expression of *AtRAP* gene, which is known to have a negative role in plant disease resistance [Katiyar-Agarwal et al., 2007].

Thanks to the chimeric biosensor, plants could readily activate the defence response mechanism in a pathogen-specific manner by the internalization of AtlsiRNA-1, stopping the

pathogen spreading as soon as the infection took place, even in absence of resistance genes activating ETI.

Several reports have already proposed and applied the utilisation of small dsRNAs to efficiently stimulate the endogenous RNA interference machinery of plants to protect them from pest invasions [Fletcher et al., 2020; Mezzetti et al., 2020; Zotti et al., 2018]. Nevertheless, one of the main topics that researchers are facing is about finding convenient solutions of applications of small dsRNAs to plants, since transgenic crops producing pest-specific dsRNAs have still many restrictions and hence the transformation of many crop species is not applicable [Fletcher et al., 2020; Zotti et al., 2018]. Recent innovations concern topical applications of dsRNAs by foliar spray or root drenching to induce gene silencing as a new strategy for plant protection [Fletcher et al., 2020; Mezzetti et al., 2020; Zotti et al., 2018]. A clear example of efficient foliar spray of dsRNAs was applied by Mitter and colleagues, which explored the use of dsRNA complexed with layered double hydroxide nanosheets, also termed BioClay, which conferred 20 or more days of plant protection from viral infections [Mitter et al., 2017].

In this view, the amelioration that I tried to introduce with this work is to render the internalization of a dsRNA associated to the plant defence stimulation an event totally dependent to the presence of a specific plant pathogen. In this way, the synthetic chimeric biosensor aims to limit the cell load and, at the same time, it can be opportunely designed to confer plant resistance to different pathogens.

Therapeutic oligonucleotides based on small dsRNAs are also important in the human field, helping for example to limit cancer cells [Kruspe and Giangrande, 2017; McNamara et al., 2006; Thiel and Giangrande, 2010]. So far, the main problems regarding the application of small dsRNAs to cells concern their polyanionic nature, which limits their cell-penetration because of poor transit across lipid bilayers; and their poor specificity to the target [Kruspe and Giangrande, 2017; McNamara et al., 2006]. Therefore, the necessity to design and apply efficient carriers to help the cell-internalization of therapeutic dsRNAs is one of the key points in order to develop an effective therapy based on dsRNAs both for humans and plants.

In this view, the use of aptamers complexed to small dsRNAs to form chimeras to specifically deliver therapeutic oligonucleotides to the target cells has been already efficiently exploited in the human field [Kruspe and Giangrande, 2017; McNamara et al., 2006; Thiel and Giangrande, 2010].

Therefore, a similar approach was applied in this work to efficiently stimulate the plant defence response in a pathogen specific manner thanks to the combination of a specific plant cell-internalizing aptamer, a small dsRNA involved in defence stimulation and an aptamer specific to the pathogen detection. Moreover, since little is known about cell-penetration of nucleic acids, this work

was also designed to contribute to study the internalization of oligonucleotides in plants, by using oligonucleotide aptamers.

6.2 Cell-SELEX on plant cells

Nowadays, the research work concerning Cell-SELEX and Cell-internalization SELEX focuses on human therapeutics and diagnostic fields. Due to the relative novelty of the interest in developing aptamers for applications in the plant field, Cell-SELEX and Cell-internalization SELEX have never been applied to plant cells (to my knowledge).

Therefore, as a part of the preliminary experimentation, pilot experiments were focused on the design of a Cell-SELEX protocol suitable for plant cells.

The protocol was based on the buffers used to sustain the plant protoplasts [Yoo et al., 2007]. WI buffer was exploited as washing buffer to remove non-specifically bound oligonucleotides, while MMg buffer was supplemented with BSA, herring sperm DNA and RNA type-IV according to Sefah et al. [2010] and used as incubation buffer to block unspecific sites on plant cells and to help the aptamer folding. For rounds 7 and 8 a new modality to perform the elution step was introduced, namely the WI buffer was supplemented with NaCl and acetic acid in order to increase the stringency and help the removal of unspecific- and specifically membrane bound- oligonucleotides [Hernandez et al., 2013].

The developed Cell-SELEX protocol succeeded since the protoplasts maintained their integrity throughout all rounds and the non-specifically bound oligonucleotides were apparently washed-away. Even though, the results about the potential aptamer internalization described at the bottom indicated that the elution- and probably also the washing- steps needed to be further optimized. Apparently, neither the more stringent elution step helped, since the HRM analysis of round 8 still highlighted the big variability among the recovered oligonucleotides.

Since my intention was to recover both potential aptamers which specifically bound membrane cells and/or internalized into cell cytoplasm, I found that the ideal elution temperature to recover the first aptamer group maintaining the cell-integrity was of 45 °C. Anyway, at this elution temperature, some protoplasts did not preserve their integrity. Therefore, the choice of this temperature was a compromised to permit at the same time the recovering of both eluting- and internalizing- aptamers. At this stage of the protocol development a complete separation of the two aptamer groups was not achieved. I also consecutively designed a buffer to lyse the remaining cells and recover the second aptamer group.

I performed the Cell-SELEX II assay until round 8, and for cell-internalizing aptamers of round 6, which actually had shown a shift of the melting peak to higher temperature, then I successively proceeded with the evaluation of their capability to internalize into plant cells.

The Cell-SELEX II, starting from round 6, showed the appearance of extra DNA bands at lower molecular weight compared the target size, in both standard- and Real Time- PCR amplifications, presumably primer-dimers. To get rid of these DNA bands, before to proceed with sequencing, I performed multiple gel isolations of the band of interest and re-amplifications by PCR.

The sequence analysis of the products of round 6 showed large sequence diversity in the random region, suggesting the need to continue the Cell-SELEX for more rounds in order to improve the selection and reduce the diversity among the sequences or an absence of internalization-specific sequence signals. Moreover, the multiple consecutive PCRs performed to avoid the DNA bands at low molecular weight may have introduced amplification bias that could contribute to the registered variability among the random regions.

Nevertheless, the sequencing of random regions of the oligonucleotides selected in round 6 allowed the identification of octamers that, with two miss-matches allowed, occur most frequently within in the random regions of the selected sequences.

According to the results of the aptamer internalization assays, putative aptamer 132 internalized approximatively 89 folds more than aptamer 106 and 136 folds more than aptamer 120, while putative aptamers 118 and 35-259 internalized approximatively 63 folds more than aptamer 106 and 96 folds more than aptamer 120 into plant cells. As stated above, the designed protocol did not allow the complete separation between eluted- and internalized- aptamers. Moreover, probably also the washing step was not totally effective. Therefore, the evaluation of the aptamer internalization by Real Time PCR was disturbed presumably by the aptamers which were binding the cell membranes and by non-specific oligonucleotides. In this view, fluorescence microscopy analysis of the plant cells incubated with the putative aptamers bringing a fluorescent tag could help the evaluation of the effective aptamer internalization even in very small amounts. A bioimaging technique *in vivo* to follow the binding of the putative aptamers to the cell membranes and/or their cell-internalization needs therefore to be performed in support to the Real Time PCR results.

Considering the small internalized amount of the aptamers of round 6, probably one crucial aspect could be represented by LIB1.0 library. Its rather short random region and its nature to be a DNA library may have turned out to be limiting choices, especially regarding the main purpose to get cell-internalizing aptamers. In fact, a lot of experimentation about Cell-SELEX and especially Cell-internalization SELEX on animal cells is led with RNA aptamers. This because RNA aptamers can form more diverse and intricate three-dimensional structures thanks to the ability of RNA nucleotides

to make non-Watson-Crick base pairing [Guo, 2010; Zhu et al., 2015], increasing the possibility to form tight interactions with the target. Moreover, RNA aptamers tend to be smaller in size compared DNA aptamers of the same length, helping their internalization into cells [Germer et al., 2013].

Notwithstanding, working with RNA aptamers is more expensive and more time consuming than DNA aptamers. Therefore, being this work the first attempt to get aptamers which specific recognize the membrane cell and/or internalize into cell cytoplasm in plants, probably it made more sense proceeding with DNA aptamers.

Furthermore, there is evidence that extracellular DNA is actively perceived and adsorbed from the soil by various organisms including plants [Mazzoleni et al., 2015]. Hypothesizing that internalization of DNA into cells was a fairly common phenomenon; presumably the DNA needs to be complexed with something else which helps its passage through the cell membranes.

Based on the results about the potential aptamer internalization, in future work the elution step would have to be reconsidered in order to guarantee a complete separation between eluted- and internalizing- aptamers, and as consequence, also the washing step has to be re-designed to efficiently remove the non-specifically bound oligonucleotides. In the end, to help for the specific aptamer internalization could be necessary introduce chemical modifications within the random region of LIB1.0 library with the aim to expand its chemical repertoire.

6.3 SELEXs on pathogen biomarkers

Pto is a well-known pathogen used in experimental infection of *Arabidopsis thaliana* plants. In this work, specific DNA aptamers against its flagellin, previously *in vitro* expressed and purified, were selected.

Flagellin is the main component of bacterial flagella and it is expressed by both plant and human pathogens. It is constituted by four domains: D0, D1, D2 and D3 [Yonekura et al., 2003]. D0 and D1 domains are localized at the N- and C- termini of the protein, respectively, and are very conserved; the recognition of plant- and human- immune receptors and the protein polymerization is based on these domains. D2 and D3 domains instead are widely variable, are localized in the central part of the protein and generate the antigenic diversity described as H-serotypes [Malandrin and Sanson, 1999].

The flagellin was chosen as a target because it is present in all flagellated bacteria and its D2 and D3 central domains are highly specific for each bacterial strain.

In this work *Pto*-flagellin gene was *in vitro* cloned and the protein was expressed, purified and refolded. The protein was fully expressed into the insoluble fraction of *E. coli* as also reported in similar works by Behrouz et al. [2016] and Goudarzi et al. [2009], as the recovery from the soluble fraction has proved not possible. This is commonly regarded as a drawback, because the re-establishment of the native state usually is not completely possible.

To help flagellin expression into the cytoplasm of *E. coli,* different tags could be exploited. Many reports described the efficacy of maltose-binding protein (MBP) fusion as a general strategy to express target proteins into the soluble fraction of *E. coli* [Hewitt et al., 2011]. Others experienced the use of a dual hexa-histidine–maltose-binding protein affinity tag (6×His–MBP) that had the additional advantage of allowing the fusion protein to be purified by immobilized metal affinity chromatography (IMAC) instead of or in addition to amylose affinity chromatography [Sun et al., 2011].

Nonetheless, flagellin purification from the urea-solubilized inclusion bodies of *E. coli* was attempted and successfully performed under denaturing conditions. Urea at high concentrations is commonly used as denaturing agent to destroy secondary protein structure and bring otherwise-insoluble proteins into solution. Urea disrupts hydrogen bonds and hydrophobic interactions both between and within proteins [Zou et al., 1998].

In order to restore the flagellin native state the denaturing agent has to be removed gradually in order to avoid protein aggregation and precipitation, with an empirically determined suitable protein buffer. Ionic strength, buffering system and pH are the main parameters that need be optimized. Ions concentration directly depend by the hydrophilicity of the protein, the pH usually is 1.0-2.0 unit far from the predicted pI of the protein and the buffer is related to the chosen pH.

The *Pto*-flagellin native state was successfully achieved in this work using 20 mM Tris pH 9 as protein buffer, since the predicted pI of the protein was around 7 and because there was evidence that high salt concentrations tend to promote the flagellin polymerization *in vitro* [Asakura et al., 1964]. Despite these precautions, however, the protein tended to precipitate after a few days.

The SELEX experiment was nevertheless successfully conducted on *Pto*-flagellin until the round 8: the protein was renatured as soon as it was needed to start each selection round.

Since the first round potential aptamers have been selected according to the shift of the melting peak to a higher melting temperature. The sequencing confirmed the HRM analysis results and showed the appearance of similar motives among the random regions of the sequences. The SELEX performed on *Pto*-flagellin was a preliminary experiment necessary to investigate if specific potential aptamers could be selected on a not completely stable target as the flagellin. This SELEX allowed to

lay the foundations for the SELEX which will be conducted starting from MH35 library in presence of the cubane, in order to specifically bind the D2 and D3 flagellin domains.

A SELEX in presence of cubane-modified aptamers or cubamers was performed against the *Plasmodium falciparum* (*Pf*) lactate dehydrogenase in order to learn how to menage chemical modification on aptamers. *Pf* is the most virulent parasite among *Plasmodium* spp. that causes malaria in humans. The *Pf* lactate dehydrogenase (*Pf*LDH) is considered as a potential molecular target for antimalarials, due to the parasite dependence on glycolysis for energy production [Penna-Coutinho et al., 2011]. Therefore, *Pf*LDH is also an important biomarker for the detection of malaria. An efficient diagnostic tool should be able to specifically distinguish the same molecular biomarker among the different parasite species, but canonical DNA aptamers are not so sensitive [Cheung et al., 2020]. In this work, cubamers have been introduced to try to reach this goal since a cubamer highly specific for *Plasmodium vivax* LDH (*Pv*LDH) was recently isolated [Cheung et al., 2020].

To conclude, the flagellin polymerization to form the flagella is naturally occurring both *in vivo* and *in vitro* [Asakura et al., 1964], but SELEX can be performed on this target, as showed here, and it is therefore not convenient to search for technical solutions to help the protein solubility. Moreover, the protein sites which will be available for the binding with aptamers will be those ones which presumably will be not involved in the protein polymerization, suggesting, that the late stages of the selection should be performed starting from a mature form of the protein.

7. CONCLUSION

This work provides a contribute to the development of innovative ways to protect plants from diseases exploiting plant immunity without genetic manipulation. Here, the specificity provided by the aptamers, would permit the stimulation of the plant immune system in a pathogen-specific manner thanks to the specific internalization of AtlsiRNA-1.

For the first time a Cell-SELEX approach was applied to plant cells, with the design of a suitable Cell-SELEX protocol that, however, still needs to be optimized at the washing and elution steps.

Another technological advance reported in this thesis concerns the SELEX carried out on the flagellin isolated from *Pseudomonas syringae* pv. *tomato* DC3000, highlighting that, even though the protein was not completely stable, the selection of potential aptamers could be reached by renaturing the protein just in time for the inclusion in the assay.

Finally, this work provided further support to the incorporation of cubane in aptamers as means to increase the affinity to the target, laying the foundations of a SELEX in presence of cubane-modified aptamers to specifically recognize the D2 and D3 domains of *Pto*-fagellin.

Although there is still a long way to go toward the accomplishment of the initial goal of the project, this demonstrated its technical feasibility and provided a solid basis for further development. Accordingly, a first preliminary model of a structure switching aptamer-based biosensor which enable the plant cell-internalization of AtlsiRNA-1 in a pathogen-specific manner to specifically stimulate *in vivo* the plant defence response was already conceived and presented.

8. BIBLIOGRAPHY

Asakura S, Eguchi G, Iino T. 1964. Reconstitution of bacterial flagella *in vitro*. *Journal of Molecular Biology*. 10(1): 42-56.

Bayat P, Nosrati R, Alibolandi M, Rafatpanah H, Abnous K, Khedri M, Ramezani M. 2018. SELEX methods on the road to protein targeting with nucleic acid aptamers. *Biochimie*. 154: 132-155.

Behrouz B, Amirmozafari N, Khoramabadi N, Bahroudi M, Legaee P, Mahdavi M. 2016. Cloning, Expression, and Purification of *Pseudomonas aeruginosa* Flagellin, and Characterization of the Elicited Anti-Flagellin Antibody. *Iranian Red Crescent Medical Journal*. 18(6): e28271.

Bianchini M, Radrizzani M, Brocardo MG, Reyes GB, Gonzalez Solveyra C, Santa-Coloma TA. 2001. Specific oligobodies against ERK-2 that recognize both the native and the denatured state of the protein. *Journal of Immunological Methods*. 252(1-2): 191-197.

Bigeard J, Colcombet J, Hirt H. 2015. Signaling Mechanisms in Pattern-Triggered Immunity (PTI). *Molecular Plant*. 8(4): 521-539.

Buell CR, Joardar V, Lindeberg M, Selengut J, Paulsen IT, Gwinn ML, Dodson RJ, Deboy RT, Durkin AS, Kolonay JF, Madupu R, Daugherty S, Brinkac L, Beanan MJ, Haft DH, Nelson WC, Davidsen T, Zafar N, Zhou L, Liu J, Yuan Q, Khouri H, Fedorova N, Tran B, Russell D, Berry K, Utterback T, Van Aken SE, Feldblyum TV, D'Ascenzo M, Deng WL, Ramos AR, Alfano JR, Cartinhour S, Chatterjee AK, Delaney TP, Lazarowitz SG, Martin GB, Schneider DJ, Tang X, Bender CL, White O, Fraser CM, Collmer A. 2003. The complete genome sequence of the *Arabidopsis* and tomato pathogen *Pseudomonas syringae* pv. *tomato* DC3000. *Proceedings of the National Academy of Sciences*. 100(18): 10181-10186.

Cai S, Yan J, Xiong H, Liu Y, Peng D, Liu Z. 2018. Investigations on the interface of nucleic acid aptamers and binding targets. *The Analyst*. 143(22): 5317-5338.

Carothers JM, Goler JA, Kapoor Y, Lara L, Keasling JD. 2010. Selecting RNA aptamers for synthetic biology: investigating magnesium dependence and predicting binding affinity. *Nucleic Acids Research*. 38(8): 2736-2747.

Chang AY, Chau VWY, Landas JA, Pang Y. 2017. Preparation of calcium competent *Escherichia coli* and heat-shock transformation. *JEMI Methods*. 1: 22-25.

Chen M, Yu Y, Jiang F, Zhou J, Li Y, Liang C, Dang L, Lu A, Zhang G. 2016. Development of Cell-SELEX Technology and Its Application in Cancer Diagnosis and Therapy. *International Journal of Molecular Sciences*. 17(12): 2079.

Cheung YW, Röthlisberger P, Mechaly AE, Weber P, Levi-Acobas F, Lo Y, Wong AWC, Kinghorn AB, Haouz A, Savage GP, Hollenstein M, Tanner JA. 2020. Evolution of abiotic cubane chemistries in a nucleic acid aptamer allows selective recognition of a malaria biomarker. *Proceedings of the National Academy of Sciences*. 117(29): 16790-16798.

Ciancio DR, Vargas MR, Thiel WH, Bruno MA, Giangrande PH, Mestre MB. 2018. Aptamers as Diagnostic Tools in Cancer. *Pharmaceuticals*. 11(3): 86.

Civit L, Fragoso A, O'Sullivan CK. 2012. Evaluation of techniques for generation of single-stranded DNA for quantitative detection. *Analytical Biochemistry*. 431(2): 132-138.

Civit L, Taghdisi SM, Jonczyk A, Haßel SK, Gröber C, Blank M, Stunden HJ, Beyer M, Schultze J, Latz E, Mayer G. 2017. Systematic evaluation of cell-SELEX enriched aptamers binding to breast cancer cells. *Biochimie*. 145: 53-62.

Colombo M, Mizzotti C, Masiero S, Kater MM, Pesaresi P. 2010. Peptide aptamers: The versatile role of specific protein function inhibitors in plant biotechnology. *Journal of Integrative Plant Biology*. 57(11): 892-901.

Colombo M, Masiero S, Rosa S, Caporali E, Toffolatti SL, Mizzotti C, Tadini L, Rossi F, Pellegrino S, Musetti R, Velasco R, Perazzolli M, Vezzulli S, Pesaresi P. 2020. NoPv1: a synthetic antimicrobial peptide aptamer targeting the causal agents of grapevine downy mildew and potato late blight. *Scientific Reports*. 10(1): 17574.

Dangl JL and Jones JDG. 2001. Plant pathogens and integrated defence responses to infection. *Nature*. 411(6839): 826-833.

Davydova A, Vorobjeva M, Pyshnyi D, Altman S, Vlassov V, Venyaminova A. 2016. Aptamers against pathogenic microorganisms. *Critical Reviews in Microbiology*. 42(6): 847-865.

Diafa S and Hollenstein M. 2015. Generation of Aptamers with an Expanded Chemical Repertoire. *Molecules*. 20(9): 16643-16671.

Ellington A and Szostak J. 1990. In vitro selection of RNA molecules that bind specific ligands. *Nature*. 346(6287): 818-822.

Famulok M. 1994. Molecular Recognition of Amino Acids by RNA-Aptamers: An L-Citrulline Binding RNA Motif and Its Evolution into an L-Arginine Binder. *Journal of the American Chemical Society*. 116(5): 1698-1706.

Famulok M and Mayer G. 2014. Aptamers and SELEX in Chemistry & Biology. *Chemistry & Biology*. 21(9): 1055-1058.

Fletcher SJ, Reeves PT, Hoang BT, Mitter N. 2020. A Perspective on RNAi-Based Biopesticides. *Frontiers in Plant Science*. 11(51): 1-10.

Gao S, Zheng X, Jiao B, Wang L. 2016. Post-SELEX optimization of aptamers. *Analytical and Bioanalytical Chemistry*. 408(17): 4567-4573.

Germer K, Leonard M, Zhang X. 2013. RNA aptamers and their therapeutic and diagnostic applications. *International journal of biochemistry and molecular biology*. 4(1): 27-40.

Gopinath SCB. 2016. Aptamers. *Encyclopedia of Analytical Chemistry*. 1-33.

Gopinath SCB, Lakshmipriya T, Chen Y, Arshad MKMd, Kerishnan JP, Ruslinda AR, Al-Douri Y, Voon CH, Hashim U. 2016. Cell-targeting aptamers act as intracellular delivery vehicles. *Applied Microbiology and Biotechnology*. 100(16): 6955-6969.

Goudarzi G, Sattari M, Roudkenar MH, Montajabi-Niyat M, Zavaran-Hosseini A, Mosavi-Hosseini K. 2009. Cloning, expression, purification, and characterization of recombinant flagellin isolated from *Pseudomonas aeruginosa*. *Biotechnology Letters*. 31(9): 1353-1360.

Guo P. 2010. The Emerging Field of RNA Nanotechnology. *Nature Nanotechnology*. 5(12): 833-842.

Guo KT, Ziemer G, Paul A, Wendel H. 2008. CELL-SELEX: Novel Perspectives of Aptamer-Based Therapeutics. *International Journal of Molecular Sciences*. 9(4): 668-678.

Hermann T and Patel DJ. 2000. Adaptive Recognition by Nucleic Acid Aptamers. *Science*. 287(5454): 820-825.

Hernandez L, Flenker K, Hernandez F, Klingelhutz A, McNamara J, Giangrande P. 2013. Methods for Evaluating Cell-Specific, Cell-Internalizing RNA Aptamers. *Pharmaceuticals*. 6(3): 295-319.

Hewitt SN, Choi R, Kelley A, Crowther GJ, Napuli AJ, Van Voorhis WC. 2011. Expression of proteins in *Escherichia coli* as fusions with maltose-binding protein to rescue non-expressed targets in a high-throughput protein-expression and purification pipeline. *Acta Crystallographica Section F Structural Biology and Crystallization Communications.* 67(9): 1006-1009.

Houston SD, Fahrenhorst-Jones T, Xing H, Chalmers BA, Sykes ML, Stok JE, Farfan Soto C, Burns JM, Bernhardt PV, De Voss JJ, Boyle GM, Smith MT, Tsanaktsidis J, Savage GP, Avery VM, Williams CM. 2019. The cubane paradigm in bioactive molecule discovery: further scope, limitations and the cyclooctatetraene complement. *Organic & Biomolecular Chemistry*. 17(28): 6790-6798.

Islam W, Noman A, Qasim M, Wang L. 2018. Plant Responses to Pathogen Attack: Small RNAs in Focus. *International Journal of Molecular Sciences*. 19(2): 515.

Jayasena S. 1999. Aptamers: An Emerging Class of Molecules That Rival Antibodies in Diagnostics. *Clinical Chemistry*. 45(9): 1628-1650.

Jin Q, Thilmony R, Zwiesler-Vollick J, He SY. 2003. Type III protein secretion in *Pseudomonas syringae*. *Microbes and Infection*. 5(4): 301-310.

Jones JDG and Dangl JL. 2006. The plant immune system. *Nature*. 444: 323-329.

Katagiri F, Thilmony R, He SY. 2002. The Arabidopsis Thaliana-Pseudomonas Syringae Interaction. *The Arabidopsis Book*. 1:1-35.

Katiyar-Agarwal S, Gao S, Vivian-Smith A, Jin H. 2007. A novel class of bacteria-induced small RNAs in *Arabidopsis*. *Genes & Development*. 21(23): 3123-3134.

Kim YS and Gu MB. 2014. Advances in Aptamer Screening and Small Molecule Aptasensors. *Advances in Biochemical Engineering/Biotechnology*. 140: 29-67.

Kruspe S and Giangrande PH. 2017. Aptamer-siRNA Chimeras: Discovery, Progress, and Future Prospects. *Biomedicines*. 5(4): 45.

Kuduva SS, Craig DC, Nangia A, Desiraju GR. 1999. Cubanecarboxylic Acids. Crystal Engineering Considerations and the Role of C−H···O Hydrogen Bonds in Determining O−H···O Networks. *Journal of the American Chemical Society*. 121(9): 1936-1944.

Lapa SA, Chudinov AV, Timofeev EN. 2016. The Toolbox for Modified Aptamers. *Molecular Biotechnology*. 58(2): 79-92.

Lionetti V, Cervone F, De Lorenzo G. 2015. A lower content of de-methylesterified homogalacturonan improves enzymatic cell separation and isolation of mesophyll protoplasts in Arabidopsis. *Phytochemistry*. 112(1): 188-194.

Lopez-Ochoa L, Ramirez-Prado J, Hanley-Bowdoin L. 2006. Peptide Aptamers That Bind to a Geminivirus Replication Protein Interfere with Viral Replication in Plant Cells. *Journal of Virology*. 80(12): 5841-5853.

Lu S, Tian Q, Zhao W, Hu B. 2017. Evaluation of the Potential of five Housekeeping Genes for Identification of Quarantine *Pseudomonas syringae*. *Journal of Phytopathology*. 165(2): 73-81.

Luo Z, He L, Wang J, Fang X, Zhang L. 2017. Developing a combined strategy for monitoring the progress of aptamer selection. *The Analyst*. 142(17): 3136-3139.

Luzi E, Minunni M, Tombelli S, Mascini M. 2003. New trends in affinity sensing. *Trends in Analytical Chemistry*. 22(11): 810-818.

Mairal T, Özalp VC, Lozano Sánchez P, Mir M, Katakis I, O'Sullivan CK. 2008. Aptamers: molecular tools for analytical applications. *Analytical and Bioanalytical Chemistry*. 390(4): 989-1007.

Malandrin L and Samson R. 1999. Serological and Molecular Size Characterization of Flagellins of *Pseudomonas syringae* Pathovars and Related Bacteria. *Systematic and Applied Microbiology*. 22(4): 534-545.

Marimuthu C, Tang TH, Tominaga J, Tan SC, Gopinath SCB. 2012. Single-stranded DNA (ssDNA) production in DNA aptamer generation. *The Analyst*. 137(6): 1307-1315.

Mayer G. 2009. The Chemical Biology of Aptamers. *Angewandte Chemie International Edition*. 48(15): 2672-2689.

Mazzoleni S, Cartenì F, Bonanomi G, Senatore M, Termolino P, Giannino F, Incerti G, Rietkerk M, Lanzotti V, Chiusano ML. 2015. Inhibitory effects of extracellular self-DNA: a general biological process?. *New Phytologist*. 206(1): 127-132.

McNamara JO, Andrechek ER, Wang Y, Viles KD, Rempel RE, Gilboa E, Sullenger BA, Giangrande PH. 2006. Cell type–specific delivery of siRNAs with aptamer-siRNA chimeras. *Nature Biotechnology*. 24(8): 1005-1015.

Mencin N, Šmuc T, Vraničar M, Mavri J, Hren M, Galeša K, Krkoč P, Ulrich H, Šolar B. 2014. Optimization of SELEX: Comparison of different methods for monitoring the progress of in vitro selection of aptamers. *Journal of Pharmaceutical and Biomedical Analysis*. 91: 151-159.

Mendoza-Figueroa JS, Soriano-García M, Valle-Castillo LB, Méndez-Lozano J. 2014. Peptides and Peptidomics: A Tool with Potential in Control of Plant Viral Diseases. *Advances in Microbiology*. 4(9): 539-548.

Mercier MC, Dontenwill M, Choulier L. 2017. Selection of nucleic acid aptamers targeting tumor cell-surface protein biomarkers. *Cancers*. 9(12): 69.

Mezzetti B, Smagghe G, Arpaia S, Christiaens O, Dietz-Pfeilstetter A, Jones H, Kostov K, Sabbadini S, Opsahl-Sorteberg HG, Ventura V, Taning CNT, Sweet J. 2020. RNAi: What is its position in agriculture?. *Journal of Pest Science*. 93(4): 1125-1130.

Mitter N, Worrall EA, Robinson KE, Li P, Jain RG, Taochy C, Fletcher SJ, Carroll BJ, Lu GQ, Xu ZP. 2017. Clay nanosheets for topical delivery of RNAi for sustained protection against plant viruses. *Nature Plants*. 3(2): 16207.

Moruzzi S, Firrao G, Polano C, Borselli S, Loschi A, Ermacora P, Loi N, Martini M. 2017. Genomic-assisted characterisation of *Pseudomonas* sp. strain Pf4, a potential biocontrol agent in hydroponics. *Biocontrol Science and Technology*. 27(8): 969-991.

Mulet M, Lalucat J, García-Valdés E. 2010. DNA sequence-based analysis of the *Pseudomonas* species. *Environmental Microbiology*. 12(6): 1513-1530.

Musheev MU and Krylov SN. 2006. Selection of aptamers by systematic evolution of ligands by exponential enrichment: Addressing the polymerase chain reaction issue. *Analytica Chimica Acta*. 564(1): 91-96.

Ni S, Yao H, Wang L, Lu J, Jiang F, Lu A, Zhang G. 2017. Chemical Modifications of Nucleic Acid Aptamers for Therapeutic Purposes. *International Journal of Molecular Sciences*. 18(8): 1683.

Nomura K, Melotto M, He SY. 2005. Suppression of host defense in compatible plant–*Pseudomonas syringae* interactions. *Current Opinion in Plant Biology*. 8(4): 361-368.

O'Sullivan CK. 2002. Aptasensors – the future of biosensing?. *Analytical and Bioanalytical Chemistry*. 372(1): 44-48.

Ohuchi S. 2012. Cell-SELEX Technology. *BioResearch Open Access*. 1(6): 265-272.

Özalp VC, Bilecen K, Kavruk M, Öktem HA. 2013. Antimicrobial aptamers for detection and inhibition of microbial pathogen growth. *Future Microbiology*. 8(3): 387-401.

Ozer A, Pagano JM, Lis JT. 2014. New Technologies Provide Quantum Changes in the Scale, Speed and Success of SELEX Methods and Aptamer Characterization. *Molecular Therapy – Nucleic Acids*. 3: e183.

Penna-Coutinho J, Cortopassi WA, Oliveira AA, França TCC, Krettli, AU. 2011. Antimalarial Activity of Potential Inhibitors of *Plasmodium falciparum* Lactate Dehydrogenase Enzyme Selected by Docking Studies. *PLoS ONE*. 6(7): e21237.

Preston G. 2000. *Pseudomonas syringae* pv. *tomato*: the right pathogen, of the right plant, at the right time. *Molecular Plant Pathology*. 1(5): 263-275.

Reyes MI, Nash TE, Dallas MM, Ascencio-Ibanez JT, Hanley-Bowdoin L. 2013. Peptide Aptamers That Bind to Geminivirus Replication Proteins Confer a Resistance Phenotype to *Tomato Yellow Leaf Curl Virus* and *Tomato Mottle Virus* Infection in Tomato. *Journal of Virology*. 87(17): 9691-9706.

Rico A and Preston G. 2008. *Pseudomonas syringae* pv. *tomato* DC3000 Uses Constitutive and Apoplast-Induced Nutrient Assimilation Pathways to Catabolize Nutrients That Are Abundant in the Tomato Apoplast. *Molecular Plant-Microbe Interactions*®. 21(2): 269-282.

Rohloff JC, Gelinas AD, Jarvis TC, Ochsner UA, Schneider DJ, Gold L, Janjic N. 2014. Nucleic Acid Ligands With Protein-like Side Chains: Modified Aptamers and Their Use as Diagnostic and Therapeutic Agents. *Molecular Therapy - Nucleic Acids*. 3: e201.

Röthlisberger P and Hollenstein M. 2018. Aptamer chemistry. *Advanced Drug Delivery Reviews*. 134: 3-21.

Rudolph C, Schreier PH, Uhrig JF. 2003. Peptide-mediated broad-spectrum plant resistance to tospoviruses. *Proceedings of the National Academy of Sciences*. 100(8): 4429-4434.

Sambrook J and Russell DW. 2001. Molecular Cloning: A Laboratory Manual (Third Edition). "Commonly Used Techniques in Molecular Cloning," Appendix 8, Volume 3, 3rd edition.

Sefah K, Shangguan D, Xiong X, O'Donoghue MB, Tan W. 2010. Development of DNA aptamers using Cell-SELEX. *Nature Protocols*. 5(6): 1169-1185.

Sivakumar P, Kim S, Kang HC, Shim MS. 2019. Targeted siRNA delivery using aptamer-siRNA chimeras and aptamer-conjugated nanoparticles. *Wiley Interdisciplinary Reviews: Nanomedicine and Nanobiotechnology*. 11(3): e1543.

Song K, Lee S, Ban C. 2012. Aptamers and Their Biological Applications. *Sensors*. 12(1): 612-631.

Stoltenburg R, Reinemann C, Strehlitz B. 2005. FluMag-SELEX as an advantageous method for DNA aptamer selection. *Analytical and Bioanalytical Chemistry*. 383(1): 83-91.

Stoltenburg R, Reinemann C, Strehlitz B. 2007. SELEX—A (r)evolutionary method to generate high-affinity nucleic acid ligands. *Biomolecular Engineering*. 24(4): 381-403.

Strehlitz B, Reinemann C, Linkorn S, Stoltenburg R. 2012. Aptamers for pharmaceuticals and their application in environmental analytics. *Bioanalytical Reviews*. 4(1): 1-30.

Studier FW. 2005. Protein production by auto-induction in high-density shaking cultures. *Protein Expression and Purification*. 41(1): 207-234.

Sun P, Tropea JE, Waugh DS. 2011. Enhancing the Solubility of Recombinant Proteins in *Escherichia coli* by Using Hexahistidine-Tagged Maltose-Binding Protein as a Fusion Partner. *Methods in Molecular Biology*. 705(1): 259-274.

Svobodová M, Pinto A, Nadal P, O' Sullivan CK. 2012. Comparison of different methods for generation of single-stranded DNA for SELEX processes. *Analytical and Bioanalytical Chemistry*. 404(3): 835-842.

Tan SY, Acquah C, Sidhu A, Ongkudon CM, Yon LS, Danquah MK. 2016. SELEX Modifications and Bioanalytical Techniques for Aptamer–Target Binding Characterization. *Critical Reviews in Analytical Chemistry*. 46(6): 521-537.

Thiel KW and Giangrande PH. 2010. Intracellular delivery of RNA-based therapeutics using aptamers. *Therapeutic Delivery*. 1(6): 849-861.

Thiel KW, Hernandez LI, Dassie JP, Thiel WH, Liu X, Stockdale KR, Rothman AM, Hernandez FJ, McNamara JO, Giangrande PH. 2012. Delivery of chemo-sensitizing siRNAs to HER2+-breast cancer cells using RNA aptamers. *Nucleic Acids Research*. 40(13): 6319-6337.

Tolle F and Mayer G. 2013. Dressed for success – applying chemistry to modulate aptamer functionality. *Chemical Science*. 4(1): 60-67.

Tolle F, Wilke J, Wengel J, Mayer G. 2014. By-product formation in repetitive PCR amplification of DNA libraries during SELEX. *PLoS ONE*. 9(12): 1-12.

Tuerk C and Gold L. 1990. Systematic evolution of ligands by exponential enrichment: RNA ligands to bacteriophage T4 DNA polymerase. *Science*. 249(4968): 505-510.

Uppalapati SR, Ishiga Y, Wangdi T, Urbanczyk-Wochniak E, Ishiga T, Mysore KS, Bender CL. 2008. Pathogenicity of *Pseudomonas syringae* pv. *tomato* on Tomato Seedlings: Phenotypic and Gene Expression Analyses of the Virulence Function of Coronatine. *Molecular Plant-Microbe Interactions*®. 21(4): 383-395.

Vanbrabant J, Leirs K, Vanschoenbeek K, Lammertyn J, Michiels L. 2014. reMelting curve analysis as a tool for enrichment monitoring in the SELEX process. *The Analyst*. 139(3): 589-595.

Walter JG, Stahl F, Scheper T. 2012. Aptamers as affinity ligands for downstream processing. *Engineering in Life Sciences*. 12(5): 496-506.

Wang T, Chen C, Larcher LM, Barrero RA, Veedu RN. 2019. Three decades of nucleic acid aptamer technologies: Lessons learned, progress and opportunities on aptamer development. *Biotechnology Advances*. 37(1): 28-50.

Weisburg WG, Barns SM, Pelletier DA, Lane DJ. 1991. 16S ribosomal DNA amplification for phylogenetic study. *Journal of Bacteriology*. 173(2): 697-703.

Whalen MC, Innes RW, Bent AF, Staskawicz BJ. 1991. Identification of *Pseudomonas syringae* Pathogens of *Arabidopsis* and a Bacterial Locus Determining Avirulence on Both *Arabidopsis* and Soybean. *The Plant Cell*. 3(1): 49-59.

Wilson K. 1997. Preparation of Genomic DNA from Bacteria. In: Ausubel FM, Brent G, Kingston RE, Moore DD, Seidman JG, Smith JA, Struhl K, editors. "Current Protocols in Molecular Biology". John Wiley & Sons Inc; ringbou edition (December 4, 2003). UNITS 2.4.1-2.4.5.

Xiang D, Zheng C, Zhou SF, Qiao S, Tran PHL, Pu C, Li Y, Kong L, Kouzani AZ, Lin J, Liu K, Li L, Shigdar S, Duan W. 2015. Superior Performance of Aptamer in Tumor Penetration over Antibody: Implication of Aptamer-Based Theranostics in Solid Tumors. *Theranostics*. 5(10): 1083-1097.

Xiao Z, Levy-Nissenbaum E, Alexis F, Lupták A, Teply BA, Chan JM, Shi J, Digga E, Cheng J, Langer R, Farokhzad OM. 2012. Engineering of Targeted Nanoparticles for Cancer Therapy Using Internalizing Aptamers Isolated by Cell-Uptake Selection. *ACS Nano*. 6(1): 696–704.

Yamamoto S, Kasai H, Arnold DL, Jackson RW, Vivian A, Harayama S. 2000. Phylogeny of the genus *Pseudomonas*: intrageneric structure reconstructed from the nucleotide sequences of *gyrB* and *rpoD* genes. *Microbiology*. 146(10): 2385-2394.

Ye M, Hu J, Peng M, Liu J, Liu J, Liu H, Zhao X, Tan W. 2012. Generating Aptamers by Cell-SELEX for Applications in Molecular Medicine. *International Journal of Molecular Sciences*. 13(3): 3341-3353.

Yokoyama R, Kuki H, Kuroha T, Nishitani K. 2016. Arabidopsis Regenerating Protoplast: A Powerful Model System for Combining the Proteomics of Cell Wall Proteins and the Visualization of Cell Wall Dynamics. *Proteomes*. 4(4): 34.

Yonekura K, Maki-Yonekura S, Namba K. 2003. Complete atomic model of the bacterial flagellar filament by electron cryomicroscopy. *Nature*. 424(6949): 643-650.

Yoo SD, Cho YH, Sheen J. 2007. *Arabidopsis* mesophyll protoplasts: a versatile cell system for transient gene expression analysis. *Nature Protocols*. 2(7): 1565-1572.

Yüce M, Ullah N, Budak H. 2015. Trends in aptamer selection methods and applications. *The Analyst*. 140(16): 5379-5399.

Zadeh JN, Steenberg CD, Bois JS, Wolfe BR, Pierce MB, Khan AR, Dirks RM, Pierce NA. 2011. NUPACK: Analysis and design of nucleic acid systems. *Journal of Computational Chemistry*. 32(1): 170-173.

Zhang Y, Lai B, Juhas M. 2019. Recent Advances in Aptamer Discovery and Applications. *Molecules*. 24(5): 941.

Zhou J and Rossi J. 2017. Aptamers as targeted therapeutics: current potential and challenges. *Nature Reviews Drug Discovery*. 16(3): 181-202.

Zhu Q, Liu G, Kai M. 2015. DNA Aptamers in the Diagnosis and Treatment of Human Diseases. *Molecules*. 20(12): 20979-20997.

Zhuo Z, Yu Y, Wang M, Li J, Zhang Z, Liu J, Wu X, Lu A, Zhang G, Zhang B. 2017. Recent Advances in SELEX Technology and Aptamer Applications in Biomedicine. *International Journal of Molecular Sciences*. 18(10): 2142.

Zotti M, dos Santos EA, Cagliari D, Christiaens O, Taning CNT, Smagghe G. 2018. RNA interference technology in crop protection against arthropod pests, pathogens and nematodes. *Pest Management Science*. 74(6): 1239-1250.

Zou Q, Habermann-Rottinghaus SM, Murphy KP. 1998. Urea effects on protein stability: Hydrogen bonding and the hydrophobic effect. *Proteins: Structure, Function, and Genetics*. 31(2): 107-115.

9. SUPPLEMENTARY MATERIALS

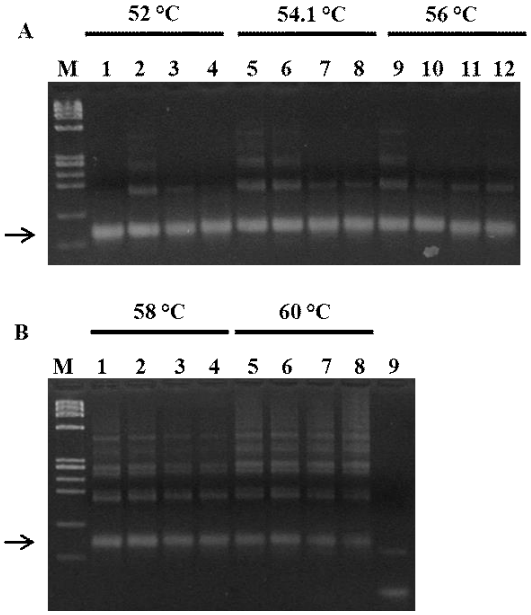

Figure S10- A and B. Gradient PCR of LIB1.0 library with 52 °C, 54.1 °C, 56 °C, 58 °C and 60 °C as annealing temperatures. **(A)** M is ΦX174 DNA BsuRI (HaeIII) marker (1 353 bp, 1 078 bp, 872 bp, 603 bp, 310 bp, 281 bp, 271 bp, 234 bp, 194 bp, 118 bp and 72 bp). Lanes 1, 2, 5, 6, 9 and 10 are 10 ng of LIB1.0 library. Lanes 3, 4, 7, 8, 11 and 12 are 100 ng of LIB1.0 library. **(B)** M is ΦX174 DNA BsuRI (HaeIII) marker (1 353 bp, 1 078 bp, 872 bp, 603 bp, 310 bp, 281 bp, 271 bp, 234 bp, 194 bp, 118 bp and 72 bp). Lanes 1, 2, 5 and 6 are 10 ng LIB1.0 library. Lanes 3, 4, 7 and 8 are 100 ng LIB1.0 library. Lane 9 is the negative control. Expected amplicon sizes are of 80 bp (black arrows).

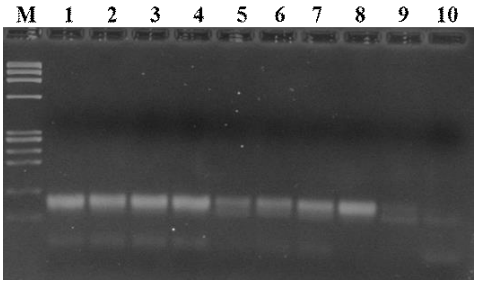

Figure S16. Gel electrophoresis of Real Time PCR products. M is ΦX174 DNA BsuRI (HaeIII) marker (1 353 bp, 1 078 bp, 872 bp, 603 bp, 310 bp, 281 bp, 271 bp, 234 bp, 194 bp, 118 bp and 72 bp). Lane 1 is eluted oligonucleotides 1 µl. Lanes 2, 3 and 4 are the eluted oligonucleotides 1:10 diluted, of 1 µl, 2.5 µl and 5 µl, respectively. Lanes 5, 6 and 7 are the eluted oligonucleotides 1:100 diluted, of 1 µl, 2.5 µl and 5 µl, respectively. Lane 8 is the cell-extracted oligonucleotides 1 µl. Lanes 9 and 10 are the negative controls.

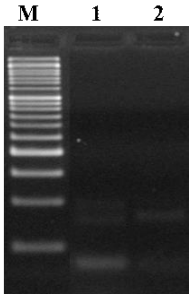

Figure S17. Gel electrophoresis of Real Time PCR products. M is *SHARPMASS*™ 50 marker (1 500 bp, 1 200 bp, 1 000 bp, 900 bp, 800 bp, 700 bp, 600 bp, 500 bp, 450 bp, 400 bp, 350 bp, 300 bp, 250 bp, 200 bp, 150 bp, 100 bp and 50 bp). Lane 1 is cell-extracted oligonucleotides. Lane 2 is the negative control.

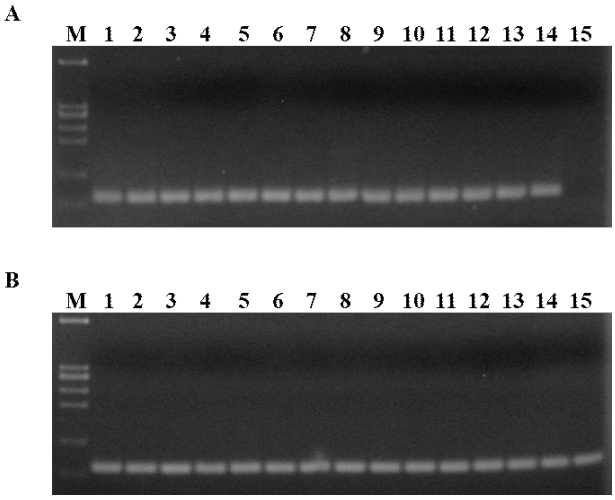

Figure S18- A and B. Colony-PCR on cells transformed with the cell-extracted oligonucleotides of Cell-SELEX I round 2. **(A)** M is ΦX174 DNA BsuRI (HaeIII) marker (310 bp, 281 bp, 271 bp, 234 bp, 194 bp, 118 bp and 72 bp). Lanes 1 to 14 are the screened colonies from number 1 to number 14. Lane 15 is the negative control. **(B)** M is ΦX174 DNA BsuRI (HaeIII) marker (310 bp, 281 bp, 271 bp, 234 bp, 194 bp, 118 bp and 72 bp). Lanes 1 to 15 are the screened colonies from number 15 to number 29.

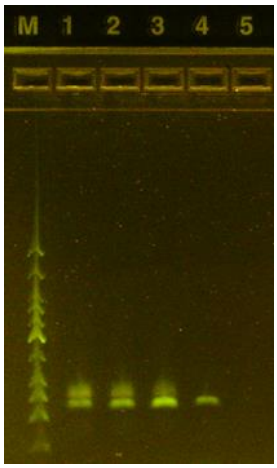

Figure S19. Electrophoresis on agarose gel of Real Time PCR products. M is Low Molecular Weight DNA Ladder (766 bp, 500 bp, 350 bp, 300 bp, 250 bp, 200 bp, 150 bp, 100 bp, 75 bp, 50 bp and 25 bp). Lanes 1, 2, 3 and 4 are MH35 library 100 nM, 10 nM, 1 nM and 0.1 nM, respectively. Lane 5 is the negative control.

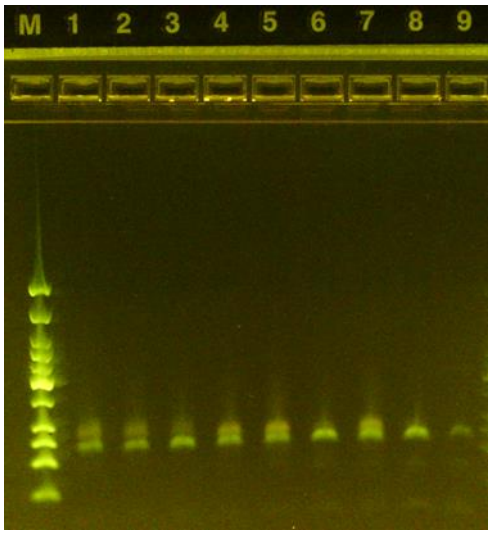

Figure S20. Electrophoresis on agarose gel of Real Time PCR products. M is Low Molecular Weight DNA Ladder (766 bp, 500 bp, 350 bp, 300 bp, 250 bp, 200 bp, 150 bp, 100 bp, 75 bp, 50 bp and 25 bp). Lanes 1, 2 and 3 are MH35 library prior selection of 1 nM, 0.5 nM and 0.2 nM, respectively. Lane 4 is round 3. Lanes 5 and 6 are round 6 dilution 1:2000 and dilution 1:10000, respectively. Lanes 7 and 8 are round 10 dilution 1:2000 and dilution 1:10000, respectively. Lane 9 is the negative control.

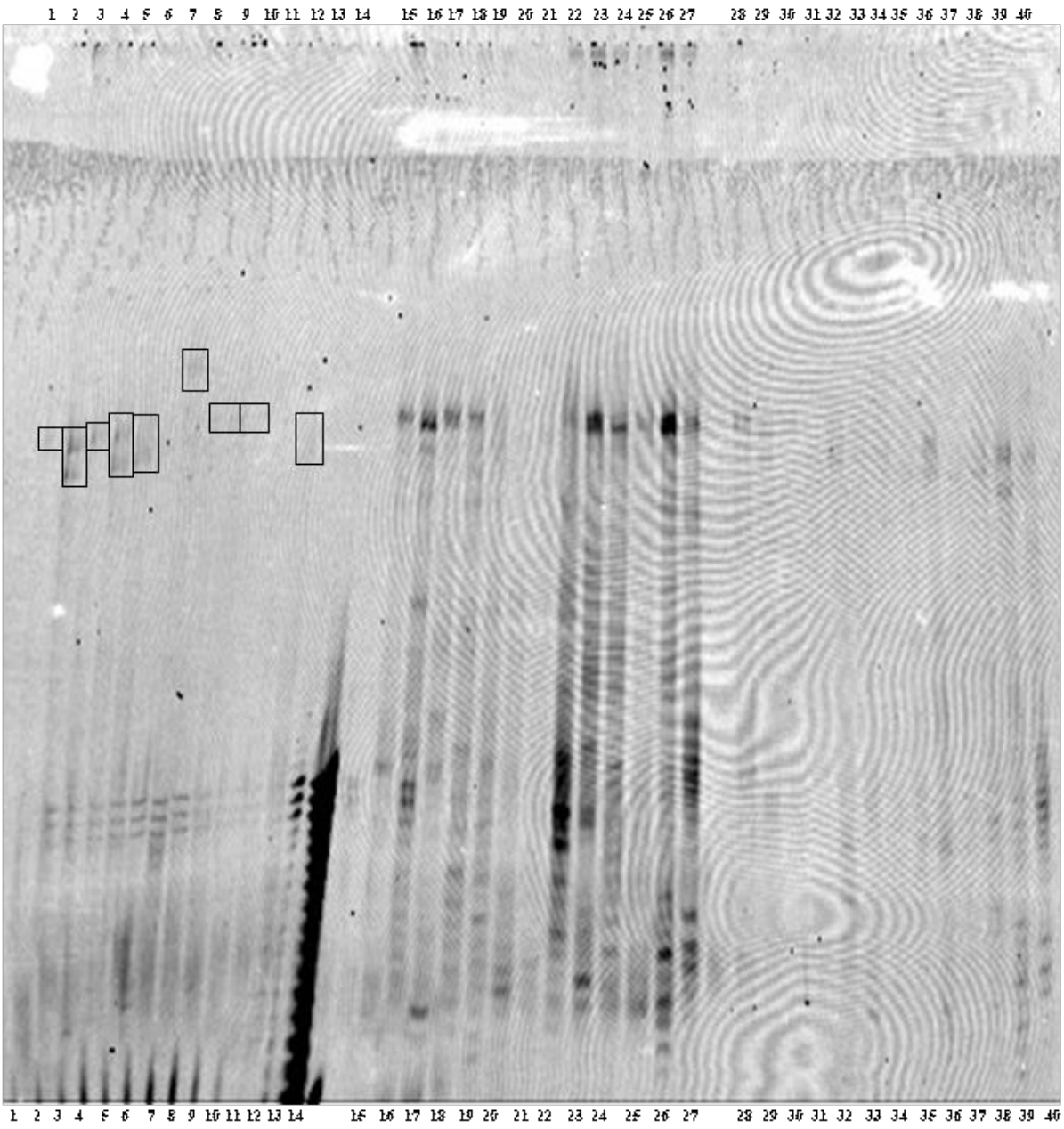

Figure S22. Denaturing polyacrylamide gel of elution (lanes 1 to 13), flow-through (lanes 15 to 27) and wash (lanes 28 to 40) steps of potential aptamers from round 10. Colony n° 2 is lanes 1, 15 and 28; n° 10 is lanes 2, 16 and 29; n° 16 is lanes 3, 17 and 30; n° 22 is lanes 4, 18 and 31; n° 38 is lanes 5, 19 and 32; n° 44 is lanes 6, 20 and 33; n° 49 is lanes 7, 21 and 34; n° 50 is lanes 8, 22 and 35; n° 53 is lanes 9, 23 and 36; n° 62 is lanes 10, 24 and 37; n° 67 is lanes 11, 25 and 38; n° 70 is lanes 12, 26 and 39; n° 71 is lanes 13, 27 and 40. Lane 14 is [6FAM]MH36 primer. Black squares highlight the specificity of some potential aptamers to the target.

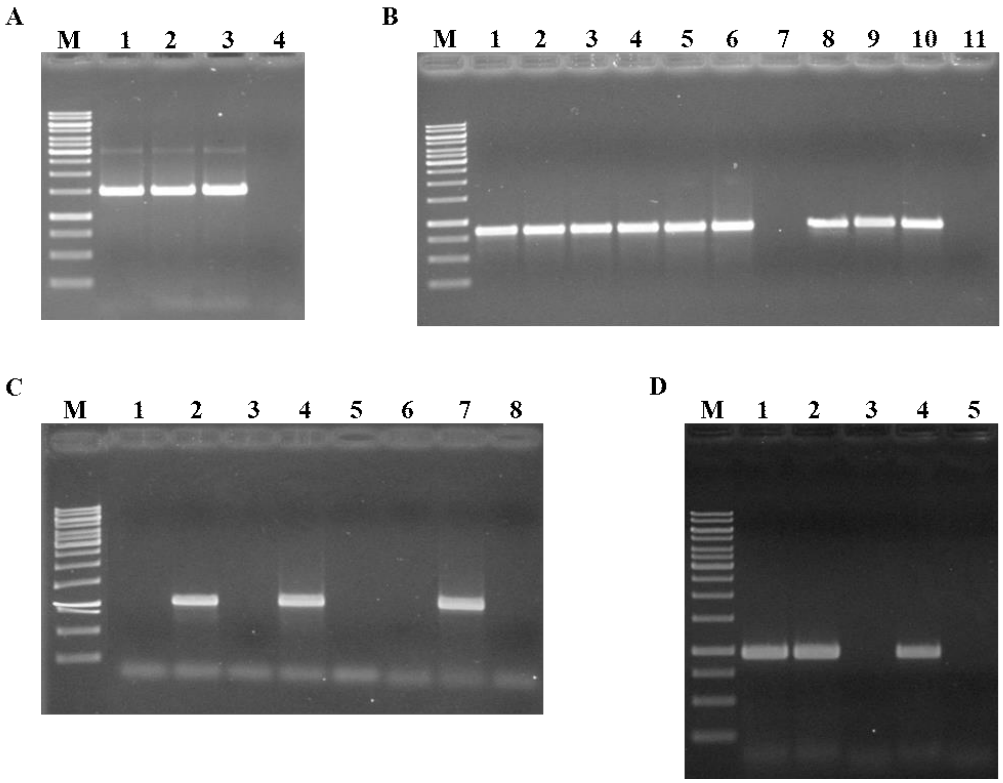

Figure S23- A, B, C and D. (A) Standard PCR amplification of 16S rDNA genes of *Pto*, *Pta* and *Pf4* gDNAs. M is GeneRuler^{TM} 1 Kb DNA Ladder (10 000 bp, 8 000 bp, 6 000 bp, 5 000 bp, 4 000 bp, 3 500 bp, 3 000 bp, 2 500 bp, 2 000 bp, 1 500 bp, 1 000 bp, 750 bp, 500 bp and 250 bp) marker. Lane 1 is *Pto*. Lane 2 is *Pta*. Lane 3 is *Pf4*. Lane 4 is the negative control. Expected amplicon sizes are of 1 504 bp. **(B)** Gradient PCR amplification with F0 and R0 primers of flagellin genes of *Pto*, *Pta* and *Pf4* gDNAs. M is GeneRuler^{TM} 1 Kb DNA Ladder marker (10 000 bp, 8 000 bp, 6 000 bp, 5 000 bp, 4 000 bp, 3 500 bp, 3 000 bp, 2 500 bp, 2 000 bp, 1 500 bp, 1 000 bp, 750 bp, 500 bp and 250 bp). Lanes 1, 2 and 3 are *Pto* at 54 °C, 53 °C and 52 °C, respectively. Lanes 4, 5 and 6 are *Pta* at 54 °C, 53 °C and 52 °C, respectively. Lane 7 is PsF0 / PsR0 negative control. Lanes 8, 9 and 10 are *Pf4* at 54 °C, 53 °C and 52 °C, respectively. Lane 11 is Pf4F0 / Pf4R0 negative control. **(C)** Standard PCR amplification with F1 and R1 primers of flagellin genes of *Pto*, *Pta* and *Pf4* gDNAs. M is GeneRuler^{TM} 1 Kb DNA Ladder marker (10 000 bp, 8 000 bp, 6 000 bp, 5 000 bp, 4 000 bp, 3 500 bp, 3 000 bp, 2 500 bp, 2 000 bp, 1 500 bp, 1 000 bp, 750 bp, 500 bp and 250 bp). Lanes 1 and 2 are *Pto* with 10 and 30 amplification cycles, respectively. Lanes 3 and 4 are *Pta* with 10 and 30 amplification cycles, respectively. Lane 5 is PsF1 / PsR1 negative control. Lanes 6 and 7 are *Pf4* with 10 and 30 amplification cycles, respectively. Lane 8 is Pf4F1 / Pf4R1 negative control. **(D)** Standard PCR amplification with F2 and R2 primers of F1 - R1 PCR products. M is GeneRuler^{TM} 1 Kb DNA Ladder marker (10 000 bp, 8 000 bp, 6 000 bp, 5 000 bp, 4 000 bp, 3 500 bp, 3 000 bp, 2 500 bp, 2 000 bp, 1 500 bp, 1 000 bp, 750 bp, 500 bp and 250 bp). Lane 1 is *Pto*. Lane 2 is *Pta*. Lane 3 is PsF2 / PsR2 negative control. Lane 4 is *Pf4*. Lane 5 is Pf4F2 / Pf4R2 negative control.

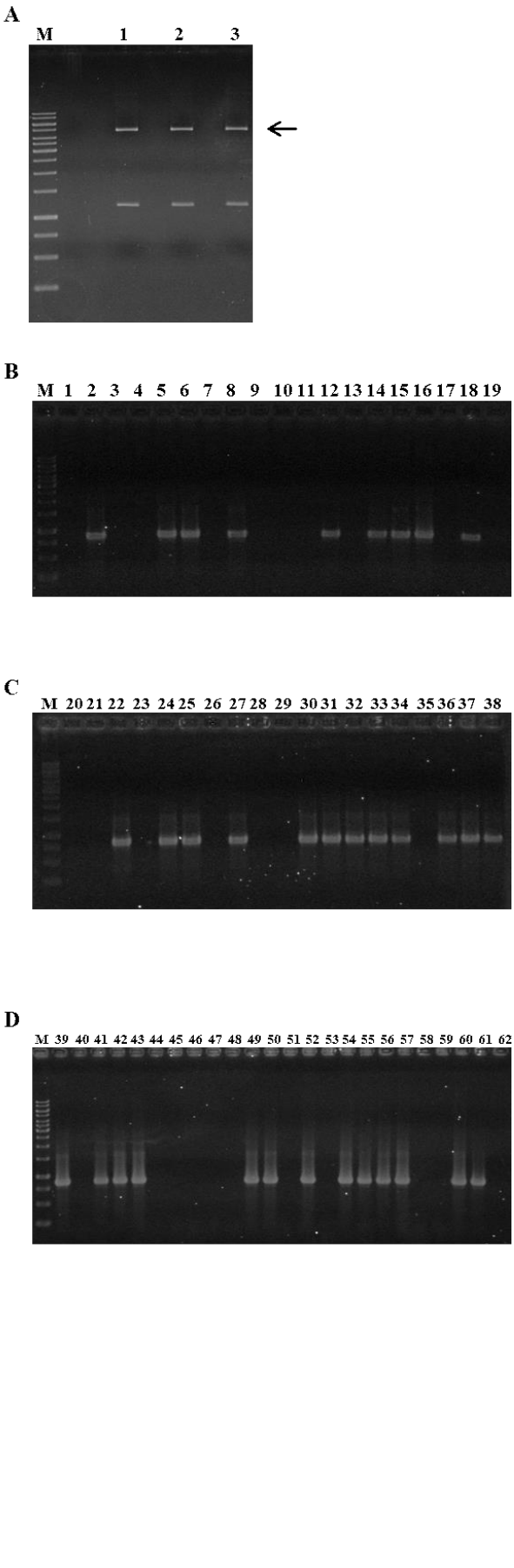
A
M 1 2 3
B
M 1 2 3 4 5 6 7 8 9 10 11 12 13 14 15 16 17 18 19
C
M 20 21 22 23 24 25 26 27 28 29 30 31 32 33 34 35 36 37 38
D
M 39 40 41 42 43 44 45 46 47 48 49 50 51 52 53 54 55 56 57 58 59 60 61 62
E
M 1 2 3 4 5 6 7 8 9 10 11 12 13 14 15 16 17 18 19
F
M 20 21 22 23 24 25 26 27 28 29 30 31 32 33 34 35 36 37 38
G
M 39 40 41 42 43 44 45 46 47 48 49 50 51 52
H
M 1 2 3 4 5 6 7 8 9 10 11 12 13 14 15 16 17 18 19
I
M 20 21 22 23 24 25 26 27 28 29 30 31 32 33 34 35 36 37 38
J
M 39 40 41 42 43 44 45 46 47 48 49 50 51 52

Figure S24- A, B, C, D, E, F, G, H, I and J. (A) pET-14b plasmid vector double-digested with *Xba*I and *Bam*HI restriction enzymes. M is GeneRuler^{TM} 1 Kb DNA Ladder marker (10 000 bp, 8 000 bp, 6 000 bp, 5 000 bp, 4 000 bp, 3 500 bp, 3 000 bp, 2 500 bp, 2 000 bp, 1 500 bp, 1 000 bp, 750 bp, 500 bp and 250 bp). Lanes 1, 2 and 3 are the digestion products. The black arrow indicates the linearized pET-14b plasmid vector. **(B-C-D)** Colony-PCR on JM101 cells transformed with ligation product of pET-14b plasmid vector and *Pto*-flagellin. M is GeneRuler^{TM} 1 Kb DNA Ladder marker (10 000 bp, 8 000 bp, 6 000 bp, 5 000 bp, 4 000 bp, 3 500 bp, 3 000 bp, 2 500 bp, 2 000 bp, 1 500 bp, 1 000 bp, 750 bp, 500 bp and 250 bp). Lanes 1 to 60 are the screened colonies from number 1 to number 60. Lane 61 is *Pto* gDNA. Lane 62 is the negative control. **(E-F-G)** Colony-PCR on JM101 cells transformed with ligation product of pET-14b plasmid vector and *Pta*-flagellin. M is GeneRuler^{TM} 1 Kb DNA Ladder marker (10 000 bp, 8 000 bp, 6 000 bp, 5 000 bp, 4 000 bp, 3 500 bp, 3 000 bp, 2 500 bp, 2 000 bp, 1 500 bp, 1 000 bp, 750 bp, 500 bp and 250 bp). Lanes 1 to 50 are the screened colonies from number 1 to number 50. Lane 51 is *Pta* gDNA. Lane 52 is the negative control. **(H-I-J)** Colony-PCR on JM101 cells transformed with ligation product of pET-14b plasmid vector and *Pf4*-flagellin. M is GeneRuler^{TM} 1 Kb DNA Ladder marker (10 000 bp, 8 000 bp, 6 000 bp, 5 000 bp, 4 000 bp, 3 500 bp, 3 000 bp, 2 500 bp, 2 000 bp, 1 500 bp, 1 000 bp, 750 bp, 500 bp and 250 bp). Lanes 1 to 50 are the screened colonies from number 1 to number 50. Lane 51 is *Pf4* gDNA. Lane 52 is the negative control.

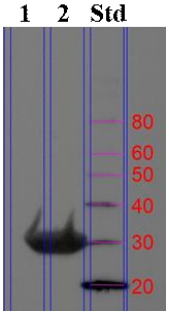

Figure S25. Western Blot of soluble and insoluble fractions of *E. coli* before protein purification. Lane 1 is the soluble fraction. Lane 2 is the insoluble fraction. M are the Protein Standards (80 kDa, 60 kDa, 50 kDa, 40 kDa, 30 kDa and 20 kDa).

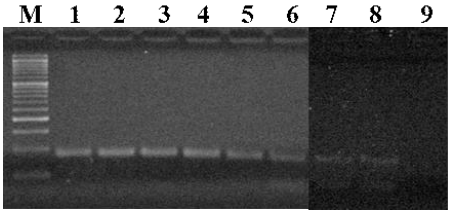

Figure S26. Gel electrophoresis of Real Time PCR products. M is *SHARPMASS*^{TM} 50 marker (1 500 bp, 1 200 bp, 1 000 bp, 900 bp, 800 bp, 700 bp, 600 bp, 500 bp, 450 bp, 400 bp, 350 bp, 300 bp, 250 bp, 200 bp, 150 bp, 100 bp and 50 bp). Lanes 1 to 8 are SELEX rounds 1 to 8, respectively. Lane 9 is the Real Time PCR negative control.

ACKNOWLEDGEMENTS

I would like to thank my Supervisor Prof. Giuseppe Firrao who always supported me through all these intense three years and helped me to grow up from a scientific point of view.

I would like to thank my External Supervisor Dr. Marcel Hollenstein who hosted me in his laboratory for my research period abroad and gave me the opportunity to work in an extremely stimulating scientific environment.

I would like to thank all my colleagues-friends both in Udine and Paris whom I shared important moments both at work and outside.

To all my family and friends
who always sustained me in every moment
helping me to take the right decisions,
thanks to them I am the person who I am.